

1 ***INDITTO2* transposon conveys auxin-mediated *DRO1* transcription for rice**
2 **drought avoidance**

3

4 Yiting Zhao^{1,2,3,8*}, Lixia Wu^{1,2,3*}, Qijing Fu^{1,2,3*}, Dong Wang⁶, Jing Li⁷, Baolin Yao⁷,
5 Si Yu¹, Li Jiang¹, Jie Qian¹, Xuan Zhou^{1,2,3}, Li Han^{1,2,3}, Shuanglu Zhao¹, Canrong Ma⁵,
6 Yanfang Zhang¹, Chongyu Luo^{1,2,3}, Qian Dong¹, Saijie Li¹, Lina Zhang¹, Xi Jiang¹,
7 Youchun Li¹, Hao Luo¹, Kuixiu Li^{1,2,3}, Jing Yang^{1,2,3}, Qiong Luo^{1,2,3}, Lichi Li⁹, Sheng
8 Peng^{1,2,3}, Huichuan Huang^{1,2,3}, Zhili Zuo⁶, Changning Liu⁷, Lei Wang⁵, Chengyun
9 Li^{1,2,3}, Xiahong He^{1,2,3}, Jiří Friml⁴, Yunlong Du^{1,2,3#}

10

11 ¹ College of Plant Protection, Yunnan Agricultural University, Kunming 650201,
12 China.

13 ² State Key Laboratory for Conservation and Utilization of Bio-Resources in Yunnan,
14 Yunnan Agricultural University, Kunming 650201, China.

15 ³ Key Laboratory of Agro-Biodiversity and Pest Management of Education Ministry
16 of China, Yunnan Agricultural University, Kunming 650201, China.

17 ⁴ Institute of Science and Technology Austria (IST Austria), Klosterneuburg, Austria.

18 ⁵ Key Laboratory of Economic Plants and Biotechnology, Yunnan Key Laboratory for
19 Research and Development of Wild Plant Resources, Kunming Institute of Botany,
20 Chinese Academy of Sciences, Kunming 650201, China.

21 ⁶ State Key Laboratory of Phytochemistry and Plant Resources in West China,
22 Kunming Institute of Botany, Chinese Academy of Sciences, Kunming 650201,
23 Yunnan, China.

24 ⁷ CAS Key Laboratory of Tropical Plant Resources and Sustainable Use,
25 Xishuangbanna Tropical Botanical Garden, Chinese Academy of Sciences, Menglun,

26 Mengla 666303, Yunnan, China.

27 ⁸ Shanxi Agricultural University/Shanxi Academy of Agricultural Sciences. The
28 Industrial Crop Institute, Fenyang 032200, China.

29 ⁹ International Agriculture Research Institute, Yunnan Academy of Agricultural
30 Sciences. Beijing Rd.2238, Kunming 650205, China

31 * Yiting Zhao, Lixia Wu and Qijing Fu should be considered joint first authors

32 # **Corresponding authors**

33 College of Plant Protection, Yunnan Agricultural University, Kunming 650201, China.

34 Tel: +86 18206799459

35 Email: yunlongdu@aliyun.com

36 ORCID ID: [yunlongdu@aliyun.com](https://orcid.org/yunlongdu@aliyun.com)

37

38 **Funding information**

39 This work was supported by grants from the National Natural Science Foundation of
40 China (Grant Nos. 31460453, 31660501, 31860064 and 31470382); the Major Special
41 Program for Scientific Research, Education Department of Yunnan Province (Grant
42 No. ZD2015005); SRF for ROCS, SEM (Grant No. [2013] 1792); the Major Science
43 and Technique Programs in Yunnan Province (Grant No. 2016ZF001); the Key
44 Projects of Applied Basic Research Plan of Yunnan Province (Grant No. 2017FA018);
45 the National Key R&D Program of China (2018YFD0201100); the China Agriculture
46 Research System (CARS-21); the National Key Research Development Program of
47 China (2016YFD0100600), the Program for Innovative Research Team in University
48 of Yunnan Province (IRTSTYN) and the European Research Council (ERC) under the
49 European Union's Horizon 2020 Research and Innovation Programme (Grant
50 Agreement No 742985).

51

52 **Running head**

53 *INDITTO2* conveys auxin signal in rice root growth

54

55 **Abstract**

56 Transposable elements exist widely throughout plant genomes and play important
57 roles in plant evolution. Auxin is an important regulator that is traditionally associated
58 with root development and drought stress adaptation. The *DEEPER ROOTING 1*
59 (*DROI*) gene is a key component of rice drought avoidance. Here, we identified a
60 transposon that acts as an autonomous auxin-responsive promoter and its presence at
61 specific genome positions conveys physiological adaptations related to drought
62 avoidance. Rice varieties with high and auxin-mediated transcription of *DROI* in the
63 root tip show deeper and longer root phenotypes and are thus better adapted to
64 drought. The *INDITTO2* transposon contains an auxin response element and displays
65 auxin-responsive promoter activity; it is thus able to convey auxin regulation of
66 transcription to genes in its proximity. In the rice *Acuce*, which displays
67 *DROI*-mediated drought adaptation, the *INDITTO2* transposon was found to be
68 inserted at the promoter region of the *DROI* locus. Transgenesis-based insertion of
69 the *INDITTO2* transposon into the *DROI* promoter of the non-adapted rice variety
70 *Nipponbare* was sufficient to promote its drought avoidance. Our data identify an
71 example of how transposons can act as promoters and convey hormonal regulation to
72 nearby loci, improving plant fitness in response to different abiotic stresses.

73 **Keywords:** Indoleacetic acid, *Oryza*, Drought, DNA transposable elements, Stress

74

75 **Introduction**

76 Transposons are important mobile DNA elements and are frequently found cross the
77 genome. Transposons have been found to be involved in a broad range of phenotypes,
78 including changes in gene promoter activity (Bureau et al., 1996; Sun et al., 2013),
79 genome diversity (Oki et al., 2008), plant responses to drought stress (Yan et al.,
80 2011), plant morphogenesis (Jiang et al., 2003; Kikuchi et al., 2003; Momose et al.,
81 2010; Nakazaki et al., 2003) as well as encoding transposases (Zhang et al., 2001;
82 Zhang et al., 2004). Miniature inverted-repeat transposable element (MITE) families,
83 including *Tourist* and *Stowaway*, play important roles in rice genome diversity (Oki et
84 al., 2008). The *Tourist* transposable elements, including a non-autonomous DNA
85 transposon named *INDITTO*, have been found in the genomes of rice, maize, barley
86 and sorghum (Bureau & Wessler, 1992, 1994; Jiang & Wessler, 2002). *Tourist*
87 elements can be present within the proximal promoter of auxin-binding protein 1 in
88 maize and teosinte and form multimers in the maize genome (Elrouby & Bureau,
89 2000, 2012; Jiang & Wessler, 2001). This implies that cross-talk between auxin and
90 the *Tourist* elements may be involved in plant development. However, the possible
91 developmental and physiological roles of *INDITTO* and its homologues remain
92 unclear.

93 Drought avoidance is of critical importance in the development of many plants.
94 Drought avoidance is the mechanism by which plants alter the angles of root growth
95 to take up water and nutrients from the soil, or roll their leaves to reduce transpiration
96 (Kadioglu et al., 2012; Uga et al., 2015a). The major plant hormone auxin is involved
97 in the regulation of rice drought avoidance. Auxin may be associated with the binding
98 of auxin response elements (AREs) and may also negatively regulate the level of rice
99 *DEEPER ROOTING 1 (DROI)* gene, which functions to enhance rice drought

100 avoidance (Uga et al., 2013). The *DROI* gene, located on chromosome 9, has been
101 identified as a major quantitative trait locus (QTL) controlling rice root growth angle
102 and promoting rice yield (Arai-Sanoh et al., 2014; Uga et al., 2011). The rice variety
103 Kinandang Patong, which contains full *DROI* sequences, shows stronger drought
104 avoidance than the variety IR64, which has a nucleotide adenine (A) deletion in exon
105 4 that results in the pre-termination of *DROI* translation (Uga et al., 2013).
106 Furthermore, the function of *DROI* may be regulated by a few major QTLs located on
107 chromosomes 2, 4, 6 and 7 (Kitomi et al., 2015; Uga et al., 2015b). The *DROI* gene is
108 a member of the IGT family (Dardick et al., 2013; Guseman et al., 2017), which also
109 includes the *OsTAC1*, *OsLAZY1* and *qSOR1* genes (Godbole et al., 1999; Kitomi et al.,
110 2020; Li et al., 2007; Yoshihara & Iino, 2007; Yu et al., 2007). The *DROI*
111 homologues in rice (Kitomi et al., 2020), *Arabidopsis* and peach also regulate root and
112 shoot architecture (Guseman et al., 2017). The rice auxin efflux carrier from the
113 PIN-FORMED (PIN) family is known to play an important role in adventitious root
114 emergence (Xu et al., 2005), tiller number and tiller angle (Chen et al., 2012), and root
115 growth angle and crown root development (Wang et al., 2018; Zhang et al., 2012) by
116 regulating polar auxin transport. Recombinant OsARF1 protein can bind to the AREs
117 of the rice *DROI* promoter as well as other *cis*-regulatory elements involved in the
118 expression divergence of *DROI-like* wheat homologues (Ashraf et al., 2019; Uga et
119 al., 2013). However, the mechanism underlying the enhancement of rice root drought
120 avoidance by *DROI* remains poorly understood. We hypothesize that auxin may
121 interact with some kinds of genes to regulate *DROI* transcription involving in rice
122 root drought avoidance mediated by controlling auxin transport.

123 The *indica* rice Acuce is a paddy rice landrace with a more than 100 years of
124 planting history in the Yuanyang Hani's terraced fields at altitudes of 1600-2000 m in

125 Yunnan Province, China. Acuce is a dominant rice variety with favourable agronomic
126 traits, including stable yields and resistance to pathogens. Revealing the genetic basis
127 of the excellent Acuce agronomic traits, especially that of root development and
128 particularly with regard to *DROI* and transposons, will be of great value in improving
129 rice responses to abiotic and biotic stresses in agricultural production.

130 Here, we found that the *DROI* gene controls root architecture via a mechanism
131 related to auxin transport. Further study revealed that an *INDITTO2* transposon
132 located in the upstream promoter region of the Acuce *DROI* gene has promoter
133 activity and can convey auxin-dependent transcriptional regulation of *DROI* to
134 enhance rice drought avoidance. These findings provide new insights into how
135 transposons can regulate plant fitness under different environmental stresses.

136

137 **Materials and Methods**

138 **Plant materials**

139 The rice varieties used in this study included Nipponbare, Li jiang xin tuan hei gu
140 (LTH) and Wen lu dao 4 (Wld) with *japonica* background; IR64 with *indica*
141 background; and Kasalath with *aus* background. The following rice germplasms
142 Acuce (*Oryza sativa* cv. *indica*, Acuce), Ai jiao gu (Ajg), Ai zhe gu (Azg), Bai gu (Bg),
143 Ban jiu gu (Bjg), Che bu (Cb), Che jia (Cj), Che zuo (Cz), Chuan bai gu (Cbg), Da
144 leng shui (Dls), Da pi gu (Dpg), Duo dian (Dd), Ga niang hong gu (Gnhg), Gan di gu
145 (Gdg), Gan tian nuo (Gtn), Hei gu (Hg), Hong jiao lao geng (Hjlg), Hong yang 1 (Hy
146 1), Hua ke nuo (Hkn), Jian shui gu (Jsg), Jiu yue nuo (Jyn), Kou ni he lve (Knhl), Le
147 che che ma (Lccm), Ma xian gu (Mxg), Ma zhe nuo (Mzn), Man che hong nuo
148 (Mchn), Mao lai gu (Mlg), Meng la gu (Mlg), Meng la nuo (Mln), Qi xian gu (Qxg),
149 Shi yue bai gu (Sybg), Si ma che (Smc), Xi bai gu (Xbg), Xiao gu (Xg), Xiao hua gu

150 (Xhg), Xiao hua nuo (Xhn), Xiao pi gu (Xpg), Ye bai gu (Ybg), Yun hui 290 (Yh 290)
151 and Yun xiang (Yx) (Supplemental Table S1) are paddy rice landraces, all obtained
152 from the Yuanyang Hani's terraced fields, Yunnan Province, China.

153

154 **Drought treatment of rice seedlings**

155 Rice seeds were germinated in water and grown for three weeks, and then the
156 seedlings were transplanted into experimental fields located in Kunming and Jinghong,
157 Yunnan Province, China. The root architectures of rice seedlings grown under
158 irrigation and drought conditions for three months were observed.

159 To observe the root phenotypes of rice seedlings grown under polyethylene
160 glycol-6000 (PEG6000) treatment, rice seeds were surface-sterilized with 70%
161 alcohol for 90 seconds, treated with 2% sodium hypochlorite for 14 minutes, and then
162 washed five times with sterilized water. Seeds were cultured on Murashige-Skoog
163 (MS) medium for two days under dark conditions, and seedlings were then transferred
164 to MS medium containing with or without 15% PEG6000 to simulate drought stress
165 as previously reported (Liu et al., 2017), and they were grown for four days under
166 light conditions.

167

168 **Antibody preparation and immune detection**

169 In order to test subcellular localization of auxin efflux carrier, we conducted an
170 immunocytochemical experiment. To prepare the anti-OsPIN1 and anti-OsPIN2
171 antibodies, the synthetic peptides QSSRNPTPRGSSFNC and QTSREPTPRASSFNC
172 for OsPIN1b (Os02g0743400) and OsPIN2 (Os06g0660200), respectively, were
173 separately injected into rabbit, and the rabbit serum was then purified to obtain the
174 antibodies. All the antibodies were prepared at Huaan Company (Hangzhou Huaan

175 Biotechnology Co., LTD). Rice seeds were germinated and grown on MS medium for
176 2 days in the dark, and the rice seedlings were then transferred to MS medium
177 containing with 15% PEG6000 and grown for 3 days under 12 h light per day. The
178 primary root tips from the rice seedlings were then subjected to whole-mount root
179 immune detection as previously described (Sauer et al., 2006). The primary anti-rabbit
180 OsPIN1 antibody (1:200) and anti-rabbit OsPIN2 antibody (1:200) were used
181 separately to incubate with the rice root tips. The secondary antibody was anti-rabbit
182 IgG Alexa488-conjugated antibody (Jackson Immuno Research) (1:500).

183

184 **Genomic DNA isolation and cloning of the *DRO1* gene, *INDITTO2* and**
185 ***INDITTO4* transposons**

186 Genomic DNA from each of the rice varieties Nipponbare, LTH, Wld, IR64, Kasalath
187 as well as 40 rice varieties collected from the Yuanyang Hani's terraced fields
188 (including Acuce) (Supplemental Table S1) was isolated using the CTAB method. The
189 gene-specific primer pairs Transposon-FP and Transposon-RP, PDI-FP and PDI-RP,
190 Cas9-FP and Cas9-RP and PUV3-R and gRNA-R5 were used to clone the *INDITTO2*/
191 *INDITTO4* transposons, the *INDITTO2* transposon containing a flanking sequence
192 from the partial *DRO1* promoter, *Cas9* and *gRNA* in different rice varieties,
193 respectively (Supplemental Table S2). The PCR mix contained 0.3 μ L of DNA
194 template, 4 μ L of 5 \times Transtart FastPfu Fly buffer, 0.4 μ L of Transtart FastPfu Fly
195 DNA polymerase (TransGen Biotech, Beijing), 1.5 μ L of 2.5 mM dNTPs, and 1.5 μ L
196 of each 10 μ M primer pair. PCR was performed under the following conditions:
197 denaturation at 95°C for 3 minutes, followed by 30 cycles of 95°C for 50 seconds,
198 56°C for 50 seconds and 72°C for 90 seconds, and a final extension at 72°C for 10
199 minutes. The PCR products of the *INDITTO2* and *INDITTO4* transposons were

200 checked using electrophoresis on 2% agarose gels and sent to the Tsingke Company
201 for sequencing.

202

203 **RNA isolation, cDNA synthesis and real-time PCR analysis**

204 Primary roots or leaves derived from rice seedlings that were grown in experimental
205 fields or tissue culture seedlings that were grown on different plates were pooled
206 together. The total RNA from the pooled tissues was isolated with the *EasyPure*[®]
207 Plant RNA kit (TransGen Biotech). To synthesize first-strand cDNA, 100 ng of DNase
208 I-treated RNA, oligo-dT primer and TransScript[®] II One-Step gDNA Removal and
209 cDNA Synthesis Super Mix (TransGen Biotech) were used to perform the reverse
210 transcription reactions. The relative quantitative expression levels of the *DRO1*,
211 *OsYUCCA2a*, *OsYUCCA5b*, *GUS*, *OsPIN1b*, *OsPIN2* and *OsPIN3t* genes were
212 determined using an ABI QuantStudio 7 Flex Real-Time PCR system (Applied
213 Biosystems, USA). The 10 μ L reaction mixture was prepared with 5 μ L PowerUp[™]
214 SYBR[™] Green Master Mix (Thermo Fisher Scientific) containing 0.8 μ L the primer
215 pairs DRO1-rFP and DRO1-rRP, OsYUCCA2a-rFP and OsYUCCA2a-rRP,
216 OsYUCCA5b-rFP and OsYUCCA5b-rRP, GUS-rFP and GUS-rRP, OsPIN1b-rFP and
217 OsPIN1b-rRP, OsPIN2-5FP and OsPIN2-5RP, and OsPIN3t-FP and OsPIN3t-RP
218 (Supplemental Table S2) for *DRO1*, *OsYUCCA2a*, *OsYUCCA5b*, *GUS*, *OsPIN1b*,
219 *OsPIN2* and *OsPIN3t*, respectively, and 0.5 μ L cDNA template. The *actin* gene
220 (GenBank no. AK060893.1) acted as the internal control, and was amplified with the
221 primer pair OsActin-FP and OsActin-RP (Supplemental Table S2). PCR was
222 performed under the following conditions: denaturation at 95°C for 2 minutes,
223 followed by 40 cycles of 95°C for 45 seconds, 56-58°C for 30 seconds and 72°C for 1
224 minute. Three biological replicates were made. The relative expression level was

225 calculated using the $2^{-\Delta\Delta C_t}$ method. SPSS version 19.0 (IBM, Inc., Armonk, NY, USA)
226 was used to analyze the differences in gene expression. $P < 0.05$ indicated a statistical
227 difference, and $P < 0.01$ indicated a statistically significant difference.

228

229 **Results**

230 **Acuce roots showed drought avoidance**

231 To analyze root development in response to drought stress, the *indica* rice Acuce and
232 the *japonica* rice Nipponbare were grown in fields either with irrigation (Figure 1A,
233 Supplemental Figure S1A) or under drought conditions (Figure 1B, Supplemental
234 Figure S1B) conditions. The above-ground parts of Acuce grew better than that of
235 Nipponbare (Figure 1B, Supplemental Figure S1B) under drought stress. Furthermore,
236 Acuce showed a deep-rooting phenotype with a smaller root growth angle (Figure 1G,
237 1I) than Nipponbare (Figure 1C), which had a shallow-root phenotype when grown in
238 fields with irrigation. Acuce also showed a smaller root growth angle (Figure 1H, 1I)
239 than Nipponbare (Figure 1D) when exposed to drought stress. Nipponbare showed a
240 larger root growth angle when grown under drought stress (Figure 1D, 1I) than when
241 under irrigation conditions (Figure 1C, 1I). In contrast, the Acuce root growth angle
242 did not show a significant difference (Figure 1I) between growth under irrigation
243 conditions (Figure 1G) and drought stress (Figure 1H). The root lengths of Acuce
244 (Supplemental Figure S1D, S1H) and Nipponbare (Supplemental Figure S1C, S1G)
245 did not show any significant difference when grown under irrigation conditions
246 (Supplemental Figure S1K). However, under drought stress, Acuce (Supplemental
247 Figure S1F, S1J S1K) had a longer root length than did Nipponbare (Supplemental
248 Figure S1E, S1I, S1K). Overall, Acuce had a higher root fresh weight than
249 Nipponbare (Supplemental Figure S1L). To further investigate the root phenotypes,

250 Acuce and Nipponbare were grown on medium containing 15% PEG6000. Compared
251 with the unstressed control (Supplemental Figure S2A, S2C), root growth was normal
252 in Acuce seedlings (Supplemental Figure S2B, S2E), but the primary root of
253 Nipponbare was shorter than that of the control (Supplemental Figure S2D, S2E).
254 These results demonstrated that the Acuce rice variety is better adapted to drought
255 than Nipponbare, and its root development showed obvious drought avoidance.

256

257 **Acuce roots had high *DRO1* expression**

258 Next, we tested whether the previously identified *DRO1* gene, which is known to be
259 involved in rice drought avoidance (Uga et al., 2013), might underpin this difference
260 between the Acuce and Nipponbare varieties. The Acuce *DRO1* amino acid sequences
261 shared 99.6%, 99.6% and 89.6% identity with the *DRO1* proteins from the rice
262 varieties Kinandang Patong, Nipponbare and IR64, respectively (Supplemental Figure
263 S3). We further analyzed the deduced tertiary structures of the *DRO1* proteins from
264 the rice varieties Acuce, Kinandang Patong, Nipponbare and IR64. The *DRO1* amino
265 acid sequence from Acuce is differs at position 163 from the varieties Nipponbare,
266 Kinandang Patong and IR64 (Supplemental Figure S3); however, the different amino
267 acid did not alter the deduced tertiary structures of the *DRO1* proteins from Acuce,
268 Kinandang Patong and Nipponbare, although that of IR64 was different
269 (Supplemental Figure S4). Next, we tested the transcription of the *DRO1* gene in the
270 primary root, revealing that *DRO1* levels were strongly upregulated in the meristem
271 region but showed no obvious change in the elongation and differentiation zones in
272 Acuce grown under drought stress (Supplemental Figure S2F). However, *DRO1*
273 transcription was not altered in Nipponbare (Supplemental Figure S2F). These
274 observations show that the drought avoidance in Acuce correlates with the specific

275 capability of this variety to upregulate *DROI* transcription in the root meristem region
276 in response to drought stress.

277

278 ***DROI* mutation altered the root architecture**

279 To test whether the *DROI* gene was relevant to the drought-mediated changes in
280 Acuce root development, we obtained *dro1-cc* mutant lines using the CRISPR/Cas9
281 method. In the Acuce *dro1-cc* mutant, one additional nucleotide, thymine (T), was
282 inserted into the second exon, thereby altering the open reading frame and leading to
283 the pre-terminated translation of DRO1 protein (Supplemental Figure S5A, S5B).
284 When the Acuce homozygous *dro1-cc* mutant was grown in a greenhouse with
285 irrigation, we found that compared with wild-type plants (Supplemental Figure S6A),
286 it showed shallow root (Supplemental Figure S6A) and short root length phenotypes
287 (Supplemental Figure S6B). The expression levels of *OsPIN1b* and *OsPIN3t* were
288 upregulated and downregulated, respectively, but the level of *OsPIN2* showed no
289 obvious change in the Acuce *dro1-cc* mutant root (Supplemental Figure S6C). These
290 results suggested the involvement of *DROI* in regulating auxin transport in root
291 growth.

292 *DROI* is a member of the IGT family (Dardick et al., 2013; Guseman et al., 2017).
293 To further analyze the role of *DROI* in root growth, we searched the IGT family
294 genes and *DROI* homologues in Nipponbare, including the *OsLAZY1*, *OsTAC1* and
295 *qSOR1* genes, which contain IGT and EAR-like motifs (Supplemental Figure S7). The
296 expression analysis of IGT family genes revealed low expression levels of *OsLAZY1*,
297 *OsTAC1* and *qSOR1*, but high expression levels of *DROI* in rice roots (Supplemental
298 Figure S8). Next, we generated Nipponbare *dro1-cc* mutants using the CRISPR/Cas9
299 method (Supplemental Figure S9). We obtained 11 *dro1-cc* mutant lines and randomly

300 selected 3 lines (#5, #10 and #17) to analyze the root phenotype. These T2 *dro1-cc*
301 lines showed a shorter root length than the original Nipponbare variety (Figure 2F).
302 When the homozygous rice *dro1-cc* line #17, in which the CRISPR cassette Cas9 was
303 selected out (Supplemental Figure S10), was grown under irrigation conditions, it
304 showed a shallower root phenotype (Figure 1E) than wild-type Nipponbare (Figure
305 1C, 1D), with a significantly larger root growth angle (Figure 1I). However, when line
306 #17 was grown under drought stress (Figure 1F), it was small (Figure 1B) and had a
307 shallow root phenotype (Figure 1F, 1I). When the rice seedlings were grown in MS
308 medium supplemented either without (Supplemental Figure S11A, S11C) or with
309 (Supplemental Figure S11B, S11D) 15% PEG6000, both Nipponbare and *dro1-cc*
310 (#17) rice seedlings showed shorter root lengths under drought stress compared with
311 the control (Supplemental Figure S11E). Additionally, the *dro1-cc* (#17)
312 (Supplemental Figure S11C, S11E) seedlings also showed a shorter root length than
313 the wild-type (Supplemental Figure S11A, S11E) when grown on MS medium.

314 We then determined the expression levels of the auxin biosynthesis genes
315 *OsYUCCA2a* and *OsYUCCA5b* in the Nipponbare *dro1-cc* (#17) mutant grown under
316 drought stress. Under drought conditions, the *OsYUCCA5b* gene was upregulated, but
317 the levels of *OsYUCCA2a* were not obviously different in wild-type Nipponbare and
318 the *dro1-cc* (#17) mutant (Supplemental Figure S12). When seedlings of wild-type
319 Nipponbare and the *dro1-cc* (#17) mutant were grown on MS medium supplemented
320 with 15% PEG6000 plus either DMSO (as a control) (Supplemental Figure S13A,
321 S13C) or 1 μ M auxin biosynthesis inhibitor L-Kynurenine (Kyn) (He et al., 2011)
322 (Supplemental Figure S13B, S13D), both wild-type and *dro1-cc* (#17) mutant
323 seedlings had longer root lengths (Supplemental Figure S13E). These data suggest
324 that *DROI* does not function to regulate auxin biosynthesis.

325 Root architecture is largely determined by auxin and, in particular, by polarized
326 auxin transport, which is dependent on PIN auxin exporters (Adamowski & Friml,
327 2015; Benkova et al., 2003). Therefore, we analyzed the influence of DRO1 activity
328 on PIN expression. Under drought conditions, expression levels of *OsPIN1b* were
329 downregulated in wild-type seedlings but were unchanged in the *dro1-cc* (#17) mutant,
330 expression levels of *OsPIN2* were unchanged in the wild-type seedlings and
331 upregulated in the *dro1-cc* (#17) mutant, and expression levels of *OsPIN3t* were
332 downregulated in the wild-type but upregulated in the *dro1-cc* (#17) mutant
333 (Supplemental Figure S11F). To further investigate whether mutation of *DRO1*
334 disturbed auxin transport, we checked the root phenotype during growth under gravity
335 stimulation. The results showed that the root of *dro1-cc* (#17), which had a larger
336 gravitropic curvature than the wild-type (Supplemental Figure S14E), was associated
337 with a disturbance in auxin transport (Supplemental Figure S14F). Compared with the
338 larger root growth angle in the wild-type treated with auxin grown under gravitropic
339 stimulation (Supplemental Figure S14C, S14E), the primary root growth angle is
340 smaller in the *dro1-cc* (#17) mutant treated with auxin (Supplemental Figure S14D,
341 S14E) and did not show significant difference compared with wild-type treated with
342 DMSO (Supplemental Figure S14E). We further investigated the subcellular
343 localization of OsPIN1b and OsPIN2 in the root meristem region of the *dro1-cc* (#17)
344 mutant grown in MS medium supplemented either without or with 15% PEG6000.
345 Compared with the wild-type grown under drought stress (Figure 3B, 3I), the
346 subcellular localization of OsPIN1b did not obviously change on the plasma
347 membrane in *dro1-cc* (#17) (Figure 3D, 3I), and OsPIN2 showed reduced localization
348 in the plasma in both the wild-type (Figure 3F, 3I) and *dro1-cc* (#17) (Figure 3H, 3I)

349 grown under drought stress. These results show that mutation of *DROI* disturbs auxin
350 transport.

351

352 **Auxin differentially regulates *DROI* transcription in Acuce and Nipponbare**

353 Auxin is known to negatively regulate the expression of *DROI* (Uga et al., 2013).
354 Therefore, we tested the potential auxin-mediated regulation of *DROI* expression in
355 Nipponbare and Acuce. Rice seedlings were treated with 0.01 μ M, 0.1 μ M and 1 μ M
356 NAA and 2,4-D (Supplemental Figure S15). An increased auxin concentration
357 inhibited the primary root length (Supplemental Figure S15M, S15N). The expression
358 levels of *DROI* increased following 0.01 μ M NAA and 2,4-D treatment in Acuce, and
359 decreased following treatment with higher concentrations of auxin (Supplemental
360 Figure S15O, S15P). In contrast, in Nipponbare, no such transcription increase was
361 observed following either treatment with 0.01 μ M NAA and 2,4-D or with higher
362 concentrations of auxin (Supplemental Figure S15O, S15P). These results suggest that
363 in Acuce, auxin has the capacity to regulate *DROI* expression.

364 We next conducted the complementary experiment and treated rice seedlings with
365 the auxin biosynthesis inhibitor Kyn. The primary roots of Acuce and Nipponbare
366 were obviously longer compared to the untreated control following treatment with
367 increasing concentrations of Kyn (Supplemental Figure S16A-I). Notably, Acuce was
368 more sensitive than Nipponbare to Kyn treatment, as 20 μ M Kyn could induce a
369 longer root length in Acuce but not in Nipponbare (Supplemental Figure S16I). In
370 addition, *DROI* gene expression was upregulated when Acuce was treated with higher
371 concentrations of 30 μ M Kyn, this is in contrast to the unchanged *DROI* expression
372 levels in Nipponbare following treatment with Kyn (Supplemental Figure S16J).
373 These data show a pronounced difference in auxin sensitivity between the Acuce and

374 Nipponbare rice varieties; both at the level of root growth and the regulation of *DROI*
375 gene expression.

376

377 **The *DROI* promoter in Acuce and many other rice varieties contains the**
378 ***INDITTO2* transposon**

379 To investigate the possible mechanism of the *DROI*-dependent differences in drought
380 avoidance and auxin-mediated *DROI* transcription regulation in Acuce, we compared
381 its *DROI* promoter to those of the varieties IR64, Nipponbare and Kinandang Patong
382 (Supplemental Figure S17). We found that the *DROI* promoters of Acuce and IR64
383 contained an additional 266 nucleotides (Supplemental Figure S17). We analyzed this
384 sequence with online software (www.repeatmasker.org, www.girinst.org) and found
385 that it shared 93.2% identity with the *INDITTO* transposon, which is a
386 non-autonomous DNA transposon belonging to the *Tourist* superfamily (Jiang &
387 Wessler, 2002). Therefore, we named the sequence inserted in the *DROI* promoter as
388 the *INDITTO2* transposon.

389 We conducted a BLAST search in the NCBI database (www.ncbi.nlm.nih.gov)
390 using the sequence of the *INDITTO2* transposon. Interestingly, a rice Teqing
391 homologue sequence was located between two genes that encoded a putative
392 ADP-glucose pyrophosphorylase subunit SH2 (GenBank no. AAB58473.1) and a
393 putative NADPH-dependent reductase A1 (GenBank no. AAB58474.1)
394 (Supplemental Figure S18A). Further analysis of this new sequence with online
395 software (www.repeatmasker.org, www.girinst.org) showed that it also belonged to
396 the *Tourist* family and shared 93.6% and 97.7% identity with the *INDITTO* and
397 *INDITTO2* transposons, respectively (Supplemental Figure S18B). Thus, we named
398 the sequence as *INDITTO3* transposon (Supplemental Figure S18A, S18B). Because

399 no homologues of *INDITTO2* were found in the *DROI* promoter region in
400 Nipponbare (Supplemental Figure S17), we further amplified the *INDITTO2*
401 transposon in the Nipponbare genome using PCR. An *INDITTO2* homologue was
402 found in the Nipponbare genome, and we named it *INDITTO4* (Supplemental Figure
403 S18B). *INDITTO4* is inserted in yet another different locus, and its sequence shared
404 95.1% and 95.5% identity with *INDITTO* and *INDITTO2*, respectively (Supplemental
405 Figure S18B). We then conducted a BLAST search using the *INDITTO4* sequence in
406 the Nipponbare genome. A total of 94 homologues of the *INDITTO4* gene were found
407 in the Nipponbare genome, of which 15 *INDITTO4* homologues were inserted into
408 known gene regions, and 12.76% genes contained an ARE (Supplemental Table S3).
409 These findings suggest that *INDITTO* transposons and its homologues can jump
410 around the rice genome and can potentially disrupt or regulate different loci.

411 To further characterize the *INDITTO2* transposon in the rice genome, we cloned
412 *INDITTO2* from the *DROI* promoter region in 45 rice lines, including IR64, Kasalath,
413 LTH, Nipponbare, Wld and 40 rice varieties collected from the Yuanyang Hani's
414 terraced fields, with gene-specific primers PDI-FP and PDI-RP using PCR
415 (Supplemental Figure S19A). We found that from 45 rice lines investigated, there
416 were 40 lines in which the homologues of the *INDITTO2* transposon could be
417 detected in the *DROI* promoter region (Supplemental Figure S19B) and show high
418 sequence conservation (Supplemental Figure S20). A BLAST search of publicly
419 available sequences further revealed that the rice varieties Shuhui498 and RP Bio-226
420 contained the *INDITTO2* transposon in the *DROI* promoter (Supplemental Figure
421 S20). These results show that the *DROI* promoter regions of many rice varieties,
422 including Acuce, contain the *INDITTO2* transposon. A phylogenetic analysis showed
423 that the *INDITTO2* transposon and its homologues formed two main subgroups,

424 which contain with or without AREs, and that these subgroups are distinct from those
425 of the *INDITTO*, *INDITTO3*, *INDITTO4* and its homologues from the different rice
426 varieties (Supplemental Figure S21).

427

428 **Presence of *INDITTO2* transposon conveys auxin-responsiveness to *DROI***
429 **expression**

430 The presence of the *INDITTO2* transposon in the *DROI* promoter of Acuce but not
431 Nipponbare (Supplemental Figure S17) provides a potential mechanism for the
432 differential *DROI* transcription regulation between these two rice varieties. Sequence
433 analysis showed that the Acuce *INDITTO2* transposon contained an ARE
434 (Supplemental Figure S17) and various transcription factor binding sites, including
435 those related to the BBR-BPC, HD-ZIP, C2H2, HD-ZIP, bZIP and the MYB-related
436 families (Supplemental Table S4). In addition, the *INDITTO2* homologue in nine of
437 the studied rice varieties (Shuhui498, RP Bio-226, Bg, Qxg, Cz, Cj, Xhn, Xhg and
438 Kasalath) contained an ARE (Supplemental Figure S20). Three further AREs also
439 occur in the *DROI* promoter outside the *INDITTO2* sequence (Supplemental Figure
440 S17).

441 The *INDITTO2* transposon contained various transcription factor binding sites
442 (Supplemental Table S4). We constructed different expression vectors to study the
443 role of the *INDITTO2* transposon in the regulation of *DROI* transcription by auxin
444 (Supplemental Figure S22A). We placed the *GUS* reporter gene under the *DROI*
445 promoter of Acuce and Nipponbare with or without the *INDITTO2* transposon
446 (Supplemental Figure S22A) and infiltrated it into tobacco leaves using an
447 *Agrobacterium tumefaciens*-mediated method. The full-length *DROI* promoter from
448 Acuce conveyed stronger *GUS* expression than the Acuce *DROI* promoter without the

449 *INDITTO2* transposon (Supplemental Figure S22B). In addition, deletion of the ARE
450 in the *INDITTO2* transposon from the Acuce *DROI* promoter also resulted in the
451 downregulation of its activity (Supplemental Figure S22B). This result implies that
452 the *INDITTO2* transposon containing the ARE is involved in the regulation of gene
453 expression. Consistent with this result, the level of the *GUS* gene controlled by the
454 Nipponbare *DROI* promoter was lower than that of the *GUS* transcribed by the Acuce
455 *DROI* promoter (Supplemental Figure S22C). However, when the *INDITTO2*
456 transposon was inserted into the Nipponbare *DROI* promoter, the expression level of
457 *GUS* was obviously upregulated (Supplemental Figure S22C).

458

459 **The *INDITTO2* transposon acts as an auxin-responsive promoter**

460 To further investigate the potential promoter function of the *INDITTO2* transposon,
461 we placed the *INDITTO2* transposon only (without the genomic context of the *DROI*
462 promoter) upstream of the *GUS* gene. Compared with the expression under the control
463 of the Acuce *DROI* promoter, *GUS* expression controlled by the *INDITTO2*
464 transposon was upregulated (Supplemental Figure S22D). However, when *GUS*
465 transcription was controlled by the *INDITTO2* transposon without the ARE, its
466 activity was obviously downregulated compared with that of the full-length
467 *INDITTO2* (Supplemental Figure S22D). These findings suggest that the *INDITTO2*
468 transposon exerts promoter activity that depends on the presence of the ARE.

469 Next, we tested whether the promoter activity of the *INDITTO2* transposon was
470 responsive to auxin. Exogenous NAA (1 μ M) was added to a solution of the
471 *Agrobacterium tumefaciens* strain EHA105 containing a full-length *INDITTO2*
472 transposon construct and infiltrated into tobacco leaves. *GUS* expression was
473 obviously upregulated relative to the untreated control (Supplemental Figure S22D).

474 Furthermore, *GUS* transcription controlled by the *INDITTO2* transposon with the
475 ARE deletion did not obviously respond to auxin treatment (Supplemental Figure
476 S22D). Taken together, these results show that the *INDITTO2* transposon exerts
477 auxin-regulated promoter activity.

478 To further investigate the role of the *INDITTO2* transposon regulated by auxin in
479 the *DROI* promoter, *Agrobacterium* strains EHA105 containing the *GUS* gene fused
480 to either the whole Acuce *DROI* promoter or with the *INDITTO2* transposon deleted
481 were infiltrated into tobacco leaves. The *GUS* expression levels were found to be
482 downregulated under NAA treatment (Supplemental Figure S22E). When the whole
483 Nipponbare *DROI* promoter or the promoter containing the *INDITTO2* transposon
484 were fused with the *GUS* gene and transiently expressed in tobacco leaves, both
485 constructs resulted in lower levels of *GUS* gene expression under NAA treatment
486 (Supplemental Figure S22F). However, when the whole Acuce *DROI* promoter with
487 ARE deletion in the *INDITTO2* transposon fused with the *GUS* gene was expressed in
488 tobacco leaves, the *GUS* gene expression levels were upregulated under NAA
489 treatment (Supplemental Figure S22E).

490 Three elements located in the *DROI* promoter can respond to auxin treatment (Uga
491 et al., 2013). To further determine the effect of these three elements in responding to
492 auxin treatment, we constructed two expression vectors containing the Acuce or
493 Nipponbare *DROI* promoter with the three AREs deleted and fused with the *GUS*
494 gene (Supplemental Figure S22A). When these two constructs were expressed in
495 tobacco leaves under NAA treatment, the expression levels of the *GUS* gene were
496 downregulated in the Acuce construct but upregulated in the Nipponbare construct
497 compared with the control without NAA treatment (Supplemental Figure S22G).

498 We further investigated the role of the *INDITTO2* transposon in regulating the
499 expression of the *DRO1* gene in rice seedlings. The *DRO1* promoter of Nipponbare
500 was inserted with the *INDITTO2* transposon containing with or without ARE and
501 fused with the genomic *DRO1* gene of Nipponbare (Figure 4A). A solution of *A.*
502 *tumefaciens* strain EHA105 transformed with the expression vector (Figure 4A) and
503 containing 30 μ M Kyn was used to infiltrate the rice leaf veins (Figure 4B).
504 Compared with the control, the *DRO1* gene expression transcribed under the
505 Nipponbare *DRO1* promoter containing the whole *INDITTO2* transposon was
506 obviously upregulated in rice leaves (Figure 4C), and this was in contrast to the
507 expression pattern of the *GUS* gene transcribed under Acuce *DRO1* or Nipponbare
508 *DRO1* containing the *INDITTO2* transposon and induced with 1 μ M NAA
509 (Supplemental Figure S22E, S22F). However, the *DRO1* gene expression transcribed
510 under the Nipponbare *DRO1* promoter containing the *INDITTO2* transposon with the
511 ARE deletion was obviously downregulated (Figure 4C), and this was in contrast to
512 the expression levels of the *GUS* gene transcribed under the Acuce *DRO1* promoter
513 carrying the *INDITTO2* transposon with the ARE deletion induced with 1 μ M NAA
514 (Supplemental Figure S22E). These results show that the ARE of the *INDITTO2*
515 transposon plays an important role in the transcriptional activity of the *DRO1*
516 promoter regulated by auxin.

517

518 **The *INDITTO2* transposon is sufficient to promote Nipponbare drought** 519 **avoidance**

520 The rice variety Nipponbare showed low drought avoidance correlating with low and
521 auxin-insensitive expression of *DRO1* (Figure 1, Supplemental Figure S2, S15). To
522 test whether the *INDITTO2* transposon, which can convey auxin regulation of *DRO1*,

523 would be sufficient to induce *DROI* transcription and enhance rice drought avoidance,
524 we obtained 11 transgenic Nipponbare rice lines expressing the *INDITTO2* transposon.
525 The *INDITTO2* transposon was inserted into the *DROI* promoter of Nipponbare
526 (Supplemental Figure S23A), and the insertion position of the *INDITTO2* transposon
527 was the same as that in the *DROI* promoter of Acuce (Supplemental Figure S17). The
528 T1 transgenic Nipponbare lines containing the *INDITTO2* transposon were verified by
529 PCR, and lines #8, #11, and #14 were grown on MS medium containing with 15%
530 PEG6000. These transgenic rice lines expressing the whole *INDITTO2* transposon
531 showed drought avoidance accompanied by an unchanged root length (Supplemental
532 Figure S23C-E, S23G-I, S23J) and upregulated *DROI* expression levels in the root
533 tips (Supplemental Figure S23K). Compared with the control grown under irrigation
534 conditions (Figure 5B-D, 5J-L), the T2 transgenic Nipponbare lines (#1, #4, and #8)
535 grown under drought stress (Figure 5F-H, 5N-P) did not show an obvious difference
536 in root growth angle (Figure 5Q) or root length (Figure 5R); however, the wild-type
537 Nipponbare showed a larger root growth angle (Figure 5Q) and a shorter root length
538 (Figure 5R). When the Nipponbare *DROI* gene containing the *INDITTO2* transposon
539 in the Nipponbare *DROI* promoter (Supplemental Figure S23A) was transformed into
540 the Nipponbare *dro1-cc* (#17) mutant (Figure 2E-F), the T1 rescued rice mutant lines
541 (#1, #5, #6, and #20) showed a longer root length compared with the wild-type
542 Nipponbare (Figure 2F). These results show that rice variety with the presence of the
543 *INDITTO2* transposon in the *DROI* locus is sufficient for enhancing drought
544 avoidance and better adaptation to drought stress.

545

546 **The *INDITTO2* transposon shows functional diversity in rice adaptation to**
547 **drought stress**

548 The *INDITTO2* transposon is involved in the regulation of *DROI* expression. We
549 next investigated root development of the rice varieties containing the *INDITTO2*
550 transposon under drought stress. We randomly selected rice varieties Kasalath and
551 Xhn, which contained the *INDITTO2* transposon with an ARE (Supplemental Figure
552 S20), and the rice varieties Knhl and Azg, which contained the *INDITTO2* transposon
553 but without ARE (Supplemental Figure S20). These four rice varieties were grown on
554 MS medium supplemented with 1 μ M NAA (Supplemental Figure S24A-H).
555 Compared with the control (Supplemental Figure S24A-D), the primary root lengths
556 of the seedlings treated with NAA were significantly shorter than those in the control
557 (Supplemental Figure S24I), and the expression levels of *DROI* were downregulated
558 in the varieties Kasalath and Xhn, unchanged in Knhl, but upregulated in the variety
559 Azg (Supplemental Figure S24J). However, when these rice varieties were grown on
560 MS medium containing with 15% PEG6000 (Supplemental Figure S25E-H), Kasalath,
561 Xhn and Knhl showed shorter primary root length, but that of Azg was not obviously
562 changed (Supplemental Figure S25I) compared with the control grown on MS
563 medium without 15% PEG6000 (Supplemental Figure S25A-D). Furthermore, the
564 expression levels of *DROI* were downregulated in Kasalath, unchanged in Xhn and
565 Knhl, but upregulated in Azg (Supplemental Figure S25J). When the four rice
566 varieties were grown in the field, compared with the control (grown with irrigation),
567 Kasalath and Xhn showed no change in root growth angles, but Knhl and Azg had
568 larger root growth angles when the rice seedlings were grown under drought stress
569 (Supplemental Figure S26I). However, compared with the control grown with
570 irrigation, Kasalath, Knhl and Azg had shorter root lengths, while Xhn did not have
571 obvious change in root length when the rice seedlings grown under drought stress
572 (Supplemental Figure S26J). This demonstrates that Xhn has a deep root phenotype

573 and that the varieties Kasalath, Knhl and Azg have a shallow root phenotype. When
574 we further analyzed this correlation between root length and root growth angle,
575 compared with seedlings grown in an irrigated field (Supplemental Figure S27A,
576 S27C, S27E, S27G), we found a significant negative correlation in both rice Xhn and
577 Knhl (Supplemental Figure S27D, S27F), no significant negative correlation in
578 Kasalath (Supplemental Figure S27B), and a positive correlation tendency in the
579 variety Azg (Supplemental Figure S27H). These results suggest that the *INDITTO2*
580 transposon is able to regulate the transcription of the *DROI* gene in a mechanism
581 mediated by auxin to enable plants to adapt to drought stress, but this effect varies
582 among the different rice genetic backgrounds.

583

584 **Discussion**

585 Rice is a worldwide crop with several different subspecies, including the *japonica* and
586 *indica*. However, drought, an important abiotic stress, may alter rice seedling
587 development and reduce crop quality and yields. Various rice cultivars exist differing
588 genetic background and plant morphogenesis (for example in root architecture) to
589 drive important adaptation in drought stress (Uga et al., 2013). In this study, we found
590 that rice drought avoidance can be enhanced through *INDITTO2* transposon-mediated
591 promoter activity and conveyed auxin-dependent transcriptional regulation of the
592 *DROI* gene.

593 Rice varieties with increased *DROI* expression had deeper root phenotypes and
594 increased root lengths than transgenic rice lines with *DROI* mutation. Furthermore,
595 *DROI* is involved in the regulation of auxin distribution and the subcellular
596 localization of the auxin transporter OsPIN1b. Furthermore, an *INDITTO2* transposon
597 inserted into the *Acuce DROI* promoter could react to auxin and show promoter

598 activity, and the transgenic Nipponbare line with an *INDITTO2* insertion in the *DROI*
599 promoter region showed enhanced drought avoidance. These observations suggest
600 that *DROI* interacts with auxin to control rice drought avoidance. *INDITTO2* conveys
601 the auxin signal to mediate *DROI* activity, thus providing a mechanism by which rice
602 can adapt to environmental drought stress.

603 During drought stress, auxin plays an important role in rice root growth. *DROI* is
604 an early auxin-response gene and is a member of the IGT family (Uga et al., 2013),
605 which controls plant architecture by forming an asymmetric auxin distributions (Dong
606 et al., 2013; Godbole et al., 1999; Li et al., 2007; Taniguchi et al., 2017; Yoshihara &
607 Iino, 2007; Yoshihara & Spalding, 2017; Yoshihara et al., 2013). In the current study,
608 mutation of *DROI* disturbed the localization and levels of the auxin efflux carrier
609 (Figure 3, Supplemental Figure S11) as well as the auxin content (Supplemental
610 Figure S14). Therefore, it was plausible that the effect of *DROI* on drought avoidance
611 was related to auxin transport. The *DROI* gene showed higher expression levels than
612 those of the other IGT family members expressed in the roots (Supplemental Figure
613 S8), which suggests that the *DROI* gene is the main regulating factor altering root
614 architecture in the control of root drought avoidance. A previous research shows that
615 auxin can negatively regulate the level of *DROI* gene (Uga et al., 2013), whereas, we
616 found that auxin could not negatively regulate the levels of *DROI* gene in certain rice
617 varieties (Supplemental Figure S24J), which implies that the role of auxin in
618 regulating the expression levels of *DROI* is dependent on the rice genetic
619 background.

620 Transposons are involved in various aspects of plant growth, including rapeseed
621 vernalization (Hou et al., 2012), potato tuber skin colour (Momose et al., 2010), rice
622 glume development and maize latitudinal adaptation (Huang et al., 2018; Nakazaki et

623 al., 2003). The rice variety IR64 has low drought avoidance resulting from a single
624 adenine nucleotide deletion in exon 4 of the *DROI* gene (Uga et al., 2013). The
625 deduced tertiary structure of Nipponbare *DROI* was not different from that of the
626 variety Acuce (Supplemental Figure S4), but that Nipponbare was sensitive to drought
627 stress while Acuce was not (Figure 1). However, given that the *INDITTO2* transposon
628 conveyed the auxin signal to regulate the transcription of the *DROI* gene (Figure 4C)
629 and promoted Nipponbare drought avoidance (Figure 5), it is plausible that drought
630 avoidance is regulated through a mechanism by which *INDITTO2* impacts on the
631 *DROI* gene, and that high levels of *DROI* are necessary for rice adaptation to drought
632 stress. However, we also noticed that the root growth phenotypes of the rice varieties
633 Xhn and Azg (Supplemental Figure S26I) were not consistent with the expression of
634 *DROI* gene when rice were grown under drought stress (Supplemental Figure S25J).
635 This suggests that unknown factors associated with the particular genetic background
636 of the variety may be involved in the regulation of drought avoidance mediated by
637 *DROI*. The *INDITTO2* transposon was found to be present in the *DROI* promoter of
638 the various rice varieties (Supplemental Figure S18, S20) and could be detected in
639 different loci of the Nipponbare genome (Supplemental Table S3). Thus, the
640 *INDITTO2* transposon increased rice genetic diversity and was enable it to adapt to
641 different abiotic stresses, including drought stress, during rice development.

642 The impact of the *INDITTO2* transposon on regulation of *DROI* is similar to that of
643 certain other transposons, which have been proposed to regulate transcription of
644 *BnFLC.A10* and *ABP1* (Elrouby & Bureau, 2000, 2012; Huang et al., 2018). However,
645 the *INDITTO2* and its homologues were found both with or without AREs and
646 putative transcription factor binding sites (Supplemental Figure S20, Supplemental
647 Table S4), which is similar to the role of *siR441* and *siR446* derived from *Stowaway1*

648 transposon to regulate ABA signalling (Yan et al., 2011). Therefore, the *INDITTO2*
649 transposon functions as an auxin-inducible promoter, which as described in *PdMLE1*
650 transposon (Sun et al., 2013), and an alternative auxin signalling pathway might
651 regulate *INDITTO2*-mediated drought avoidance. However, the *INDITTO2* could not
652 induce upregulation of *DRO1* genes in certain rice varieties under drought stress
653 (Supplemental Figure S25J). Furthermore, the four AREs that are located in the *DRO1*
654 promoter region and the *INDITTO2* transposon show different patterns when
655 responding to the transcriptional activity of the *DRO1* promoter under auxin treatment
656 (Figure 4, Supplemental Figure S22). These findings suggest that the functional
657 differences of AREs may contribute to the differential roles of *DRO1* gene in the
658 responses of rice to drought stress, and the rice genetic diversity is an important factor
659 for the role of *INDITTO2* in regulating gene expression profile.

660 The *INDITTO2* transposon was identified from the variety Acuce as well as certain
661 rice landraces collected from the Yuanyang Hani's terraced fields, and which grow on
662 terraced fields at altitudes of 1600-2000 m. This implies that the *INDITTO2*
663 transposon, jumping to different positions in the rice genome, can function as an
664 auxin-regulated promoter to accelerate the evolution of developmental and
665 physiological traits in different rice species, and its presence is sufficient to convey
666 plant adaptation under different environmental stresses in agricultural production.

667 In summary, the *INDITTO2* transposon and its homologues are found widely
668 throughout the rice genomes and are able to convey auxin-mediated *DRO1*
669 transcription to enhance rice drought avoidance through an as yet undiscovered
670 mechanism as shown in a putative model (Supplemental Figure S28). The *INDITTO2*
671 transposon and its homologues increase the rice genetic diversity and may enable it to
672 adapt to different environmental stresses.

673

674 **Acknowledgments**

675 We thank Professor Jianqiang Wu (Kunming Institute of Botany, Chinese Academy of
676 Sciences) for providing generous support for the IAA measurements. This work was
677 supported by grants from the National Natural Science Foundation of China (Grant
678 Nos. 31460453, 31660501, 31860064 and 31470382), the Major Special Program for
679 Scientific Research, Education Department of Yunnan Province (Grant No.
680 ZD2015005), SRF for ROCS, SEM (Grant No. [2013] 1792), the Major Science and
681 Technique Programs in Yunnan Province (Grant No. 2016ZF001), the Key Projects of
682 Applied Basic Research Plan of Yunnan Province (Grant No. 2017FA018), the
683 Earmarked Fund for Modern Agro-industry Technology Research System (Grant No.
684 CARS-21), the National Key Research Development Program of China
685 (2016YFD0100600), the Program for Innovative Research Team in University of
686 Yunnan Province (IRTSTYN), and the European Research Council (ERC) under the
687 European Union's Horizon 2020 Research and Innovation Programme (Grant
688 Agreement No. 742985).

689

690 **Conflict of Interest Statement**

691 The authors declare that they have no competing interests.

692

693 **Accession numbers**

694 Sequence data for the *Acuce DROI* and *Nipponbare DROI*, *qSOR1*, *OsLAZY1* and
695 *OsTAC1* genes described in this study can be found in the NCBI database under the
696 following accession numbers: MH939159, Os09g0439800, Os07g0614400,
697 Os11g0490600 and Os09g0529300, respectively.

698

699 **Authorship**

700 Y.D. conceived the original screening and research plans; Y.D. supervised the
701 experiments; Y.Z., L-X.W., Q.F., D.W., J.L., B.Y., S.Y., L.J., J.Q., X.Z., L.H., S.Z.,
702 C.M., Y-F.Z., C-Y.L., Q.D., S.L., L.Z., X.J., Y.L., H.L., and K.L. performed the
703 majority of the experiments; Y.D., J.Y., Q.L., L.L., S.P., H.H., Z.Z., C.L., L.W., C.L.,
704 X.H., and J.F. provided technical assistance to Y.Z., L-X.W., Q.F., D.W., J.L., B.Y.,
705 S.Y., S.Y., L.J., J.Q., X.Z., L.H., S.Z., C.M., Y-F.Z., C-Y.L., Q.D., S.L., L.Z., X.J.,
706 Y.L., H.L., and K.L.; Y.D., Y.Z., L-X.W., and Q.F. designed the experiments and
707 analysed the data; Y.D. conceived the project and wrote the article with contributions
708 from all the authors; Y.D. and J.F. supervised and completed the manuscript writing.
709 Y.D. agrees to serve as the author responsible for contact and will ensure
710 communication.

711

712 **Data Availability Statement**

713 The data that supports the findings of this study are available in the supplementary
714 material of this article.

715

716 **References**

- 717 Adamowski, M., & Friml, J. (2015). PIN-dependent auxin transport: action,
718 regulation, and evolution. *Plant Cell*, 27(1), 20-32.
- 719 Arai-Sanoh, Y., Takai, T., Yoshinaga, S., Nakano, H., Kojima, M., Sakakibara, H.,
720 Kondo, M., & Uga, Y. (2014). Deep rooting conferred by DEEPER
721 ROOTING 1 enhances rice yield in paddy fields. *Scientific Reports*, 4, 5563.
- 722 Ashraf, A., Rehman, O. U., Muzammil, S., Léon, J., Naz, A. A., Rasool, F., Ali, G.

723 M., Zafar, Y., & Khan, M. R. (2019). Evolution of Deeper Rooting 1-like
724 homoeologs in wheat entails the C-terminus mutations as well as gain and loss
725 of auxin response elements. *Plos One*, *14*(4), e0214145.

726 Benková, E., Michniewicz, M., Sauer, M., Teichmann, T., Seifertová, D., Jürgens, G.,
727 & Friml, J. (2003). Local, efflux-dependent auxin gradients as a common
728 module for plant organ formation. *Cell*, *115*(5), 591-602.

729 Bureau, T. E., Ronald, P. C., & Wessler, S. R. (1996). A computer-based systematic
730 survey reveals the predominance of small inverted-repeat elements in
731 wild-type rice genes. *Proceedings of the National Academy of Sciences of the*
732 *United States of America*, *93* (16), 8524-8529.

733 Bureau, T. E., & Wessler, S. R. (1992). Tourist: a large family of small inverted
734 repeat elements frequently associated with maize genes. *Plant Cell*, *4*(10),
735 1283-1294.

736 Bureau, T. E., & Wessler, S. R. (1994). Mobile inverted-repeat elements of the
737 Tourist family are associated with the genes of many cereal grasses.
738 *Proceedings of the National Academy of Sciences of the United States of*
739 *America*, *91*(4), 1411-1415.

740 Chen, Y. N., Fan, X. R., Song, W. J., Zhang, Y. L., & Xu, G. H. (2012).
741 Over-expression of OsPIN2 leads to increased tiller numbers, angle and
742 shorter plant height through suppression of OsLAZY1. *Plant Biotechnology*
743 *Journal*, *10*(2), 139-149.

744 Dardick, C., Callahan, A., Horn, R., Ruiz, K. B., Zhebentyayeva, T., Hollender, C.,
745 Whitaker, M., Abbott, A., & Scorza, R. (2013). PpeTAC1 promotes the
746 horizontal growth of branches in peach trees and is a member of a functionally
747 conserved gene family found in diverse plants species. *Plant Journal*, *75*(4),

748 618-630.

749 Dong, Z. B., Jiang, C., Chen, X. Y., Zhang, T., Ding, L., Song, W. B., Luo, H. B., Lai,
750 J. S., Chen, H. B., Liu, R. Y., Zhang, X. L., & Jin, W. W. (2013). Maize
751 LAZY1 mediates shoot gravitropism and inflorescence development through
752 regulating auxin transport, auxin signaling, and light response. *Plant*
753 *physiology*, *163*(3), 1306-1322.

754 Elrouby, N., & Bureau, T. E. (2000). Molecular characterization of the Abp1 5
755 '-flanking region in maize and the teosintes. *Plant physiology*, *124*(1),
756 369-377.

757 Elrouby, N., & Bureau, T. E. (2012). Modulation of auxin-binding protein1 gene
758 expression in maize and the teosintes by transposon insertions in its promoter.
759 *Molecular Genetics and Genomics*, *287*(2), 143-153.

760 Godbolé, R., Takahashi, H., & Hertel, R. (1999). The *lazy* mutation in rice affects a
761 step between statoliths and gravity-induced lateral auxin transport. *Plant*
762 *Biology*, *1*(4), 379-381.

763 Guseman, J. M., Webb, K., Srinivasan, C., & Dardick, C. (2017). DRO1 influences
764 root system architecture in *Arabidopsis* and *Prunus* species. *Plant Journal*,
765 *89*(6), 1093-1105.

766 He, W. R., Brumos, J., Li, H. J., Ji, Y. S., Ke, M., Gong, X. Q., Zeng, Q. L., Li, W. Y.,
767 Zhang, X. Y., An, F. Y., Wen, X., Li, P. P., Chu, J. F., Sun, X. H., Yan, C. Y.,
768 Yan, N., Xie, D. Y., Raikhel, N., Yang, Z. B., Stepanova, A. N., Alonso, J. M.,
769 & Guo, H. W. (2011). A small-molecule screen identifies L-Kynurenine as a
770 competitive inhibitor of TAA1/TAR activity in ethylene-directed auxin
771 biosynthesis and root growth in *Arabidopsis*. *Plant Cell*, *23*(11), 3944-3960.

772 Hou, J. N., Long, Y., Raman, H., Zou, X. X., Wang, J., Dai, S. T., Xiao, Q. Q., Li, C.,

773 Fan, L. J., Liu, B., & Meng, J. L. (2012). A tourist-like MITE insertion in the
774 upstream region of the BnFLC.A10 gene is associated with vernalization
775 requirement in rapeseed (*Brassica napus* L.). *BMC plant biology*, *12*, 238.

776 Huang, C., Sun, H. Y., Xu, D. Y., Chen, Q. Y., Liang, Y. M., Wang, X. F., Xu, G. H.,
777 Tian, J. G., Wang, C. L., Li, D., Wu, L. S., Yang, X. H., Jin, W. W., Doebley,
778 J. F., & Tian, F. (2018). ZmCCT9 enhances maize adaptation to higher
779 latitudes. *Proceedings of the National Academy of Sciences of the United*
780 *States of America*, *115*(2), E334-E341.

781 Jiang, N., Bao, Z. R., Zhang, X. Y., Hirochika, H., Eddy, S. R., McCouch, S. R., &
782 Wessler, S. R. (2003). An active DNA transposon family in rice. *Nature*,
783 *421*(6919), 163-167.

784 Jiang, N., & Wessler, S. R. (2001). Insertion preference of maize and rice miniature
785 inverted repeat transposable elements as revealed by the analysis of nested
786 elements. *Plant Cell*, *13*(11), 2553-2564.

787 Jiang, N., & Wessler, S. R. (2002). INDITTO: a non-autonomous DNA transposon
788 from *Oryza sativa*. *In Rebase Reports*, *2*(7), 21.

789 Kadioglu, A., Terzi, R., Saruhan, N., & Saglam, A. (2012). Current advances in the
790 investigation of leaf rolling caused by biotic and abiotic stress factors. *Plant*
791 *Science*, *182*, 42-48.

792 Kikuchi, K., Terauchi, K., Wada, M., & Hirano, H. Y. (2003). The plant MITE mPing
793 is mobilized in anther culture. *Nature*, *421*(6919), 167-170.

794 Kitomi, Y., Hanzawa, E., Kuya, N., Inoue, H., Hara, N., Kawai, S., Kanno, N., Endo,
795 M., Sugimoto, K., Yamazaki, T., Sakamoto, S., Sentoku, N., Wu, J., Kanno,
796 H., Mitsuda, N., Toriyama, K., Sato, T., & Uga, Y. (2020). Root angle
797 modifications by the DRO1 homolog improve rice yields in saline paddy

798 fields. *Proceedings of the National Academy of Sciences*, 117(35),
799 21242-21250.

800 Kitomi, Y., Kanno, N., Kawai, S., Mizubayashi, T., Fukuoka, S., & Uga, Y. (2015).
801 QTLs underlying natural variation of root growth angle among rice cultivars
802 with the same functional allele of DEEPER ROOTING 1. *Rice*, 8. doi:ARTN
803 1610.1186/s12284-015-0049-2

804 Li, P. J., Wang, Y. H., Qian, Q., Fu, Z. M., Wang, M., Zeng, D. L., Li, B. H., Wang,
805 X. J., & Li, J. Y. (2007). LAZY1 controls rice shoot gravitropism through
806 regulating polar auxin transport. *Cell Research*, 17(5), 402-410.

807 Liu, X. L., Li, X., Zhang, C., Dai, C. C., Zhou, J. Y., Ren, C. G., & Zhang, J. F.
808 (2017). Phosphoenolpyruvate carboxylase regulation in C4-PEPC-expressing
809 transgenic rice during early responses to drought stress. *Physiologia*
810 *Plantarum*, 159(2), 178-200.

811 Momose, M., Abe, Y., & Ozeki, Y. (2010). Miniature inverted-repeat transposable
812 elements of *Stowaway* are active in potato. *Genetics*, 186(1), 59-66.

813 Nakazaki, T., Okumoto, Y., Horibata, A., Yamahira, S., Teraishi, M., Nishida, H.,
814 Inoue, H., & Tanisaka, T. (2003). Mobilization of a transposon in the rice
815 genome. *Nature*, 421(6919), 170-172.

816 Oki, N., Yano, K., Okumoto, Y., Tsukiyama, T., Teraishi, M., & Tanisaka, T. (2008).
817 A genome-wide view of miniature inverted-repeat transposable elements
818 (MITEs) in rice, *Oryza sativa* ssp. *japonica*. *Genes & Genetic Systems*, 83(4),
819 321-329.

820 Sauer, M., Paciorek, T., Benková, E., & Friml, J. (2006). Immunocytochemical
821 techniques for whole-mount in situ protein localization in plants. *Nature*
822 *Protocols*, 1(1), 98-103.

823 Sun, X. P., Xu, Q., Ruan, R. X., Zhang, T. Y., Zhu, C. Y., & Li, H. Y. (2013).
824 PdMLE1, a specific and active transposon acts as a promoter and confers
825 *Penicillium digitatum* with DMI resistance. *Environmental Microbiology*
826 *Reports*, 5(1), 135-142.

827 Taniguchi, M., Furutani, M., Nishimura, T., Nakamura, M., Fushita, T., Iijima, K.,
828 Baba, K., Tanaka, H., Toyota, M., Tasaka, M., & Morita, M. T. (2017). The
829 Arabidopsis LAZY1 family plays a key role in gravity signaling within
830 statocytes and in branch angle control of roots and shoots. *Plant Cell*, 29(8),
831 1984-1999.

832 Uga, Y., Kitomi, Y., Ishikawa, S., & Yano, M. (2015a). Genetic improvement for root
833 growth angle to enhance crop production. *Breeding Science*, 65(2), 111-119.

834 Uga, Y., Kitomi, Y., Yamamoto, E., Kanno, N., Kawai, S., Mizubayashi, T., &
835 Fukuoka, S. (2015b). A QTL for root growth angle on rice chromosome 7 is
836 involved in the genetic pathway of DEEPER ROOTING 1. *Rice*, 8. doi:ARTN
837 810.1186/s12284-015-0044-7

838 Uga, Y., Okuno, K., & Yano, M. (2011). *Dro1*, a major QTL involved in deep rooting
839 of rice under upland field conditions. *Journal of Experimental Botany*, 62(8),
840 2485-2494.

841 Uga, Y., Sugimoto, K., Ogawa, S., Rane, J., Ishitani, M., Hara, N., Kitomi, Y., Inukai,
842 Y., Ono, K., Kanno, N., Inoue, H., Takehisa, H., Motoyama, R., Nagamura, Y.,
843 Wu, J. Z., Matsumoto, T., Takai, T., Okuno, K., & Yano, M. (2013). Control
844 of root system architecture by DEEPER ROOTING 1 increases rice yield
845 under drought conditions. *Nature Genetics*, 45(9), 1097-1102.

846 Wang, L. L., Guo, M. X., Li, Y., Ruan, W. Y., Mo, X. R., Wu, Z. C., Sturrock, C. J.,
847 Yu, H., Lu, C. G., Peng, J. R., & Mao, C. Z. (2018). LARGE ROOT ANGLE

848 1, encoding OsPIN2, is involved in root system architecture in rice. *Journal of*
849 *Experimental Botany*, 69(3), 385-397.

850 Xu, M., Zhu, L., Shou, H. X., & Wu, P. (2005). A PIN1 family gene, OsPIN1,
851 involved in auxin-dependent adventitious root emergence and tillering in rice.
852 *Plant and Cell Physiology*, 46(10), 1674-1681.

853 Yan, Y. S., Zhang, Y. M., Yang, K., Sun, Z. X., Fu, Y. P., Chen, X. Y., & Fang, R. X.
854 (2011). Small RNAs from MITE-derived stem-loop precursors regulate
855 abscisic acid signaling and abiotic stress responses in rice. *Plant Journal*,
856 65(5), 820-828.

857 Yoshihara, T., & Iino, M. (2007). Identification of the gravitropism-related rice gene
858 LAZY1 and elucidation of LAZY1-dependent and -independent gravity
859 signaling pathways. *Plant and Cell Physiology*, 48(5), 678-688.

860 Yoshihara, T., & Spalding, E. P. (2017). LAZY genes mediate the effects of gravity
861 on auxin gradients and plant architecture. *Plant physiology*, 175(2), 959-969.

862 Yoshihara, T., Spalding, E. P., & Iino, M. (2013). AtLAZY1 is a signaling component
863 required for gravitropism of the *Arabidopsis thaliana* inflorescence. *Plant*
864 *Journal*, 74(2), 267-279.

865 Yu, B., Lin, Z., Li, H., Li, X., Li, J., Wang, Y., Zhang, X., Zhu, Z., Zhai, W., Wang,
866 X., Xie, D., & Sun, C. (2007). TAC1, a major quantitative trait locus
867 controlling tiller angle in rice. *The Plant Journal*, 52(5), 891-898.

868 Zhang, Q., Li, J. J., Zhang, W. J., Yan, S. N., Wang, R., Zhao, J. F., Li, Y. J., Qi, Z.
869 G., Sun, Z. X., & Zhu, Z. G. (2012). The putative auxin efflux carrier OsPIN3t
870 is involved in the drought stress response and drought tolerance. *Plant Journal*,
871 72(5), 805-816.

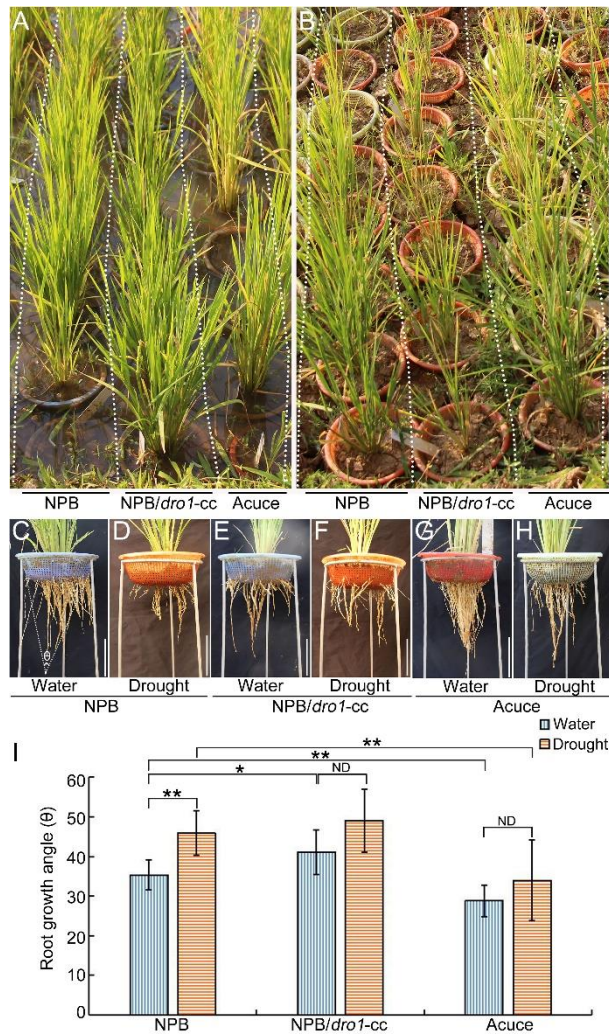
872 Zhang, X. Y., Feschotte, C., Zhang, Q., Jiang, N., Eggleston, W. B., & Wessler, S. R.

873 (2001). *P* instability factor: an active maize transposon system associated with
874 the amplification of *Tourist*-like MITEs and a new superfamily of transposases.
875 *Proceedings of the National Academy of Sciences of the United States of*
876 *America*, 98(22), 12572-12577.

877 Zhang, X. Y., Jiang, N., Feschotte, C., & Wessler, S. R. (2004). PIF- and pong-like
878 transposable elements: distribution, evolution and relationship with tourist-
879 like miniature inverted-repeat transposable elements. *Genetics*, 166(2),
880 971-986.

881

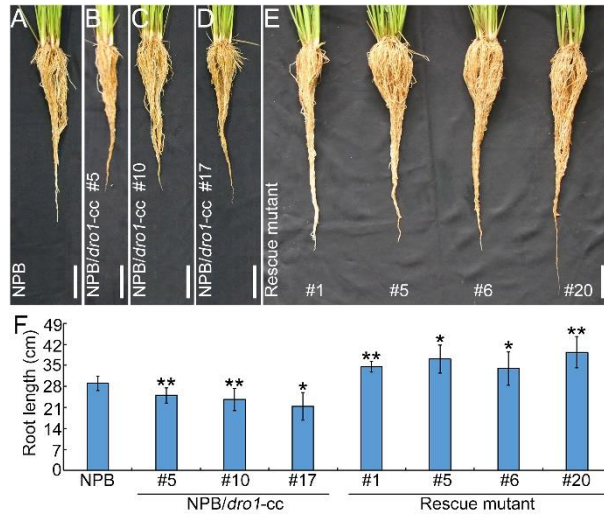
882 **Figure**



883

884 **Figure 1. Phenotypes of rice varieties grown in the field.** The rice varieties Acuce,
 885 Nipponbare, and the Nipponbare *dro1-cc* mutant were grown with irrigation
 886 conditions (A) or under drought conditions (B) for 3 months, and the root architecture
 887 was observed (C-H). Quantification of the root growth angle (I) (Acuce: $n_{\text{water}} = 13$,
 888 $n_{\text{drought}} = 11$; NPB: $n_{\text{water}} = 9$, $n_{\text{drought}} = 6$; NPB/*dro1-cc*: $n_{\text{water}} = 9$, $n_{\text{drought}} = 5$). Data are
 889 means \pm SD; * $P < 0.05$, ** $P < 0.01$ (Student's *t*-test). NPB = Nipponbare,
 890 NPB/*dro1-cc* = Nipponbare *dro1-cc* mutant, ND = no difference, θ = root growth
 891 angle. Bar = 10 cm.

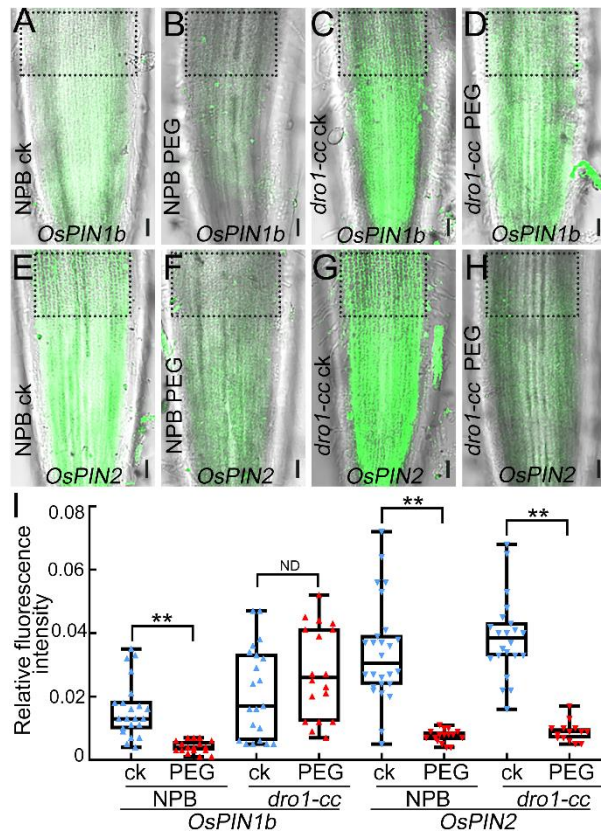
892



893

894 **Figure 2. Root lengths in the Nipponbare *dro1-cc* and rescue mutant.** Rice
 895 varieties Nipponbare (A), *dro1-cc* lines #5 (B), #10 (C), and #17 (D) and the T1
 896 rescue mutant lines (#1, #5, #6 and #20) (E) were grown in an experimental field with
 897 irrigation conditions for 3 months. Quantification of root length (F) (NPB: n=10;
 898 NPB/*dro1-cc* #5: n=7, #10: n=8, #17: n=12; rescue lines #1: n=4, #5: n=4, #6: n=8,
 899 #20: n=4). Data are means \pm SD; * $P < 0.05$, ** $P < 0.01$ (Student's *t*-test). NPB =
 900 Nipponbare. Bar = 10 cm.

901



902

903 **Figure 3. The subcellular localization of OsPIN1 and OsPIN2 in the Nipponbare**

904 ***dro1-cc* mutant.** Rice seedlings of wild-type Nipponbare (A, B, E, F) and the *dro1-cc*

905 (#17) mutant (C, D, G, H) grown on MS medium supplemented without (A, C, E, G)

906 or with (B, D, F, H) 15% PEG6000. Immunolocalization of OsPIN1b (A-D) and

907 OsPIN2 (E-H) in root epidermal cells of wild-type Nipponbare and the *dro1-cc* (#17)

908 mutant. Quantification of the fluorescence intensity of OsPIN1b and OsPIN2 at the

909 plasma membrane (I) (NPB/OsPIN1b: $n_{ck} = 22$, $n_{PEG6000} = 17$; *dro1-cc*/OsPIN1b: $n_{ck} =$

910 21, $n_{PEG6000} = 18$; NPB/OsPIN2: $n_{ck} = 26$, $n_{PEG6000} = 16$; *dro1-cc*/OsPIN2: $n_{ck} = 22$,

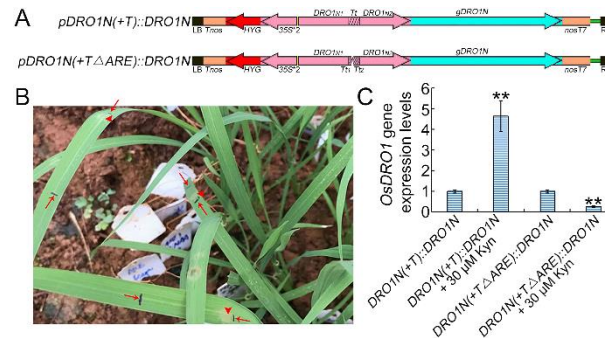
911 $n_{PEG6000} = 14$). The rectangle shows the region used to measure fluorescence intensity.

912 Data are means \pm SD; ** $P < 0.01$ (Student's *t*-test). ck = Seedlings grown on MS

913 medium. PEG = Seedlings grown on MS medium supplemented with 15% PEG6000.

914 NPB = Nipponbare. Bar = 1 cm.

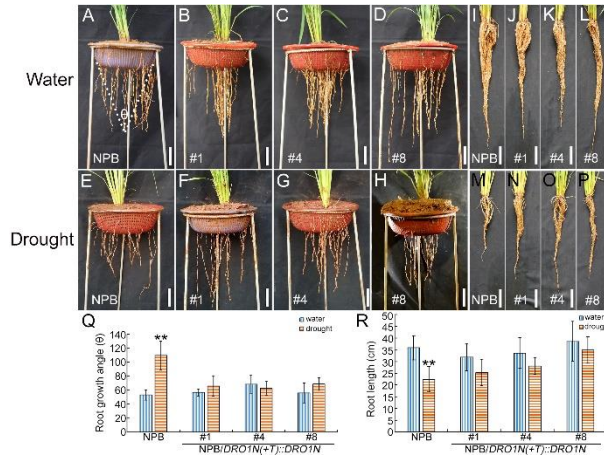
915



916

917 **Figure 4. Expression levels of the *DRO1* in Nipponbare leaves.** Schematic diagram
 918 of the rice expression constructs (A). A solution of *Agrobacterium* strain EHA105
 919 transformed with the expression vector with the addition of 30 μM L-Kynurenine was
 920 infiltrated into rice leaf veins (B). The expression levels of the *DRO1* gene in rice
 921 leaves were determined by real-time PCR (C). The *OsActin* gene was used as an
 922 internal control. Data are means ± SD. ** $P < 0.01$ (SPSS analysis). *pDRO1N*
 923 (+T)::*DRO1N* = the Nipponbare *DRO1* promoter containing the *INDITTO2*
 924 transposon and fused with the Nipponbare genomic *DRO1* gene, *pDRO1N* (+TΔ
 925 *ARE*)::*DRO1N* = the Nipponbare *DRO1* promoter containing the *INDITTO2*
 926 transposon with a deletion of the auxin response element and fused with the
 927 Nipponbare genomic *DRO1* gene. g*DRO1N* = Nipponbare genomic *DRO1* gene. Kyn
 928 = L-Kynurenine. The arrowheads point to the injection position in the leaf veins; the
 929 arrows point to the region of the *Agrobacterium* solution in the leaf veins.

930



931

932 **Figure 5. Root architectures of transgenic Nipponbare rice lines with *INDITTO2***

933 **transposon insertion in the *DRO1* promoter.** The Nipponbare (A, E, I, M) and T2

934 transgenic Nipponbare rice lines #1 (B, F, J, N), #4 (C, G, K, O) and #8 (D, H, L, P)

935 were grown with irrigation conditions (A-D, I-L) or under drought stress (E-H, M-P)

936 for 3 months. Quantification of the root growth angle (Q) (NPB: $n_{\text{water}} = 8$, $n_{\text{drought}} = 7$;

937 #1: $n_{\text{water}} = 7$, $n_{\text{drought}} = 8$; #4: $n_{\text{water}} = 7$, $n_{\text{drought}} = 9$; #8: $n_{\text{water}} = 6$, $n_{\text{drought}} = 4$) and root

938 length (R) (NPB: $n_{\text{water}} = 10$, $n_{\text{drought}} = 8$; #1: $n_{\text{water}} = 7$, $n_{\text{drought}} = 7$; #4: $n_{\text{water}} = 6$, n_{drought}

939 $= 5$; #8: $n_{\text{water}} = 7$, $n_{\text{drought}} = 7$). Data are means \pm SD; ** $P < 0.01$ (Student's *t*-test).

940 NPB = Nipponbare, θ = root growth angle. Bar = 5 cm.

941

942 **Supporting Information**

943

944 ***INDITTO2* transposon conveys auxin-mediated *DRO1* transcription for rice**
945 **drought avoidance**

946

947 Yiting Zhao^{1,2,3,8*}, Lixia Wu^{1,2,3*}, Qijing Fu^{1,2,3*}, Dong Wang⁶, Jing Li⁷, Baolin Yao⁷,
948 Si Yu¹, Li Jiang¹, Jie Qian¹, Xuan Zhou^{1,2,3}, Li Han^{1,2,3}, Shuanglu Zhao¹, Canrong Ma⁵,
949 Yanfang Zhang¹, Chongyu Luo^{1,2,3}, Qian Dong¹, Sajjie Li¹, Lina Zhang¹, Xi Jiang¹,
950 Youchun Li¹, Hao Luo¹, Kuixiu Li^{1,2,3}, Jing Yang^{1,2,3}, Qiong Luo^{1,2,3}, Lichi Li⁹, Sheng
951 Peng^{1,2,3}, Huichuan Huang^{1,2,3}, Zhili Zuo⁶, Changning Liu⁷, Lei Wang⁵, Chengyun
952 Li^{1,2,3}, Xiahong He^{1,2,3}, Jiří Friml⁴, Yunlong Du^{1,2,3#}

953

954 **Supplemental Experimental Procedures**

955 **Gravity stimulation of rice roots**

956 Rice roots were subjected to gravity stimulation as previously described (Du et al.,
957 2013). Five-day-old rice seedlings were transferred to Murashige-Skoog (MS)
958 medium containing with 0.01 μM NAA or the equivalent amount of DMSO as control.
959 The plates were then turned 90° compared with the original vertical position.
960 Seedlings were gravity stimulated for 18 hours under light conditions.

961

962 **Plasmid construction**

963 Genomic DNA of the rice varieties Acuce and Nipponbare was isolated from rice
964 leaves. To clone the *DRO1* promoter of Acuce (*DRO1A*) and Nipponbare (*DRO1N*),
965 the gene-specific primers PrDRO1-FP and PrDRO1-RP containing the *Eco31I* site
966 (Supplemental Table S2) were synthesized based on the known *DRO1* sequence

967 (GenBank no. AB689742.1). The amplification product was cloned into the vector
968 *pBWA(V)HG-ccdB* digested with *Eco31I*, and was sequenced at BGI. Constructs
969 containing the *DROI* promoter of Acuce and Nipponbare fused with the *gusA* gene
970 were named *pDROIA* and *pDROIN*, respectively.

971 To construct the expression vectors *pDROIA(ΔT)* and *pDROIA(TΔARE)* carrying
972 the *INDITTO2* transposon deletion or the *INDITTO2* transposon without the ARE,
973 respectively, the PCR fragment was amplified with the *pDROIA* template, fused with
974 the *gusA* gene, and inserted into the vector *pBWA(V)HG-ccdB*.

975 To construct the expression vector *pDROIN(+T)*, the PCR fragment of the
976 *INDITTO2* transposon was amplified and inserted into the *DROI* promoter of
977 Nipponbare, fused with the *gusA* gene, and inserted into the vector
978 *pBWA(V)HG-ccdB*.

979 To construct the expression vectors *pT* and *pT(ΔARE)* carrying the *INDITTO2*
980 transposon with or without AREs and the transcribed *gusA*, respectively, the PCR
981 fragment containing the *INDITTO2* transposon was amplified with the *pDROIA*
982 template and inserted into the vector *pBWA(V)HG-ccdB*.

983 To construct the expression vectors *pDROIA(ΔRE1/2/3)* and *pDROIN(ΔRE1/2/3)*,
984 in which the three AREs RE1 (TGTCTC), RE2 (TGTC) and RE3 (GACA) (Uga et al.,
985 2013) were deleted, respectively, the PCR fragments of the respective Acuce and
986 Nipponbare *DROI* promoters were amplified and fused with the *gusA* gene, and
987 inserted into the vector *pBWA(V)HG-ccdB*.

988 To construct the expression vectors *pDROIN(+T)::DROIN* and *pDROIN(+TΔ*
989 *ARE)::DROIN*, the PCR fragments of the *INDITTO2* transposon with or without ARE
990 were amplified with the *pDROIA* template and inserted into the *DROI* promoter of
991 Nipponbare, respectively. The insertion position of the *INDITTO2* transposon was the

992 same as that in the *Acuce DROI* promoter. The *Nipponbare DROI* gene was
993 subsequently amplified, fused with the *Nipponbare DROI* promoter, and inserted into
994 the vector *pBWA(V)HG-ccdB*.

995 All the expression vectors were constructed at BIORUN Company (Wuhan
996 BIORUN Bio-Tech Co., LTD).

997

998 **Construction of the CRISPR/Cas9 plasmids**

999 Codon-optimized hSpCas9 was linked to the maize ubiquitin promoter (UBI) in an
1000 intermediate plasmid (Cong et al., 2013), and this expression cassette was then
1001 inserted into the binary vector *pCAMBIA1300* (Cambia, Australia), containing the
1002 HPT (hygromycin B phosphotransferase) gene. The original *BsaI* site in the
1003 *pCAMBIA1300* backbone was removed using a point mutation kit (Transgen, China).

1004 A fragment comprising an *OsU6* promoter (Feng et al., 2013), a negative selection
1005 marker gene *ccdB* flanked by two *BsaI* sites and an sgRNA derived from *pX260* was
1006 inserted into this vector using the In-fusion Cloning kit (Takara, Japan) to produce the
1007 CRISPR/Cas9 binary vector *pBGK032* (Cong et al., 2013). *Escherichia coli* strain
1008 DB3.1 was used to maintain this binary vector.

1009 The 23-bp targeting sequences (including the protospacer adjacent motif (PAM))
1010 were selected within the target genes, and their targeting specificity was confirmed
1011 using a BLAST search against the rice genome (<http://blast.ncbi.nlm.nih.gov/Blast.cgi>)
1012 (Hsu et al., 2013). The designed targeting sequences were synthesized and annealed to
1013 form oligo adaptors. The vector *pBGK032* was digested with *BsaI* and purified using
1014 a DNA purification kit (Tiangen, China). A ligation reaction (10 μ L) containing 10 ng
1015 of the digested *pBGK032* vector and 0.05 mM oligo adaptor was performed and
1016 directly transformed into *E. coli* competent cells to produce CRISPR/Cas9 plasmids.

1017 The CRISPR/Cas9 vector was constructed at Biogle Company (Hangzhou Biogle Co.,
1018 LTD.)

1019

1020 **Construction of the *DRO1* knockout mutant and transgenic rice lines**

1021 The rice *dro1*-cc mutant lines were produced using the CRISPR/Cas9 method. The
1022 specific guide-RNA (gRNA) sequence was designed as follows:

1023 5'-GAAGGCGCAGAAGAATTTGC-3'. The target gene sequence that added the

1024 PAM of *DRO1* was 5'-TAAGGCGCAGAAGAATTTGCGGG-3', and the GGG

1025 trinucleotide acted as the PAM. The CRISPR/Cas9 plasmids were introduced into

1026 *Agrobacterium tumefaciens* strain EHA105. Genomic DNA was extracted from rice

1027 transformants using the CTAB method, and the primer pair OsDRO1-ccFP and

1028 OsDRO1-ccRP (Supplemental Table S2) flanking the designed target site was used for

1029 PCR amplification. The PCR products were sequenced directly and identified using

1030 the degenerate sequence decoding method (Ma et al., 2015). To obtain transgenic

1031 Nipponbare lines containing the *INDITTO2* transposon in the Nipponbare *DRO1*

1032 promoter, the construct *pDROIN(+T)::DROIN* was transformed into *Agrobacterium*

1033 *tumefaciens* strain EHA105. Rice transformation was performed as previously

1034 described by the *Agrobacterium*-mediated method at Biogle Company (Hangzhou

1035 Biogle Co., LTD) (Nishimura et al., 2006).

1036

1037 **Measurement of auxin content**

1038 Roots of the *dro1*-cc mutant were ground to a powder, and the phytohormone IAA

1039 was measured by HPLC-MS/MS as previously described (Luo et al., 2016). For IAA

1040 extraction, the root powder was dissolved with ethyl acetate spiked with 5 ng of

1041 D5-IAA (OlhemIm) as an internal standard. Multiple reaction monitoring was

1042 performed to monitor the analytic parent ion → product ion process: mass-to-charge
1043 ratio [m/z] 176.00 → 130.00 (CE, -15 V; Q1 pre bias, -19 V; Q3 pre bias, -22 V) for
1044 IAA; m/z 181.00 → 134.05 (CE, -18 V; Q1 pre bias, -23 V; Q3 pre bias, -23 V) for
1045 D5-IAA.

1046

1047 **Transient gene expression in tobacco and rice leaves**

1048 *Agrobacterium* strain EHA105 containing the expression constructs was cultured in
1049 liquid LB medium supplemented with antibiotics (50 mg/L rifampicin and 50 mg/L
1050 kanamycin) at 28°C. The precipitate of the bacterial liquid culture was washed three
1051 times with sterilized water followed by injection buffer (containing 2.132 g/L MES,
1052 10 mM CaCl₂ and 0.2 mM acetosyringone) and diluted with injection buffer to an
1053 OD₆₀₀ of 0.7. Leaves of *Nicotiana benthamiana* and Nipponbare leaf veins were
1054 infiltrated with *Agrobacterium* solution with or without 1 μM NAA or 30 μM of the
1055 auxin biosynthesis inhibitor L-Kynurenine, respectively. Infiltrated leaves of tobacco
1056 and rice were grown in chambers or greenhouse for 4 and 5 days, respectively, and
1057 then harvested to detect the expression levels of the *GUS*, *DRO1*, *NaActin* (GenBank
1058 no. JQ256516.1) and *OsActin* genes (GenBank no. AK060893.1) amplified with the
1059 gene-specific primer pairs GUS-rFP and GUS-rRP, DRO1-rFP and DRO1-rRP,
1060 NaActin-rFP and NaActin-rRP, and OsActin-FP and OsActin-RP (Supplemental Table
1061 S2), respectively, using quantitative real-time PCR performed under denaturation at
1062 95°C for 2 minutes, followed by 40 cycles of 95°C for 45 seconds, 52°C for 30
1063 seconds and 72°C for 1 minute. Three biological replicates were tested. The relative
1064 expression level was calculated using the $2^{-\Delta\Delta Ct}$ method. The *NaActin* and *OsActin*
1065 genes served as internal controls.

1066

1067 **Identification of IGT family genes in the rice genome**

1068 BLASTP searches were performed to identify the IGT family genes in Nipponbare.
1069 The homologues genes of *DROI*, *TAC1*, and *LAZY1* from *Arabidopsis* were used as
1070 query sequences against the rice protein sequences.

1071

1072 **Conserved motif analysis of IGT family proteins**

1073 The online Multiple Expectation Maximization for the Motif Elucidation (MEME)
1074 toolkit was used to identify all conserved motifs (<http://meme-suite.org/>) (Bailey et al.,
1075 2009). All IGT family protein sequences were used for the queries. The parameters
1076 were set as follows: minimum width = 6, maximum width = 150, motif number = 15
1077 and minimum number of sites = 2.

1078

1079 **Expression profile analysis of IGT family genes**

1080 All IGT gene expression data in eleven tissues (ovary, anther, embryo, pistil,
1081 inflorescence, root, lemma and palea, leaf blade, endosperm, stem, and leaf sheath) of
1082 rice were retrieved from the RiceXPro database (<https://ricexpro.dna.affrc.go.jp/>)
1083 (Sato et al., 2013). All normalized data were log₂ transformed. The expression profile
1084 was displayed in a heat map using the R package pheatmap ([https://cran.r-project.](https://cran.r-project.org/web/packages/pheatmap/index.html)
1085 [org/web/packages/pheatmap/index.html](https://cran.r-project.org/web/packages/pheatmap/index.html)).

1086

1087 **Identification of *INDITT04* copies in the Nipponbare genome**

1088 *INDITT04* copies were identified by local BLASTN. The reference sequence was the
1089 *Oryza sativa* Japonica RGAP7 genome and was used to construct the local BLASTN
1090 database. The specific parameters were set as follows: word size = 4, e-value = 1e-10,
1091 best hit score edge = 0.05 and best hit overhang = 0.25. The sequences of all

1092 *INDITT04* copies shared more than 95% identity with the original *INDITT04*. The
1093 positions of all *INDITT04* copies were compared with the positions of all genes in the
1094 *Oryza sativa* Japonica RGAP7 genome to obtain the inserted loci of all *INDITT04*
1095 copies.

1096

1097 **Phylogenetic tree construction**

1098 The sequences of *INDITTO* and its homologues in different rice varieties were used to
1099 construct a phylogenetic tree using the neighbour-joining method in MEGA 5.1. Each
1100 bootstrap value was analyzed with 1000 replicates.

1101

1102 **Analysis of the transposon and root phenotype**

1103 The online software (<http://bioinf.cs.ucl.ac.uk/introduction/>, www.repeatmasker.org
1104 and www.girinst.org) was used to analyse the tertiary structures of DRO1 and the
1105 transposons. The online software (<http://plantregmap.cbi.pku.edu.cn>) was used to
1106 analyze the transcription factor binding sites of the transposons. Vector NTI Suite 6,
1107 DNAMAN and Discovery Studio 4.0 were used to analyze the sequence alignment,
1108 protein sequence and conformation of the DRO1 protein, respectively. ImageJ 1.41
1109 was used to measure the root growth angle, root length and fluorescence intensities.
1110 To measure the root growth angle with ImageJ 1.41, the longest root tip acted as
1111 vertex and joined both sides of the most upward apex root end that emerged from the
1112 basket edge when the rice seedlings were grown in a basket. Pearson's correlation
1113 coefficient was calculated using SPSS software and used to analyze the correlation
1114 between the root length and angle. All images were processed with Photoshop.

1115

1116 **SI References**

1117 Bailey, T. L., Boden, M., Buske, F. A., Frith, M., Grant, C. E., Clementi, L., Ren, J.
1118 Y., Li, W. W., & Noble, W. S. (2009). MEME SUITE: tools for motif
1119 discovery and searching. *Nucleic Acids Research*, 37(Web Server issue),
1120 W202-W208.

1121 Cong, L., Ran, F. A., Cox, D., Lin, S. L., Barretto, R., Habib, N., Hsu, P. D., Wu, X.
1122 B., Jiang, W. Y., Marraffini, L. A., & Zhang, F. (2013). Multiplex genome
1123 engineering using CRISPR/Cas systems. *Science*, 339(6121), 819-823.

1124 Du, Y. L., Tejos, R., Beck, M., Himschoot, E., Li, H. J., Robatzek, S., Vanneste, S., &
1125 Friml, J. (2013). Salicylic acid interferes with clathrin-mediated endocytic
1126 protein trafficking. *Proceedings of the National Academy of Sciences of the*
1127 *United States of America*, 110(19), 7946-7951.

1128 Feng, Z. Y., Zhang, B. T., Ding, W. N., Liu, X. D., Yang, D. L., Wei, P. L., Cao, F.
1129 Q., Zhu, S. H., Zhang, F., Mao, Y. F., & Zhu, J. K. (2013). Efficient genome
1130 editing in plants using a CRISPR/Cas system. *Cell Research*, 23(10),
1131 1229-1232.

1132 Hsu, P. D., Scott, D. A., Weinstein, J. A., Ran, F. A., Konermann, S., Agarwala, V.,
1133 Li, Y. Q., Fine, E. J., Wu, X. B., Shalem, O., Cradick, T. J., Marraffini, L. A.,
1134 Bao, G., & Zhang, F. (2013). DNA targeting specificity of RNA-guided Cas9
1135 nucleases. *Nature Biotechnology*, 31(9), 827-832.

1136 Luo, J., Wei, K., Wang, S. H., Zhao, W. Y., Ma, C. R., Hettenhausen, C., Wu, J. S.,
1137 Cao, G. Y., Sun, G. L., Baldwin, I. T., Wu, J. Q., & Wang, L. (2016).
1138 COI1-regulated hydroxylation of jasmonoyl-L-isoleucine impairs *Nicotiana*
1139 *attenuata's* resistance to the generalist herbivore *Spodoptera litura*. *Journal of*
1140 *Agricultural and Food Chemistry*, 64(14), 2822-2831.

1141 Ma, X. L., Chen, L. T., Zhu, Q. L., Chen, Y. L., & Liu, Y. G. (2015). Rapid decoding

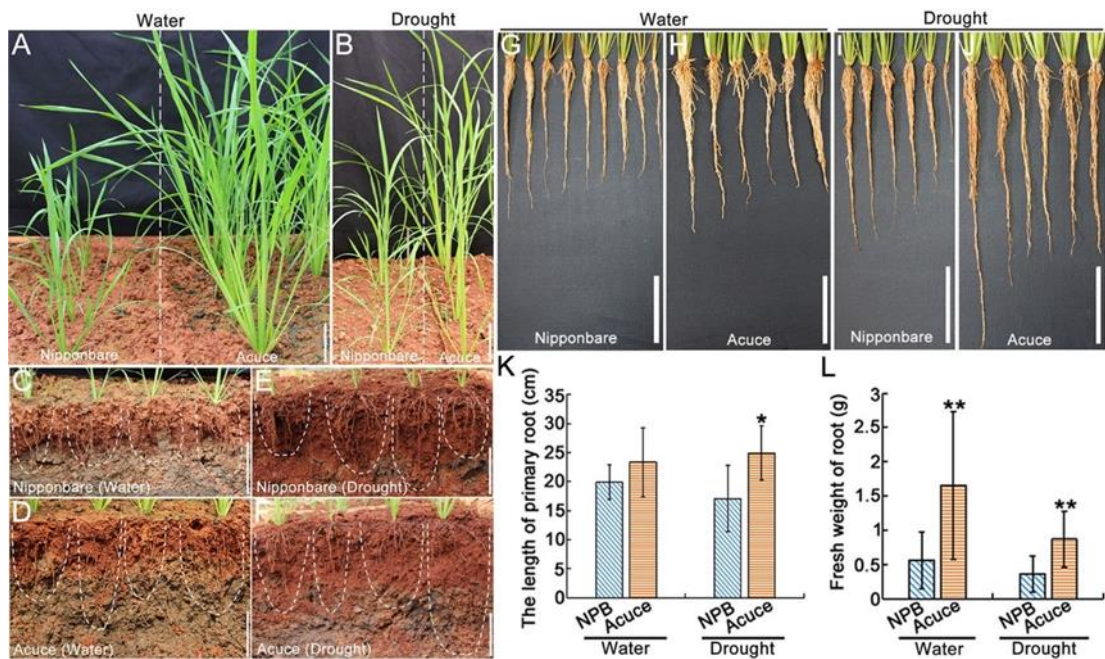
1142 of sequence-specific nuclease-induced heterozygous and biallelic mutations by
1143 direct sequencing of PCR products. *Molecular Plant*, 8(8), 1285-1287.

1144 Nishimura, A., Aichi, I., & Matsuoka, M. (2006). A protocol for
1145 *Agrobacterium*-mediated transformation in rice. *Nature Protocols*, 1(6),
1146 2796-2802.

1147 Sato, Y., Takehisa, H., Kamatsuki, K., Minami, H., Namiki, N., Ikawa, H., Ohyanagi,
1148 H., Sugimoto, K., Antonio, B. A., & Nagamura, Y. (2013). RiceXPro version
1149 3.0: expanding the informatics resource for rice transcriptome. *Nucleic Acids*
1150 *Research*, 41(D1), D1206-D1213.

1151

1152 **Supplemental Figures and Tables**



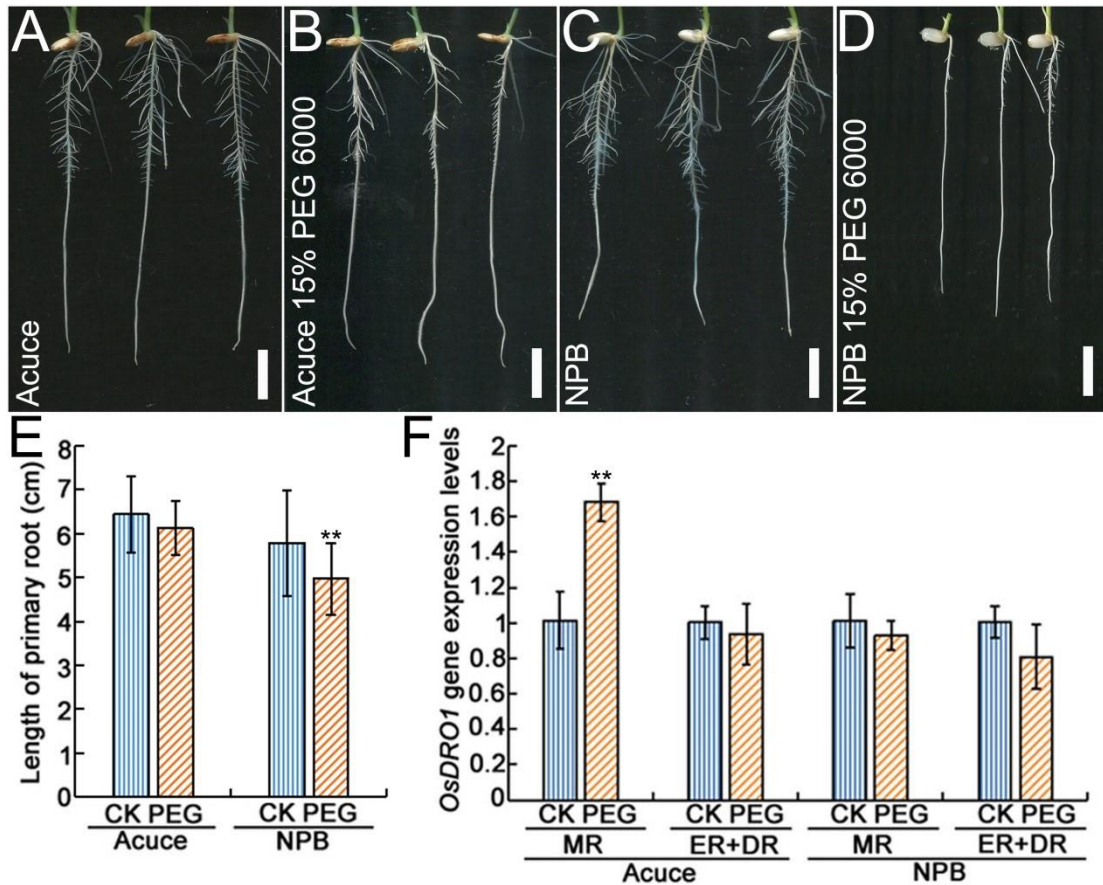
1153

1154 **Figure S1. Root phenotypes of Acuce and Nipponbare grown in the field.**

1155 Root architectures of Acuce (A, B, D, F) and Nipponbare (A, B, C, E) grown in the
 1156 field with irrigation (A, C, D) or under drought stress (B, E, F). Root phenotypes of
 1157 Acuce (H, J) and Nipponbare (G, I) grown with irrigation (G, H) or under drought
 1158 stress (I, J). Quantification of primary root length (K) (NPB: $n_{\text{water}} = 10$, $n_{\text{drought}} = 6$;
 1159 Acuce: $n_{\text{water}} = 12$, $n_{\text{drought}} = 12$) and root fresh weight (L) (NPB: $n_{\text{water}} = 11$, $n_{\text{drought}} = 7$;
 1160 Acuce: $n_{\text{water}} = 12$, $n_{\text{drought}} = 12$). Data are means \pm SD; * $P < 0.05$, ** $P < 0.01$
 1161 (Student's *t*-test). Bar = 10 cm.

1162

1163



1164

1165 **Figure S2. Root phenotypes of Acuce and Nipponbare treated with PEG6000.**

1166 Seedlings of Acuce (A and B) and Nipponbare (C and D) grown on MS medium
 1167 supplemented either with or without 15% PEG6000 for 4 days. The primary root
 1168 length was measured and quantified (E) (Acuce: $n_{CK} = 42$, $n_{PEG6000} = 30$, NPB: $n_{CK} =$
 1169 29 , $n_{PEG6000} = 30$). The expression levels of *DRO1* (F) in the root meristem region,
 1170 elongation region and differentiation region were determined using real-time PCR.
 1171 The *OsActin* gene was used as an internal control. Data are means \pm SD. ** $P < 0.01$
 1172 (Student's *t*-test for root length analysis, SPSS analysis for gene expression). CK =
 1173 rice seedlings grown on MS medium, PEG = rice seedlings grown on MS medium
 1174 supplemented with 15% PEG6000, NPB = Nipponbare, MR = meristem region, ER =
 1175 elongation region, DR = differentiation region. Bar = 1 cm.


```

IR64 MKIFSWVANKISGKQEANRFPANSSAPYRANVSDCRKDEFSDWPQSLLAIGTFGN 55
Acuce MKIFSWVANKISGKQEANRFPANSSAPYRANVSDCRKDEFSDWPQSLLAIGTFGN 55
KP MKIFSWVANKISGKQEANRFPANSSAPYRANVSDCRKDEFSDWPQSLLAIGTFGN 55
Nipponbare MKIFSWVANKISGKQEANRFPANSSAPYRANVSDCRKDEFSDWPQSLLAIGTFGN 55

IR64 KQIEEVAQVENSSDNVQSVQDTVKFTEEEVDKIRKEFETLLAIKDQAEAQRSHDD 110
Acuce KQIEEVAQVENSSDNVQSVQDTVKFTEEEVDKIRKEFETLLAIKDQAEAQRSHDD 110
KP KQIEEVAQVENSSDNVQSVQDTVKFTEEEVDKIRKEFETLLAIKDQAEAQRSHDD 110
Nipponbare KQIEEVAQVENSSDNVQSVQDTVKFTEEEVDKIRKEFETLLAIKDQAEAQRSHDD 110

IR64 DQVGLQKRADGEDNEKHIRQLINKRIIVSKSKNSLGKKGNTLKPRSVASLLKLFM 165
Acuce DQVGLQKRADGEDNEKHIRQLINKRIIVSKSKNSLGKKGNTLKPRSVASLLKLFM 165
KP DQVGLQKRADGEDNEKHIRQLINKRIIVSKSKNSLGKKGNTLKPRSVASLLKLFM 165
Nipponbare DQVGLQKRADGEDNEKHIRQLINKRIIVSKSKNSLGKKGNTLKPRSVASLLKLFM 165

IR64 CKGGFTSVVPEPRNTFPQSRMEKLLKAILQKKIHPQNSSTLVAKRHLDWKPDETE 220
Acuce CKGGFTSVVPEPRNTFPQSRMEKLLKAILQKKIHPQNSSTLVAKRHLDWKPDETE 220
KP CKGGFTSVVPEPRNTFPQSRMEKLLKAILQKKIHPQNSSTLVAKRHLDWKPDETE 220
Nipponbare CKGGFTSVVPEPRNTFPQSRMEKLLKAILQKKIHPQNSSTLVAKRHLDWKPDETE 220

IR64 INECLEVHCVI-----251
Acuce INECLEDALRDLDDDGAKWVKTDSEYIVLEM 251
KP INECLEDALRDLDDDGAKWVKTDSEYIVLEM 251
Nipponbare INECLEDALRDLDDDGAKWVKTDSEYIVLEM 251

```

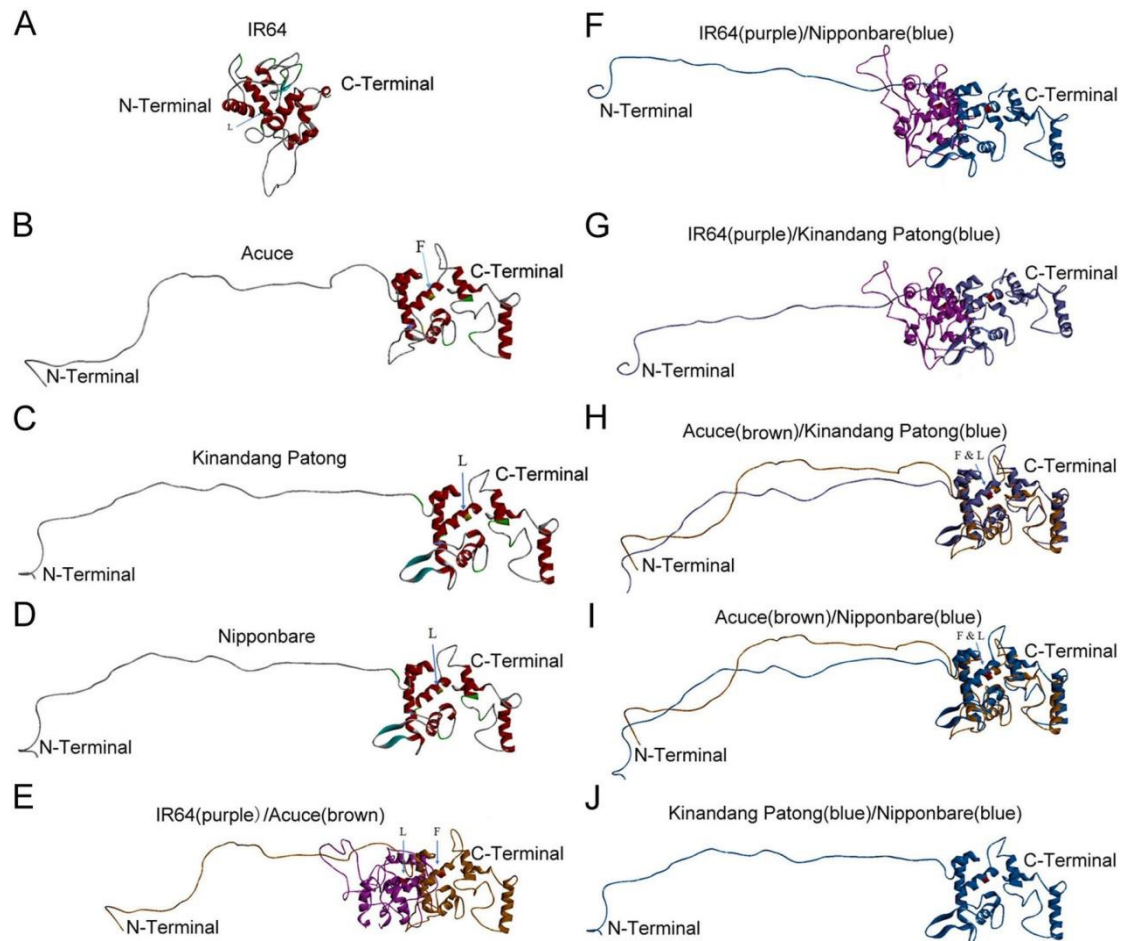
1176

1177 **Figure S3. Amino acid sequences of DRO1 in different rice varieties.**

1178 The DRO1 amino acid sequences of the *indica* rice IR64 and Acuce and the *japonica*

1179 rice Kinandang Patong and Nipponbare were aligned. KP = Kinandang Patong.

1180

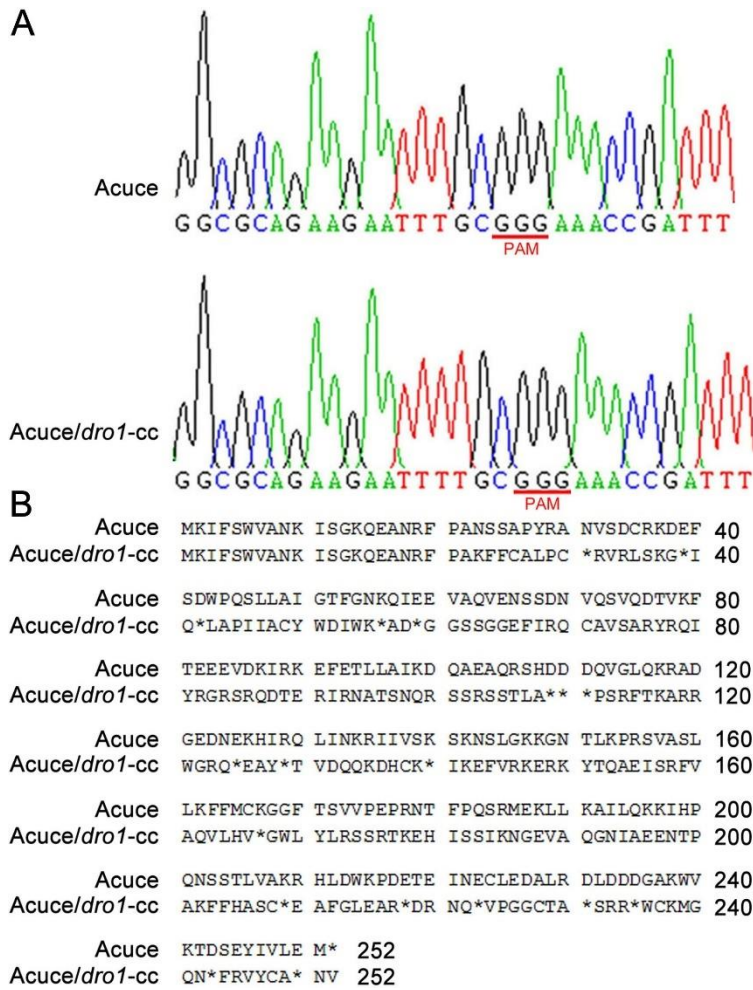


1181

1182 **Figure S4. Deduced tertiary structures of the DRO1 protein.**

1183 The deduced tertiary structures of DRO1 amino acids from IR64 (A), Acuce (B),
 1184 Kinandang Patong (C) and Nipponbare (D) were analyzed with the online software
 1185 (<http://bioinf.cs.ucl.ac.uk/introduction/>). Merged images show the structural
 1186 differences between Acuce and IR64 (E), IR64 and Nipponbare (F), IR64 and
 1187 Kinandang Patong (G), Acuce and Kinandang Patong (H), Acuce and Nipponbare (I)
 1188 and Kinandang Patong and Nipponbare (J). The amino acid of DRO1 at position 163
 1189 is labelled with a blue arrow. The capital F and L indicate Phe and Leu, respectively.

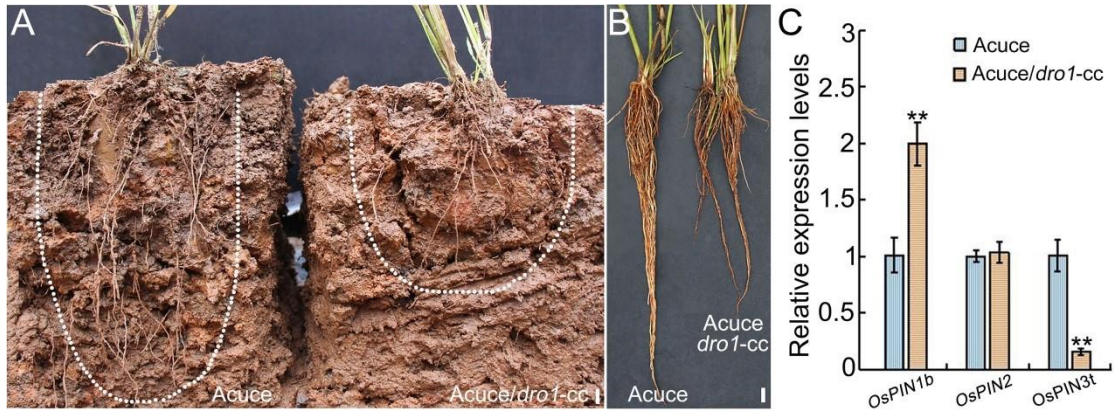
1190



1192 **Figure S5. Sequence profiles of the *DRO1* gene in Acuce and *DRO1* knockout**
 1193 **mutant.**

1194 The genomic *DRO1* gene of Acuce was knocked out using the CRISPR/Cas9 method.
 1195 Sequence map of the PCR product of the genomic *DRO1* gene (A), and the amino
 1196 acid sequences encoded by the *DRO1* gene (B) in wild-type Acuce and the *dro1-cc*
 1197 mutant. PAM = protospacer adjacent motif. Asterisks indicate translation termination.

1198



1199

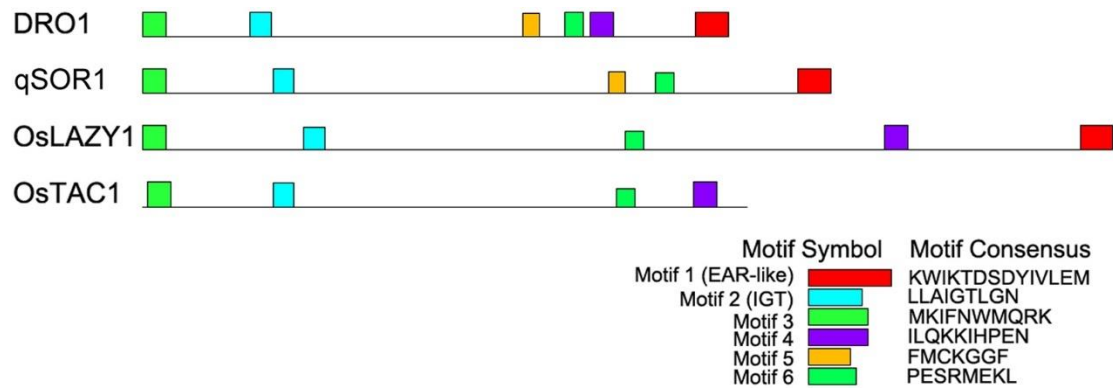
1200 **Figure S6. Root phenotypes and gene expression levels in the Acuce *dro1-cc***
 1201 **mutant.**

1202 Root phenotypes of wild-type Acuce (left) and the *dro1-cc* mutant (right) (A, B). Bar
 1203 = 5 cm. Expression levels of *OsPIN1b*, *OsPIN2* and *OsPIN3t* in the primary roots (C).

1204 Data are means \pm SD. ** $P < 0.01$ (SPSS analysis).

1205

1206



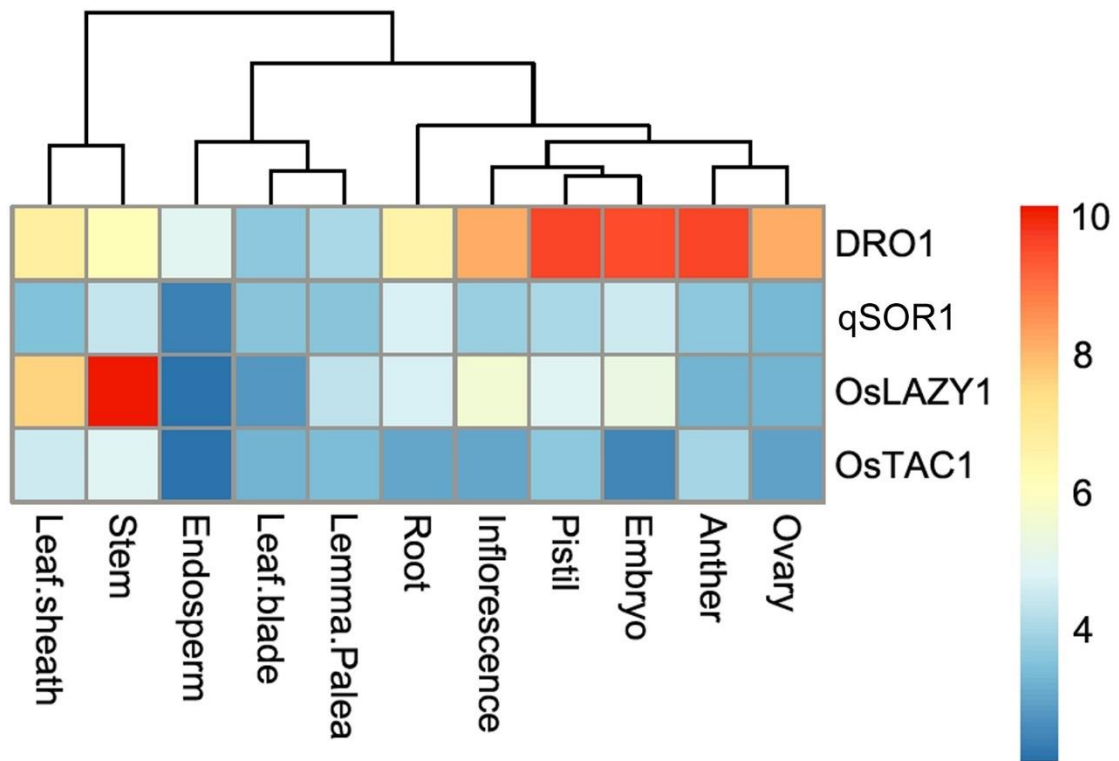
1207

1208 **Figure S7. Motif profiles in the rice IGT family.**

1209 The motifs in IGT family proteins DRO1, qSOR1, OsLAZY1 and OsTAC1 are shown

1210 in different colors. The color codes indicate different motifs.

1211

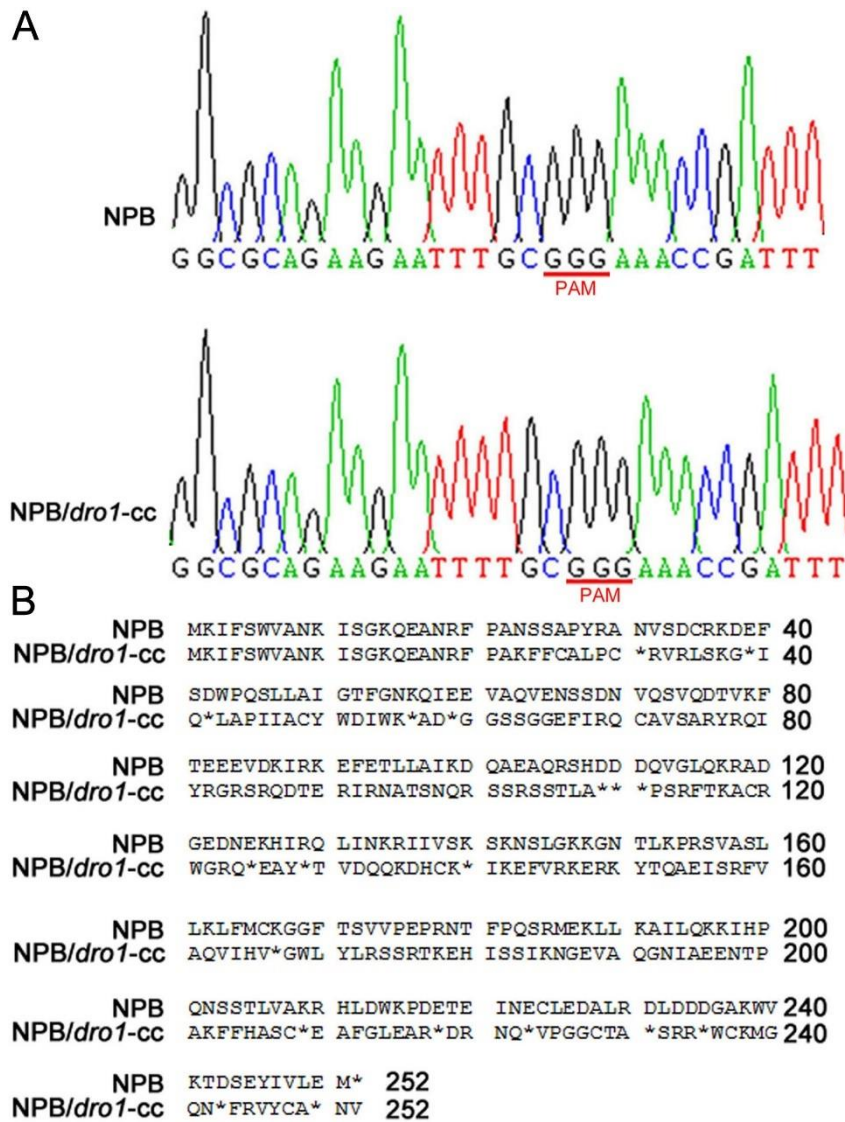


1212

1213 **Figure S8. Heat maps showing the expression profiles of IGT family genes in**
 1214 **Nipponbare.**

1215 The transcriptional levels of the IGT family genes *DRO1*, *qSOR1*, *OsLAZY1* and
 1216 *OsTAC1* in different rice tissues are indicated by different colors. The relative
 1217 expression intensity is color coded: blue = low; yellow = medium; and red = high.

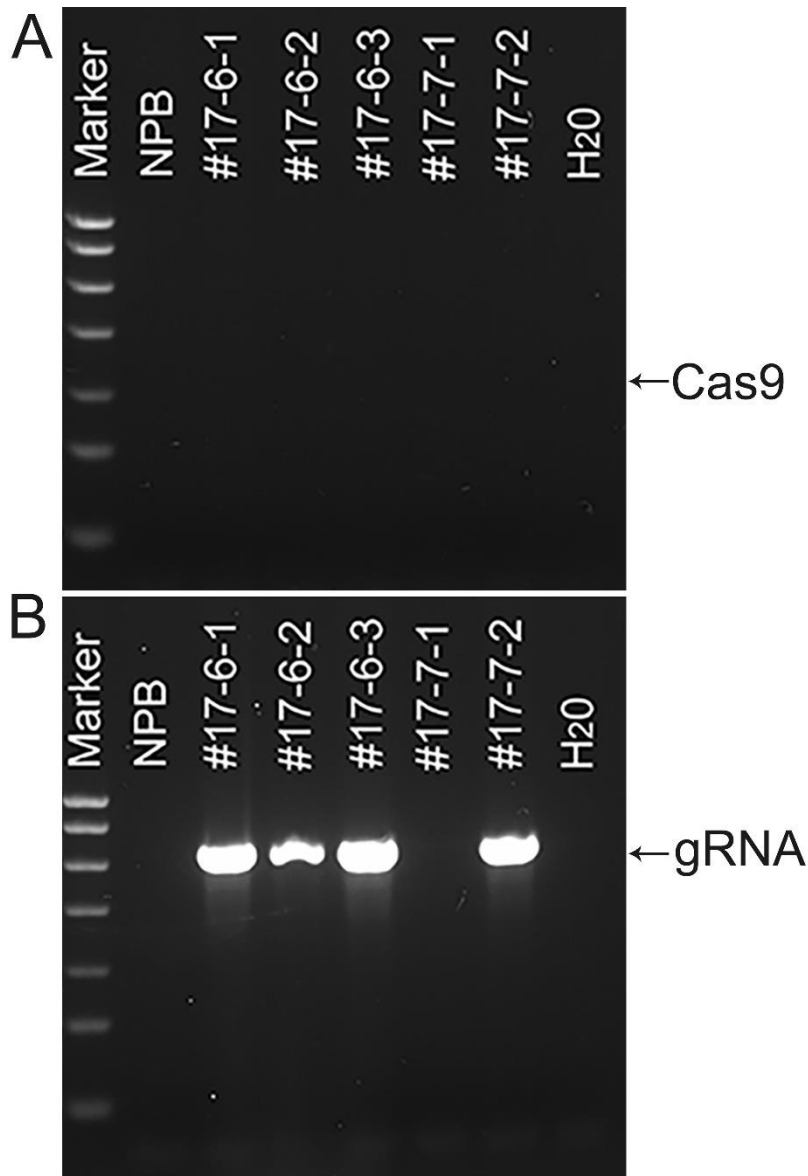
1218



1219
1220 **Figure S9. Sequence profiles of the *DROI* gene in Nipponbare and *DROI***
1221 **knockout mutant.**

1222 The genomic *DROI* gene of Nipponbare was knocked out using the CRISPR/Cas9
1223 method. Sequence map of the PCR product of the genomic *DROI* gene (A), amino
1224 acid sequences encoded by the *DROI* gene (B) in wild-type Nipponbare and the
1225 *dro1-cc* mutant. PAM = protospacer adjacent motif. Asterisks indicate translation
1226 termination.

1227

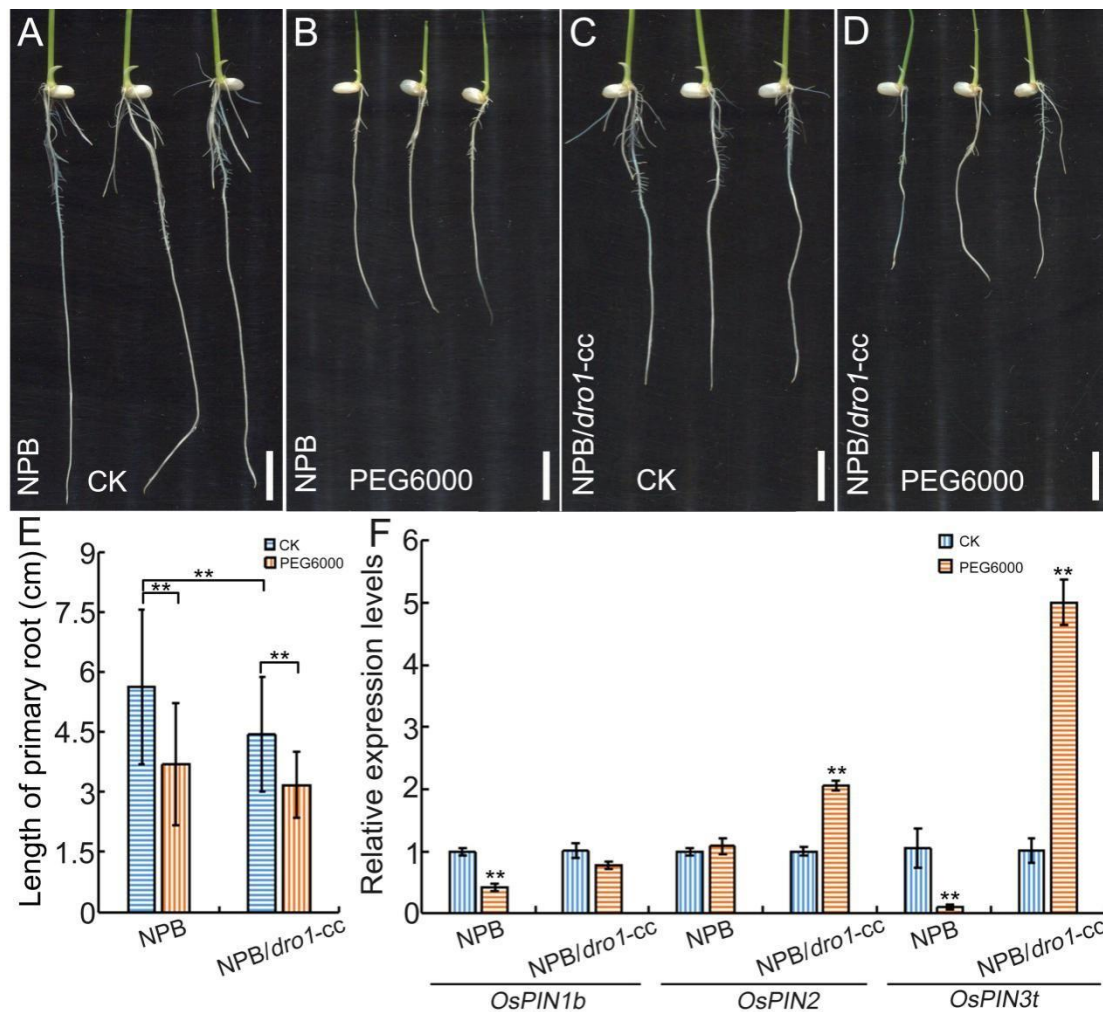


1228

1229 **Figure S10. PCR detection of the CRISPR cassette in Nipponbare *dro1-cc* line 17.**

1230 The *Cas9* (A) and *gRNA* (B) genes in the wild-type Nipponbare and *dro1-cc* mutant
 1231 line 17 (#17-6-1, #17-6-2, #17-6-3, #17-7-1, #17-7-2) genomes were amplified by
 1232 PCR using genomic DNA as the template. The arrow shows the PCR product of the
 1233 *Cas9* and *gRNA* genes with sizes of 371 bp and 550 bp, respectively. The negative
 1234 controls were used genomic DNA of wild-type Nipponbare and sterilized water as a
 1235 template in PCR. NPB = Nipponbare, gRNA = guide-RNA.

1236

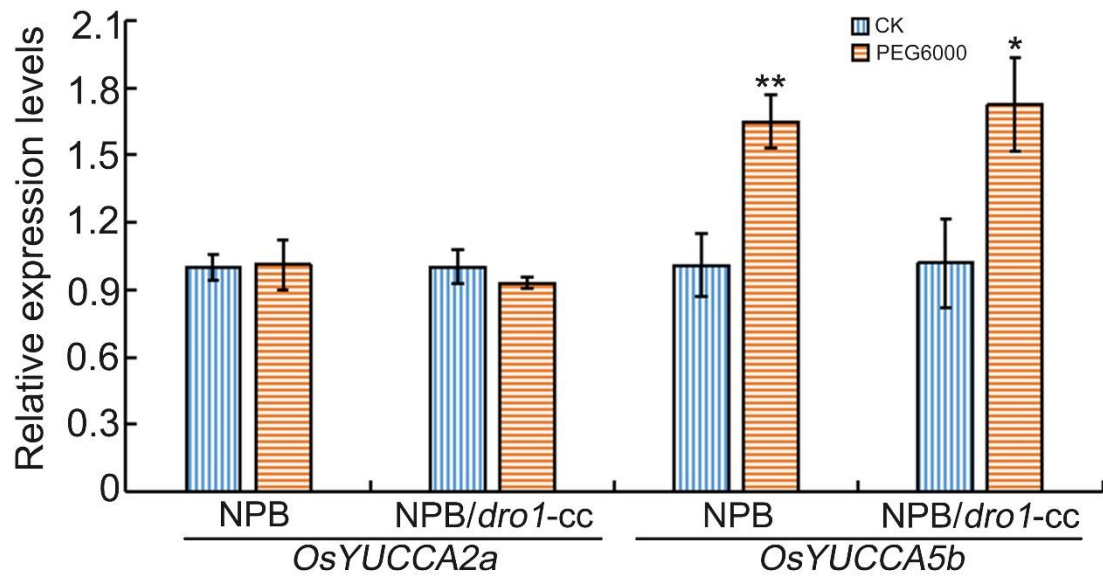


1237

1238 **Figure S11. Root phenotypes of the Nipponbare *dro1-cc* mutant.**

1239 Seedlings of Nipponbare (A, B) and the *dro1-cc* mutant (#17) (C, D) grown on MS
 1240 medium (A, C) or supplemented with 15% PEG6000 (B, D). Quantification of the
 1241 primary root lengths in Nipponbare and the *dro1-cc* mutant (E) (Nipponbare: $n_{CK}=31$,
 1242 $n_{PEG6000}=35$; NPB/*dro1-cc*: $n_{CK}=41$, $n_{PEG6000}=25$). The expression of *OsPIN1b*,
 1243 *OsPIN2* and *OsPIN3t* (F) in the primary root meristem region. CK = rice seedlings
 1244 grown on MS medium, PEG = rice seedlings grown on MS medium supplemented
 1245 with 15% PEG6000, NPB = Nipponbare. Bar = 1 cm. Data are means \pm SD; ** $P <$
 1246 0.01 (Student's *t*-test for root length analysis, SPSS analysis for gene expression).

1247

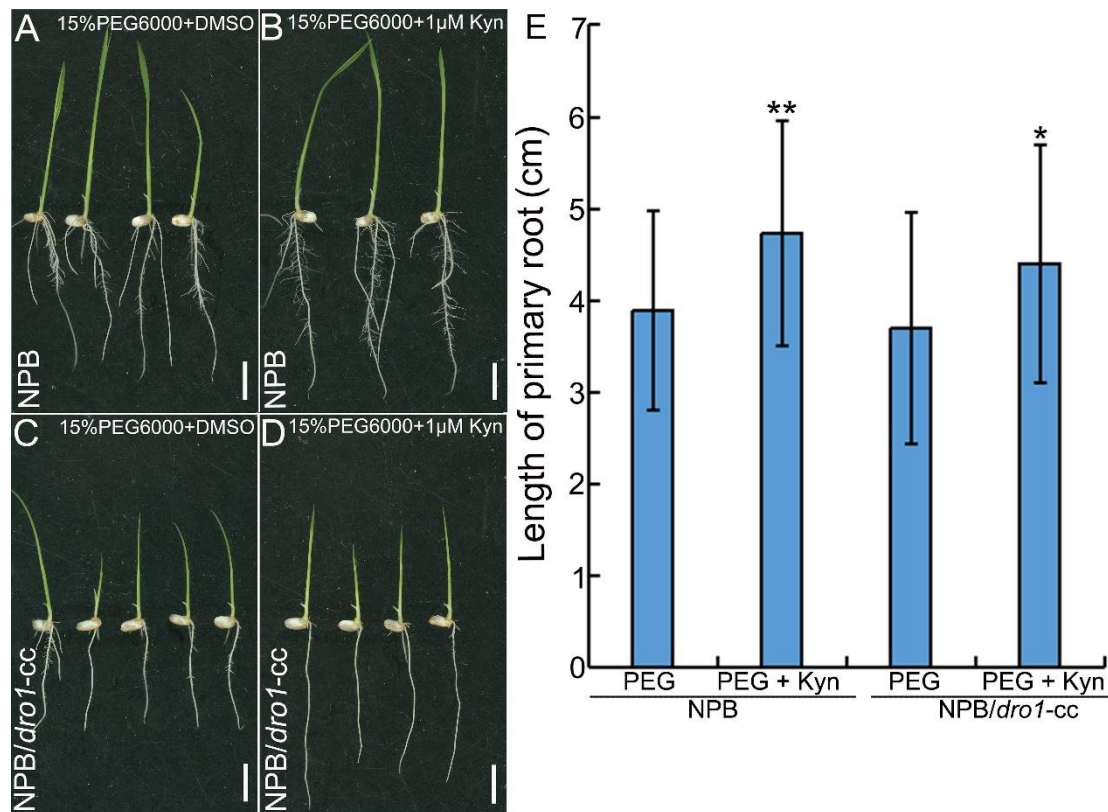


1248

1249 **Figure S12. The expression levels of *OsYUCCA2a* and *OsYUCCA5b* in the**
 1250 **Nipponbare *dro1-cc* mutant.**

1251 Seedlings of Nipponbare and the *dro1-cc* mutant grown on MS medium supplemented
 1252 with 15% PEG6000 for 4 days. The expression levels of the *OsYUCCA2a* and
 1253 *OsYUCCA5b* genes in the rice root meristem region were determined using real-time
 1254 PCR. The *OsActin* gene was used as an internal control. CK = seedlings grown on MS
 1255 medium, PEG = seedlings grown on MS medium supplemented with 15% PEG6000,
 1256 NPB = Nipponbare. Data are means \pm SD. * $P < 0.05$, ** $P < 0.01$ (SPSS analysis).

1257

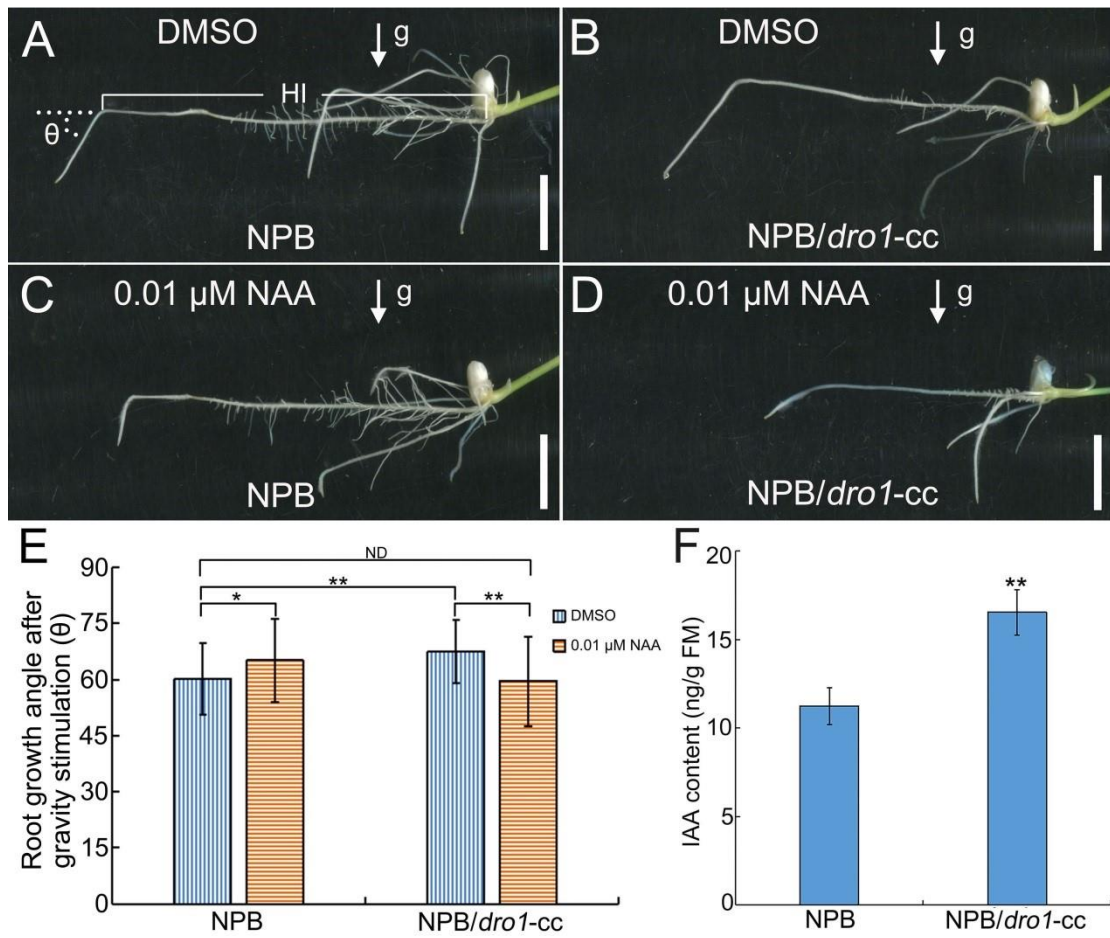


1258

1259 **Figure S13. Root lengths of the Nipponbare *dro1-cc* mutant grown under**
 1260 **drought stress co-treated with L-Kynurenine.**

1261 Seedlings of Nipponbare (A, B) and the *dro1-cc* mutant (C, D) grown on MS medium
 1262 (A, B) supplemented with 15% PEG6000 and co-treated with 1 μM Kyn (B, D) or
 1263 DMSO (A, C). Seedlings grown on the MS medium containing DMSO was acted as a
 1264 control. Quantification of primary root lengths in Nipponbare and the *dro1-cc* mutant
 1265 (E) (NPB: $n_{\text{PEG6000}} = 29$, $n_{\text{PEG6000+Kyn}} = 34$; NPB/*dro1-cc*: $n_{\text{PEG6000}} = 24$, $n_{\text{PEG6000+Kyn}} =$
 1266 30). Kyn = L-Kynurenine, NPB = Nipponbare, PEG = seedlings grown on MS
 1267 medium supplemented with 15% PEG6000. Data are means \pm SD; * $P < 0.05$, ** $P <$
 1268 0.01 (Student's *t*-test). Bar = 1 cm.

1269



1270

1271 **Figure S14. Auxin transport was disturbed in the Nipponbare *dro1-cc* mutant.**

1272 Root phenotypes of wild-type Nipponbare (A, C) and the *dro1-cc* (#17) mutant (B, D)

1273 grown on MS medium supplemented with DMSO (A, B) or 0.01 μ M NAA (C, D)

1274 under gravity stimulation. Seedlings grown on the MS medium containing DMSO

1275 was acted as a control. Quantification of root growth angles (E) (NPB: $n_{\text{DMSO}}=39$,

1276 $n_{\text{NAA}}=41$; NPB/*dro1-cc*: $n_{\text{DMSO}}=32$, $n_{\text{NAA}}=42$). IAA content in rice primary roots

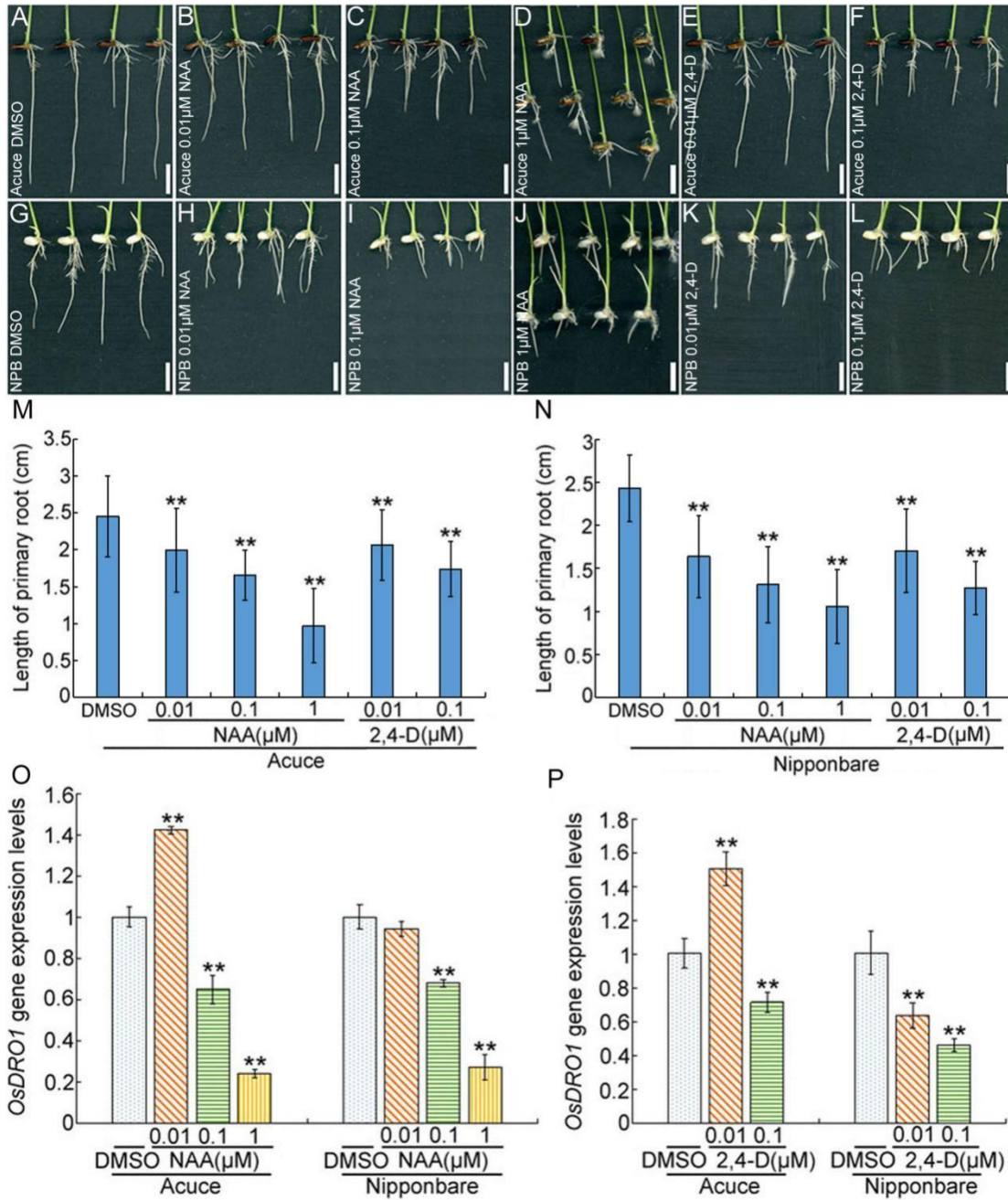
1277 grown in MS medium under gravity stimulation (F) (NPB: $n=3$, NPB/*dro1-cc*: $n=4$).

1278 Data are means \pm SD; * $P < 0.05$, ** $P < 0.01$ (Student's *t*-test). NPB = Nipponbare,

1279 HI = IAA content in parallel primary roots, g = gravity. Bar = 1 cm. The arrow shows

1280 the direction of gravity.

1281

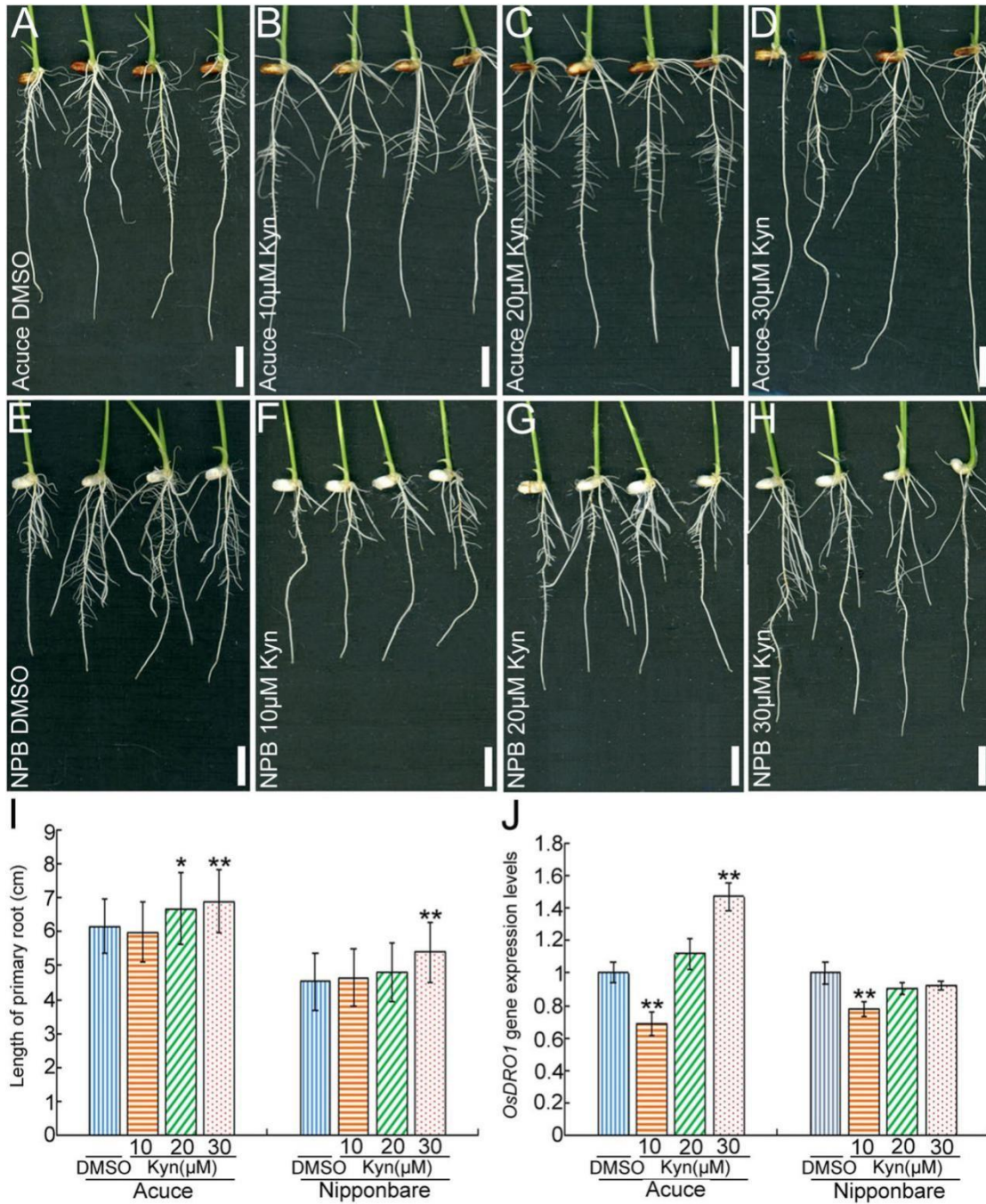


1282

1283 **Figure S15. Root phenotypes of rice seedlings treated with auxin.**

1284 Seedlings of Acuce and Nipponbare cultured with MS medium containing DMSO (A
 1285 and G), 0.01 μ M NAA (B and H), 0.1 μ M NAA (C and I), 1 μ M NAA (D and J), 0.01
 1286 μ M 2,4-D (E and K), and 0.1 μ M 2,4-D (F and L) for 4 days. Seedlings grown on the
 1287 MS medium containing DMSO was acted as a control. The primary root lengths were
 1288 measured and quantified (M and N) (Acuce: $n_{\text{DMSO}} = 49$, $n_{0.01 \mu\text{M NAA}} = 38$, $n_{0.1 \mu\text{M NAA}} =$
 1289 38 , $n_{1 \mu\text{M NAA}} = 42$, $n_{0.01 \mu\text{M 2,4-D}} = 37$, $n_{0.1 \mu\text{M 2,4-D}} = 53$; NPB: $n_{\text{DMSO}} = 23$, $n_{0.01 \mu\text{M NAA}} =$

1290 20, n_{0.1 μM NAA} = 19, n_{1 μM NAA} = 42, n_{0.01 μM 2,4-D} = 20, n_{0.1 μM 2,4-D} = 32). The expression
1291 levels of *DRO1* (O and P) in the rice root meristem region were determined using
1292 real-time PCR. The *OsActin* gene was used as an internal control. Data are means ±
1293 SD. ** $P < 0.01$ (Student's *t*-test for root length, SPSS analysis for differential gene
1294 expression). NPB = Nipponbare. Bar = 1 cm.
1295



1296

1297 **Figure S16. Root phenotypes of rice seedlings treated with L-Kynurenine.**

1298 Four-day-old seedlings of Acuce and Nipponbare cultured with MS medium
 1299 containing DMSO (A and E) or 10 μM (B and F), 20 μM (C and G), and 30 μM (D
 1300 and H) L-Kynurenine for 4 days. Seedlings grown on the MS medium containing
 1301 DMSO was acted as a control. The primary root lengths were measured and
 1302 quantified (I) (Acuce: $n_{\text{DMSO}} = 34$, $n_{10 \mu\text{M Kyn}} = 46$, $n_{20 \mu\text{M Kyn}} = 40$, $n_{30 \mu\text{M Kyn}} = 38$; NPB:

1303 $n_{\text{DMSO}} = 23$, $n_{10 \mu\text{M Kyn}} = 26$, $n_{20 \mu\text{M Kyn}} = 30$, $n_{30 \mu\text{M Kyn}} = 28$). The expression levels of
1304 *DROI* in the rice root meristem region were determined using real-time PCR (J). The
1305 *OsActin* gene was used as an internal control. Data are means \pm SD. * $P < 0.05$, ** P
1306 < 0.01 (Student's *t*-test for root length, SPSS analysis for differential gene expression).
1307 NPB = Nipponbare, Kyn = L-Kynurenine. Bar = 1 cm.
1308

IR64 ATATATATTTTGAATTCGTTCGCATACTTTTAAACCCTAAAAAGGTACGTTTCGTACGGAACTTTCTACATAGAAA 80
Acuce ATATATATTTTGAATTCGTTCGCATACTTTTAAACCCTAAAAAGGTACGTTTCGTACGGAACTTTCTACATAGAAA 80
Kinandang Patong ATATATATTTTGAATTCGTTCGCATACTTTTAAACCCTAAAAAGGTACGTTTCGTACGGAACTTTCTACATAGAAA 80
Nipponbare ATATATATTTTGAATTCGTTCGCATACTTTTAAACCCTAAAAAGGTACGTTTCGTACGGAACTTTCTACATAGAAA 80

IR64 TTGCTCTAAAATATTAACATAAATCAATTTTCCAACACTAGTAATAATTAACCTTAATTAACCATAGTAACCTTTCTTTTTT 160
Acuce TTGCTCTAAAATATTAACATAAATCAATTTTCCAACACTAGTAATAATTAACCTTAATTAACCATAGTAACCTTTCTTTTTT 160
Kinandang Patong TTGCTCTAAAATATTAACATAAATCAATTTTCCAACACTAGTAATAATTAACCTTAATTAACCATAGTAACCTTTCTTTTTT 160
Nipponbare TTGCTCTAAAATATTAACATAAATCAATTTTCCAACACTAGTAATAATTAACCTTAATTAACCATAGTAACCTTTCTTTTTT 160

IR64 TT--ATGCTCTTACTTAATCTTAATCTTTATTAGTTTCAAGCACCACCTTATTTTCATCTTTATCCCTAGCTCGTCTCC 240
Acuce TT--ATGCTCTTACTTAATCTTAATCTTTATTAGTTTCAAGCACCACCTTATTTTCATCTTTATCCCTAGCTCGTCTCC 240
Kinandang Patong TT--ATGCTCTTACTTAATCTTAATCTTTATTAGTTTCAAGCACCACCTTATTTTCATCTTTATCCCTAGCTCGTCTCC 240
Nipponbare TT--ATGCTCTTACTTAATCTTAATCTTTATTAGTTTCAAGCACCACCTTATTTTCATCTTTATCCCTAGCTCGTCTCC 240

IR64 CCAACAGTCACGGCTAAGTCCCAGCACAGTCGCACTCTCTCCCATCTTGTGCCTCCGCTCCCTCCACTAGCTTGTAGG 320
Acuce CCAACAGTCACGGCTAAGTCCCAGCACAGTCGCACTCTCTCCCATCTTGTGCCTCCGCTCCCTCCACTAGCTTGTAGG 320
Kinandang Patong CCAACAGTCACGGCTAAGTCCCAGCACAGTCGCACTCTCTCCCATCTTGTGCCTCCGCTCCCTCCACTAGCTTGTAGG 320
Nipponbare CCAACAGTCACGGCTAAGTCCCAGCACAGTCGCACTCTCTCCCATCTTGTGCCTCCGCTCCCTCCACTAGCTTGTAGG 320

IR64 TGGCTGGCGACAATGCCTCCAGGCCGCTGAAGGAGAGTGCCTGAAGGAGGAGAACGACAACCTAGCTTGTGGGATTGAGG 400
Acuce TGGCTGGCGACAATGCCTCCAGGCCGCTGAAGGAGAGTGCCTGAAGGAGGAGAACGACAACCTAGCTTGTGGGATTGAGG 400
Kinandang Patong TGGCTGGCGACAATGCCTCCAGGCCGCTGAAGGAGAGTGCCTGAAGGAGGAGAACGACAACCTAGCTTGTGGGATTGAGG 400
Nipponbare TGGCTGGCGACAATGCCTCCAGGCCGCTGAAGGAGAGTGCCTGAAGGAGGAGAACGACAACCTAGCTTGTGGGATTGAGG 400

IR64 AATTGCAGGCAAAATTTACTCTCAAAACATGTATCGAAATGATCGGTGAGCTCGGCCATGACCGAAGACCGAATATAA 480
Acuce AATTGCAGGCAAAATTTACTCTCAAAACATGTATCGAAATGATCGGTGAGCTCGGCCATGACCGAAGACCGAATATAA 480
Kinandang Patong AATTGCAGGCAAAATTTACTCTCAAAACATGTATCGAAATGATCGGTGAGCTCGGCCATGACCGAAGACCGAATATAA 480
Nipponbare AATTGCAGGCAAAATTTACTCTCAAAACATGTATCGAAATGATCGGTGAGCTCGGCCATGACCGAAGACCGAATATAA 480

IR64 AAATGATGAAATATTTTAGGTTTTACGGTTTTATATTAATTTTCGATCTTGATTTTAGAGGCTGAAGTTTTGAGAGGACC 560
Acuce AAATGATGAAATATTTTAGGTTTTACGGTTTTATATTAATTTTCGATCTTGATTTTAGAGGCTGAAGTTTTGAGAGGACC 560
Kinandang Patong AAATGATGAAATATTTTAGGTTTTACGGTTTTATATTAATTTTCGATCTTGATTTTAGAGGCTGAAGTTTTGAGAGGACC 560
Nipponbare AAATGATGAAATATTTTAGGTTTTACGGTTTTATATTAATTTTCGATCTTGATTTTAGAGGCTGAAGTTTTGAGAGGACC 560

IR64 GAAAAACCAACAAAATTAATCGGTGAGACTGAATAACCCACCCTACTCACCACGTAGCGATAAGAATGTGTGTTTGA 640
Acuce GAAAAACCAACAAAATTAATCGGTGAGACTGAATAACCCACCCTACTCACCACGTAGCGATAAGAATGTGTGTTTGA 640
Kinandang Patong GAAAAACCAACAAAATTAATCGGTGAGACTGAATAACCCACCCTACTCACCACGTAGCGATAAGAATGTGTGTTTGA 640
Nipponbare GAAAAACCAACAAAATTAATCGGTGAGACTGAATAACCCACCCTACTCACCACGTAGCGATAAGAATGTGTGTTTGA 640

IR64 AATTGACTAGAGATATCTAATTAGTAGAATTTTCGTTAGCGCTT-----CTAATCTAAACTGATAAAATTTGG 720
Acuce AATTGACTAGAGATATCTAATTAGTAGAATTTTCGTTAGCGCTTTCGTTAGCGCTTCTAATCTAAACTGATAAAATTTGG 720
Kinandang Patong AATTGACTAGAGATATCTAATTAGTAGAATTTTCGTTAGCGCTT-----CTAATCTAAACTGATAAAATTTGG 720
Nipponbare AATTGACTAGAGATATCTAATTAGTAGAATTTTCGTTAGCGCTT-----CTAATCTAAACTGATAAAATTTGG 720

IR64 TTTTGTACAATGTATTGCCACAACGTAATTTTAGTTTTGCAGA GATATATA TATATATATATATATATATA TAGCAC 800
Acuce TTTTGTACAATGTATTGCCACAACGTAATTTTAGTTTTGCAGA-----TATATATATATATATATATA TAGCAC 800
Kinandang Patong TTTTGTACAATGTATTGCCACAACGTAATTTTAGTTTTGCAGA GATATATA TATATATATATATATATATA TAGCAC 800
Nipponbare TTTTGTACAATGTATTGCCACAACGTAATTTTAGTTTTGCAGA-----TATATATATATATATATATA TAGCAC 800

IR64 TATCATGTCATGTTAGCTTGTGGTCCAGGTGCATCCACGGTCTAGTACCATTATTGCGTAGTTAATGGACGGAATAGCT 880
Acuce TATCATGTCATGTTAGCTTGTGGTCCAGGTGCATCCACGGTCTAGTACCATTATTGCGTAGTTAATGGACGGAATAGCT 880
Kinandang Patong TATCATGTCATGTTAGCTTGTGGTCCAGGTGCATCCACGGTCTAGTACCATTATTGCGTAGTTAATGGACGGAATAGCT 880
Nipponbare TATCATGTCATGTTAGCTTGTGGTCCAGGTGCATCCACGGTCTAGTACCATTATTGCGTAGTTAATGGACGGAATAGCT 880

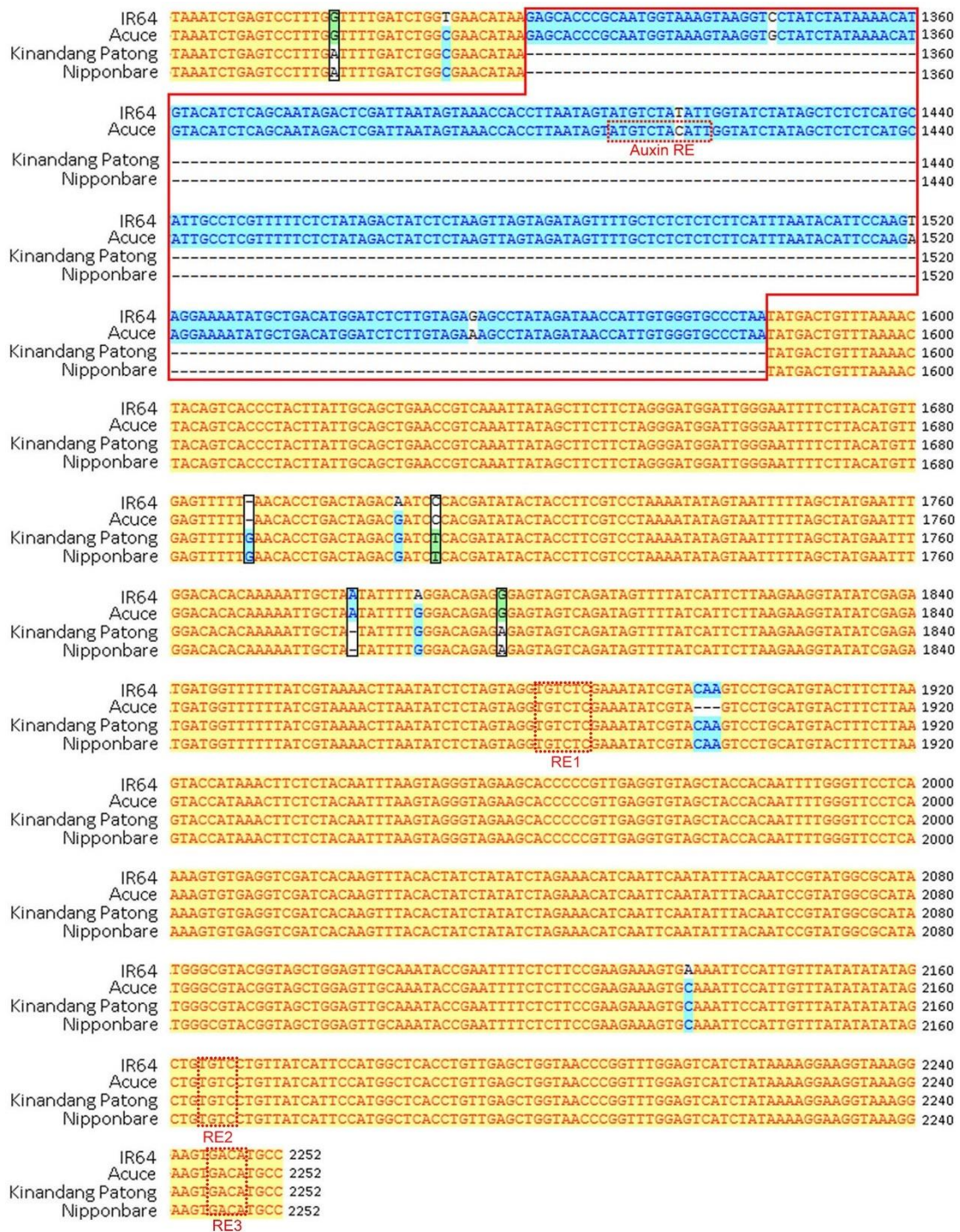
IR64 GCTAGTGGAGATGGGGGTGTACTTCAGCAGTTAACCCCGAGAACCTGATTAGCATCGGTGACGGCGCCCTCGTGTGG 960
Acuce GCTAGTGGAGATGGGGGTGTACTTCAGCAGTTAACCCCGAGAACCTGATTAGCATCGGTGACGGCGCCCTCGTGTGG 960
Kinandang Patong GCTAGTGGAGATGGGGGTGTACTTCAGCAGTTAACCCCGAGAACCTGATTAGCATCGGTGACGGCGCCCTCGTGTGG 960
Nipponbare GCTAGTGGAGATGGGGGTGTACTTCAGCAGTTAACCCCGAGAACCTGATTAGCATCGGTGACGGCGCCCTCGTGTGG 960

IR64 TTAACCAAGGCGGGCGCCCGTACTTACCCGCGCTAATGCCGGTTTTAAGGAAGTTAACACGTGATTCTGGCACACCGGT 1040
Acuce TTAACCAAGGCGGGCGCCCGTACTTACCCGCGCTAATGCCGGTTTTAAGGAAGTTAACACGTGATTCTGGCACACCGGT 1040
Kinandang Patong TTAACCAAGGCGGGCGCCCGTACTTACCCGCGCTAATGCCGGTTTTAAGGAAGTTAACACGTGATTCTGGCACACCGGT 1040
Nipponbare TTAACCAAGGCGGGCGCCCGTACTTACCCGCGCTAATGCCGGTTTTAAGGAAGTTAACACGTGATTCTGGCACACCGGT 1040

IR64 CGGGCCCGACCAAGTGCATGGGATCCGTTGCGGCGCGGTCTGACACTTGGTGCCCAACTTGCCGTCGATCTCGCCGC 1120
Acuce CGGGCCCGACCAAGTGCATGGGATCCGTTGCGGCGCGGTCTGACACTTGGTGCCCAACTTGCCGTCGATCTCGCCGC 1120
Kinandang Patong CGGGCCCGACCAAGTGCATGGGATCCGTTGCGGCGCGGTCTGACACTTGGTGCCCAACTTGCCGTCGATCTCGCCGC 1120
Nipponbare CGGGCCCGACCAAGTGCATGGGATCCGTTGCGGCGCGGTCTGACACTTGGTGCCCAACTTGCCGTCGATCTCGCCGC 1120

IR64 GCTGTACTTTATCTTAGCTAATAACTCTTCTCTCCCCCTGGAAAAAATAAACAACCGGGTTTCTCCCTTTGAGGC 1200
Acuce GCTGTACTTTATCTTAGCTAATAACTCTTCTCTCCCCCTGGAAAAAATAAACAACCGGGTTTCTCCCTTTGAGGC 1200
Kinandang Patong GCTGTACTTTATCTTAGCTAATAACTCTTCTCTCCCCCTGGAAAAAATAAACAACCGGGTTTCTCCCTTTGAGGC 1200
Nipponbare GCTGTACTTTATCTTAGCTAATAACTCTTCTCTCCCCCTGGAAAAAATAAACAACCGGGTTTCTCCCTTTGAGGC 1200

IR64 ATTGATTTTTGGATACTCTCTCGTGGCTGCAGTGAAGCGAACCCAGTGCACGGTATTCAAACAGTCTGCAATACCTGGG 1280
Acuce ATTGATTTTTGGATACTCTCTCGTGGCTGCAGTGAAGCGAACCCAGTGCACGGTATTCAAACAGTCTGCAATACCTGGG 1280
Kinandang Patong ATTGATTTTTGGATACTCTCTCGTGGCTGCAGTGAAGCGAACCCAGTGCACGGTATTCAAACAGTCTGCAATACCTGGG 1280
Nipponbare ATTGATTTTTGGATACTCTCTCGTGGCTGCAGTGAAGCGAACCCAGTGCACGGTATTCAAACAGTCTGCAATACCTGGG 1280



1310

1311 **Figure S17. Sequences of the *DRO1* promoter in different rice varieties.**

1312 Sequences of *DRO1* promoters from the rice varieties Acuce, Nipponbare, IR64 and

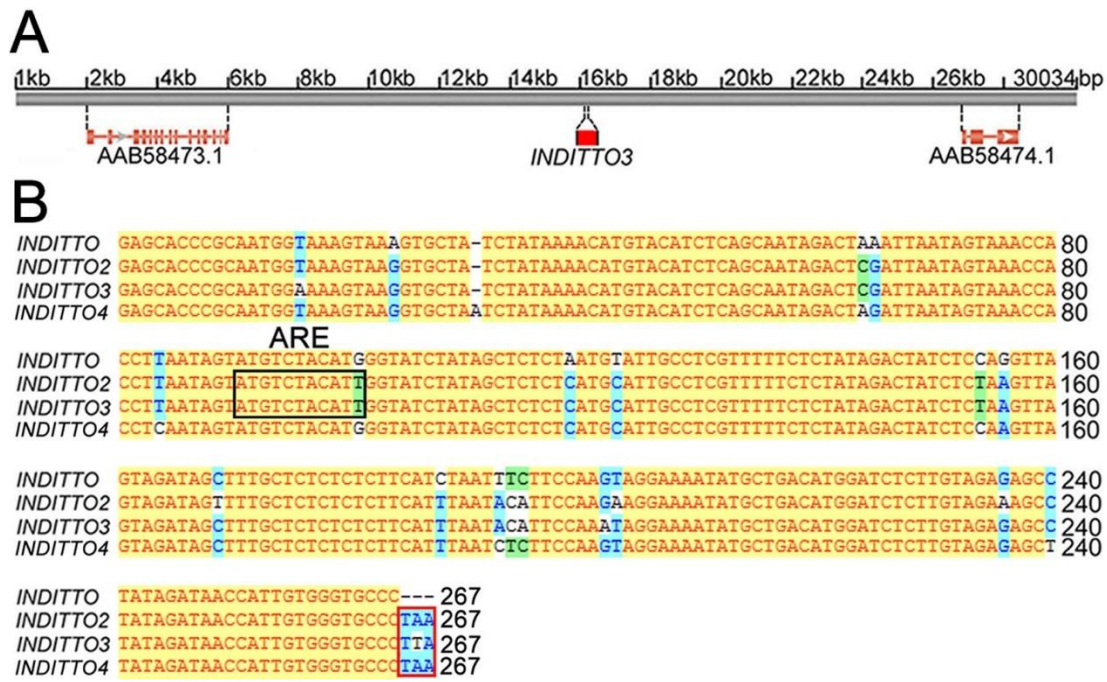
1313 Kinandang Patong were aligned. The conserved sequences are indicated by black

1314 boxes. The sequences of *INDITTO2* transposons are labelled with red boxes. Auxin

1315 RE = auxin response element. RE1, 2, 3 = auxin response element 1, 2 and 3,

1316 respectively.

1317

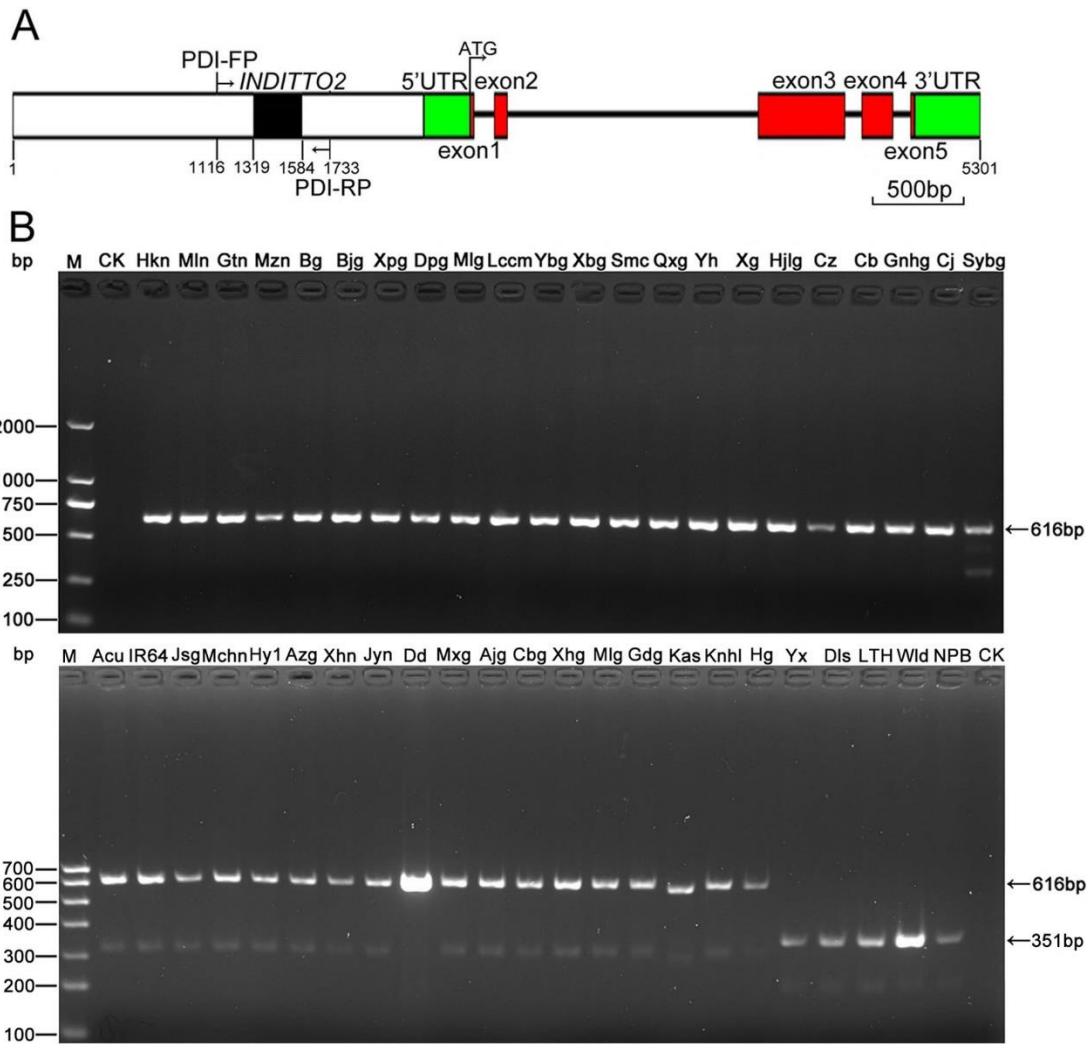


1318

1319 **Figure S18. Positions and sequences of the *INDITTO2* transposon and its**
1320 **homologues genes in different rice varieties.**

1321 Position of the *INDITTO3* transposon in the Teqing genome obtained from the NCBI
1322 database (A). Sequence alignments of the *INDITTO*, *INDITTO2*, *INDITTO3* and
1323 *INDITTO4* transposons (B). The *INDITTO4* transposon was amplified from the
1324 Nipponbare genome. The red box represents the target site duplication (TSD)
1325 sequence. The black box represents the auxin response element (ARE).

1326

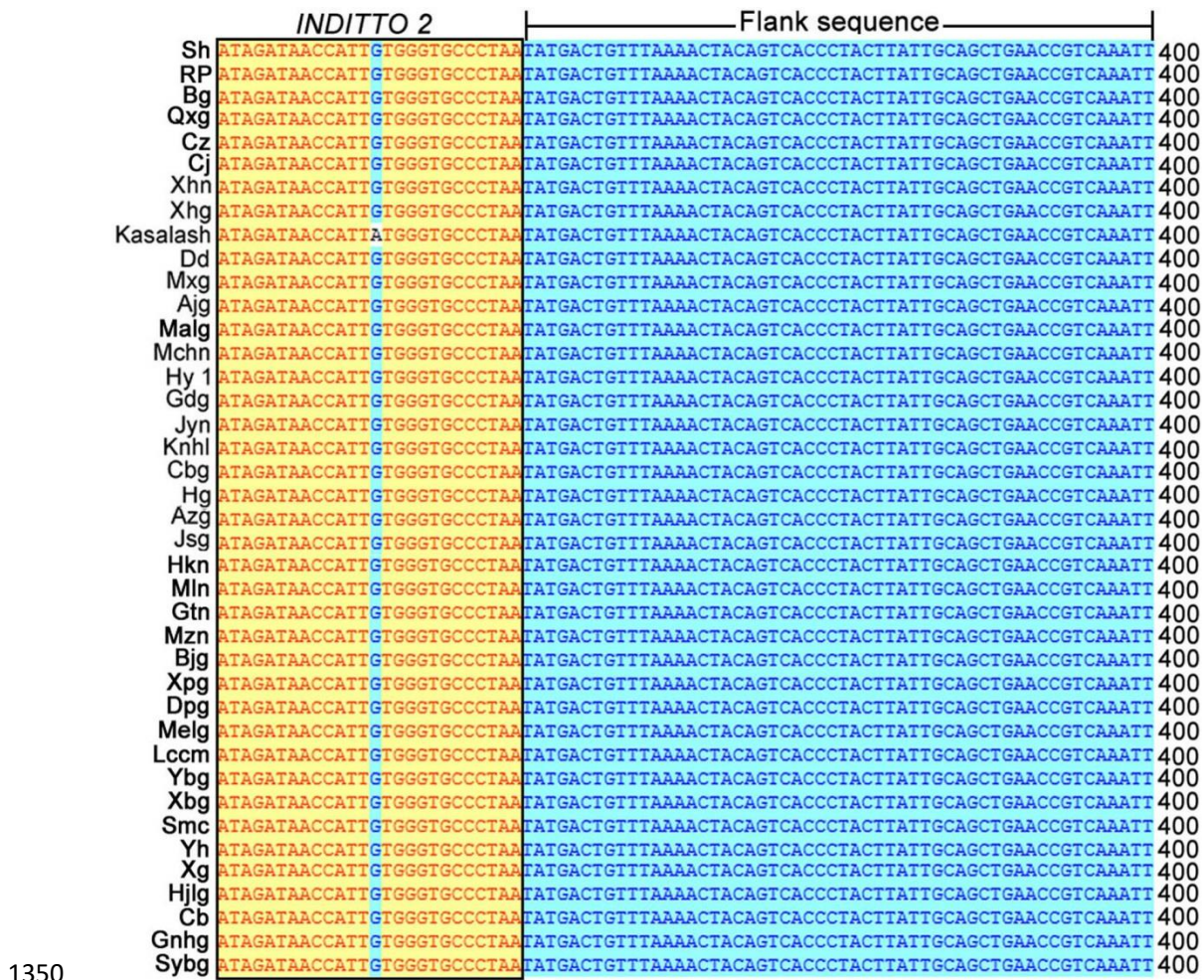


1327

1328 **Figure S19. Amplification of the *INDITTO2* transposon and its homologues genes**
 1329 **from different rice genomes.**

1330 Schematic diagram of the *INDITTO2* transposon located in the *DRO1* promoter of
 1331 *Acuce* (A). Agarose gel electrophoresis shows the PCR product of the *INDITTO2*
 1332 transposon amplified with the primer pair PDI-FP and PDI-RP from 45 rice varieties
 1333 (B). The arrow shows the PCR product of the *INDITTO2* transposon with a size of
 1334 616 bp amplified with primers PDI-FP and PDI-RP. The 351 bp PCR product was
 1335 non-specifically amplified. Acu = *Acuce*, Ajg = *Ai jiao gu*, Azg = *Ai zhe gu*, Bg =
 1336 *Bai gu*, Big = *Ban jiu gu*, Cb = *Che bu*, Cbg = *Chuan bai gu*, Cj = *Che jia*, Cz = *Che*
 1337 *zuo*, Dd = *Duo dian*, Dls = *Da leng shui*, Dpg = *Da pi gu*, Gdg = *Gan di gu*, Gnhg =
 1338 *Ga niang hong gu*, Gtn = *Gan tian nuo*, Hg = *Hei gu*, Hjljg = *Hong jiao lao geng*, Hkn

1339 = Hua ke nuo, Hy 1 = Hong yang 1, IR64 = IR64, Jsg = Jian shui gu, Jyn = Jiu yue
1340 nuo, Kas = Kasalath, Knhl = Kou ni he lve, Lccm = Le che che ma, LTH = Li jiang
1341 xin tuan hei gu, Mchn = Man che hong nuo, Mlg = Mao lai gu, Mlg = Meng la gu,
1342 Mln = Meng la nuo, Mxg = Ma xian gu, Mzn = Ma zha nuo, NPB = Nipponbare, Qxg
1343 = Qi xian gu, Smc = Si ma che, Sybg = Shi yue bai gu, Wld = Wen lu dao 4, Xbg =
1344 Xi bai gu, Xg = Xiao gu, Xhg = Xiao hua gu, Xhn = Xiao hua nuo, Xpg = Xiao pi gu,
1345 Ybg = Ye bai gu, Yh = Yun hui 290, Yx = Yun xiang. M = DNA marker, CK = H₂O,
1346 which served as a negative control.
1347



1351 **Figure S20. Sequence alignments of the *INDITTO2* transposon and its**
 1352 **homologues genes in the *DRO1* promoters of different rice varieties.**

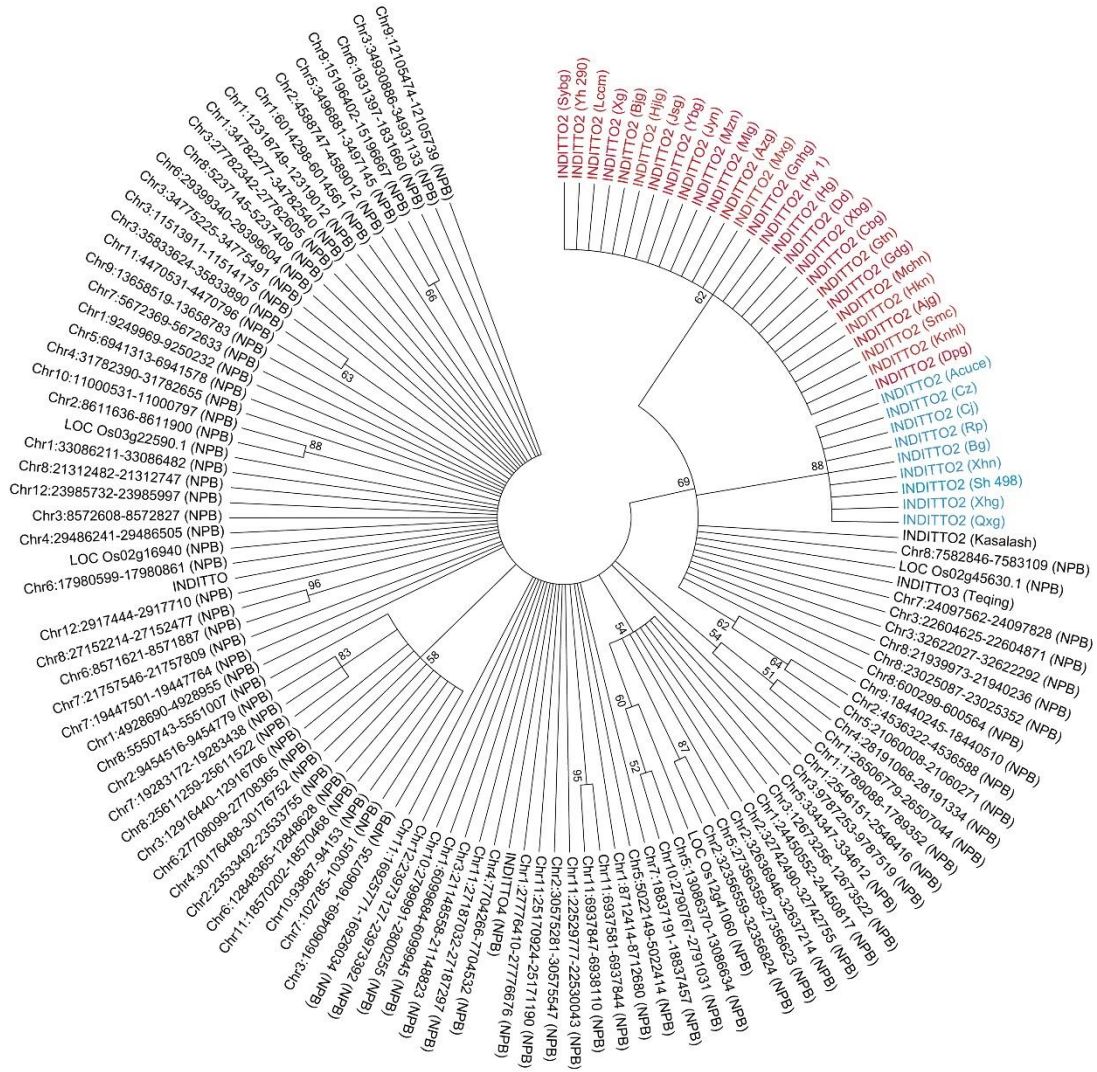
1353 Forty sequences of the *INDITTO2* transposon were amplified from 38 rice varieties
 1354 and two sequences from Shuhui498 and RP Bio-226 obtained from the NCBI
 1355 database. The red box represents an auxin response element (ARE). Ajg = Ai jiao gu,
 1356 Azg = Ai zhe gu, Bg = Bai gu, Bjg = Ban jiu gu, Cb = Che bu, Cbg = Chuan bai gu,
 1357 Cj = Che jia, Cz = Che zuo, Dd = Duo dian, Dpg = Da pi gu, Gdg = Gan di gu, Gnhg
 1358 = Ga niang hong gu, Gtn = Gan tian nuo, Hg = Hei gu, Hjlg = Hong jiao lao geng,
 1359 Hkn = Hua ke nuo, Hy 1 = Hong yang 1, Jsg = Jian shui gu, Jyn = Jiu yue nuo, Knhl =
 1360 Kou ni he lve, Lccm = Le che che ma, Malg = Mao lai gu, Mchn = Man che hong nuo,
 1361 Melg = Meng la gu, Mln = Meng la nuo, Mxg = Ma xian gu, Mzn = Ma zhe nuo, Qxg

1362 = Qi xian gu, RP = RP Bio-226, Sh = Shuhui498, Smc = Si ma che, Sybg = Shi yue

1363 bai gu, Xbg = Xi bai gu, Xg = Xiao gu, Xhg = Xiao hua gu, Xhn = Xiao hua nuo, Xpg

1364 = Xiao pi gu, Ybg = Ye bai gu, Yh = Yun hui 290.

1365

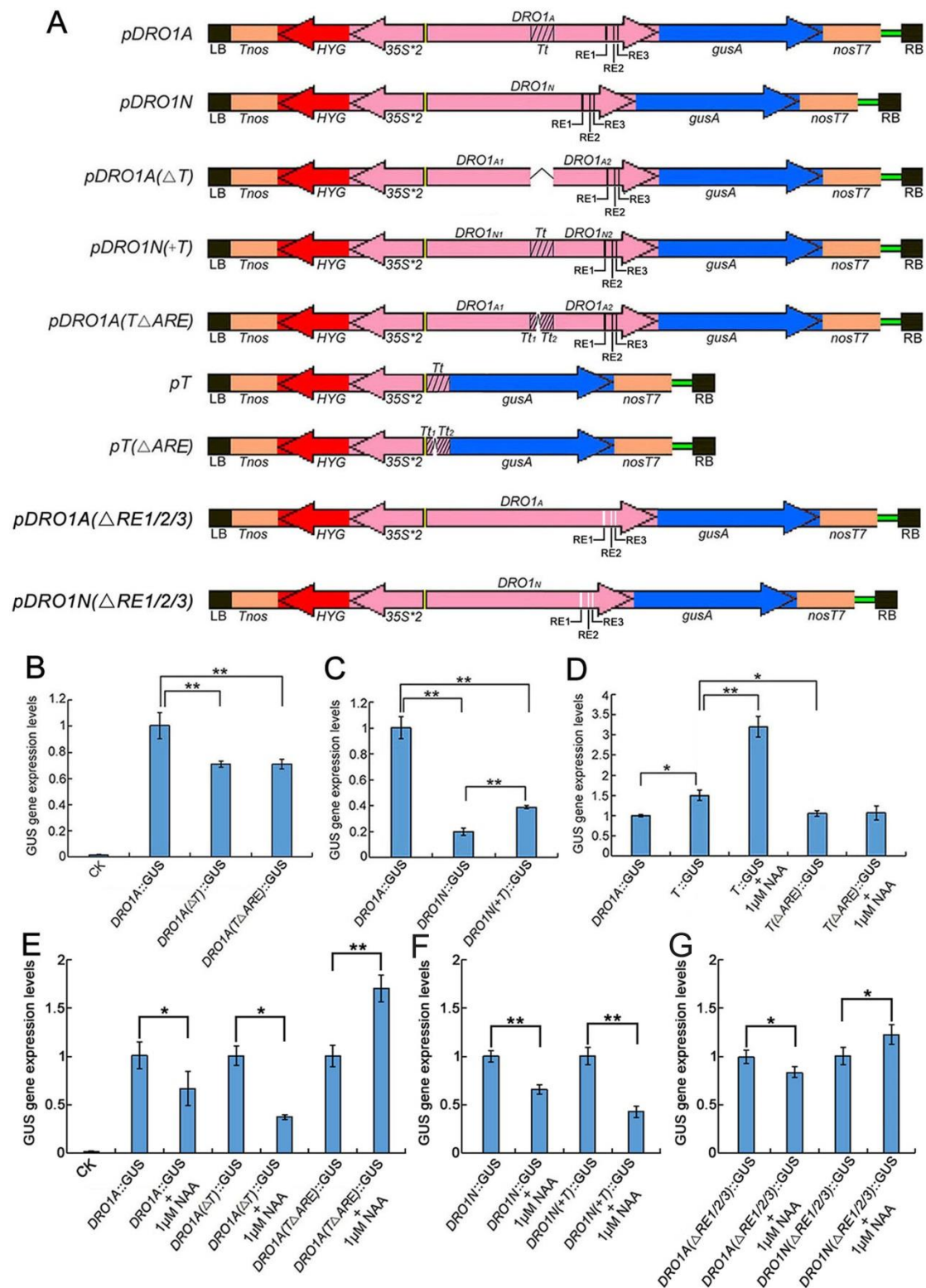


1366

1367 **Figure S21. Phylogeny of *INDITTO* and its homologues from different**
 1368 **varieties.**

1369 Phylogenetic tree constructed based on neighbour-joining (NJ) analysis. The numbers
 1370 indicate bootstrap values at the branching points. The name of homologues of the
 1371 *INDITTO4* transposon was represented by the gene position in the Nipponbare
 1372 genome. Ajg = Ai jiao gu, Azg = Ai zhe gu, Bg = Bai gu, Bjg = Ban jiu gu, Cbg =
 1373 Chuan bai gu, Cj = Che jia, Cz = Che zuo, Dd = Duo dian, Dpg = Da pi gu, Gdg =
 1374 Gan di gu, Gnhg = Ga niang hong gu, Gtn = Gan tian nuo, Hg = Hei gu, Hjlj = Hong
 1375 jiao lao geng, Hkn = Hua ke nuo, Hy 1 = Hong yang 1, Jsg = Jian shui gu, Jyn = Jiu
 1376 yue nuo, Knhl = Kou ni he lve, Lccm = Le che che ma, Mchm = Man che hong nuo,

1377 Mlg = Meng la gu, Mxg = Ma xian gu, Mzn = Ma zhe nuo, NPB = Nipponbare, Qxg
1378 = Qi xian gu, RP = RP Bio-226, Sh = Shuhui498, Smc = Si ma che, Sybg = Shi yue
1379 bai gu, Xbg = Xi bai gu, Xg = Xiao gu, Xhg = Xiao hua gu, Xhn = Xiao hua nuo, Ybg
1380 = Ye bai gu, Yh 290= Yun hui 290.
1381



1382

1383 **Figure S22. Expression levels of the *GUS* gene in tobacco leaves.**

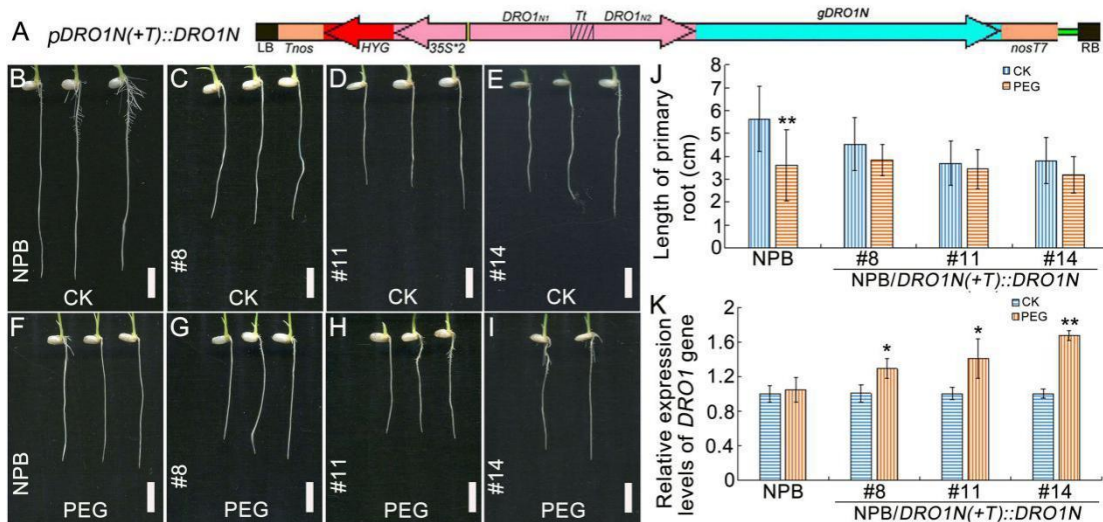
1384 Schematic diagram of the expression vector containing the *DRO1* promoter and

1385 *INDITTO2* transposon (A). A solution of *Agrobacterium* strain EHA105 transformed

1386 with the expression vector was infiltrated into tobacco leaves with or without 1 μM

1387 NAA supplementation. The expression levels of the *GUS* gene (B-G) in tobacco
1388 leaves were determined using real-time PCR. The *NaActin* gene was used as an
1389 internal control. Data are means \pm SD. * $P < 0.05$, ** $P < 0.01$ (SPSS analysis). CK =
1390 tobacco leaf without treatment (negative control). *DROIA* = the Acuce *DROI*
1391 promoter, *DROIN* = the Nipponbare *DROI* promoter, *DROIA*(ΔT) = the Acuce
1392 *DROI* promoter with deletion of the *INDITTO2* transposon, *DROIA*($T\Delta ARE$) = the
1393 Acuce *DROI* promoter containing the *INDITTO2* transposon with an ARE deletion,
1394 *DROIN*(+*T*) = the *INDITTO2* transposon inserted into the Nipponbare *DROI*
1395 promoter, *pT* = the expression construct containing the *INDITTO2* transposon, *pT*(Δ
1396 *ARE*) = the expression construct containing the *INDITTO2* transposon with an ARE
1397 deletion, *DROIA*($\Delta RE1/2/3$) = the Acuce *DROI* promoter with deletion of 3 AREs,
1398 *DROIN*($\Delta RE1/2/3$) = the Nipponbare *DROI* promoter with deletion of 3 AREs, Tt =
1399 *INDITTO2* transposon, RE 1, 2, 3 = auxin response element 1, 2 and 3, *gusA* = *GUS*
1400 gene, ARE = auxin response element.

1401

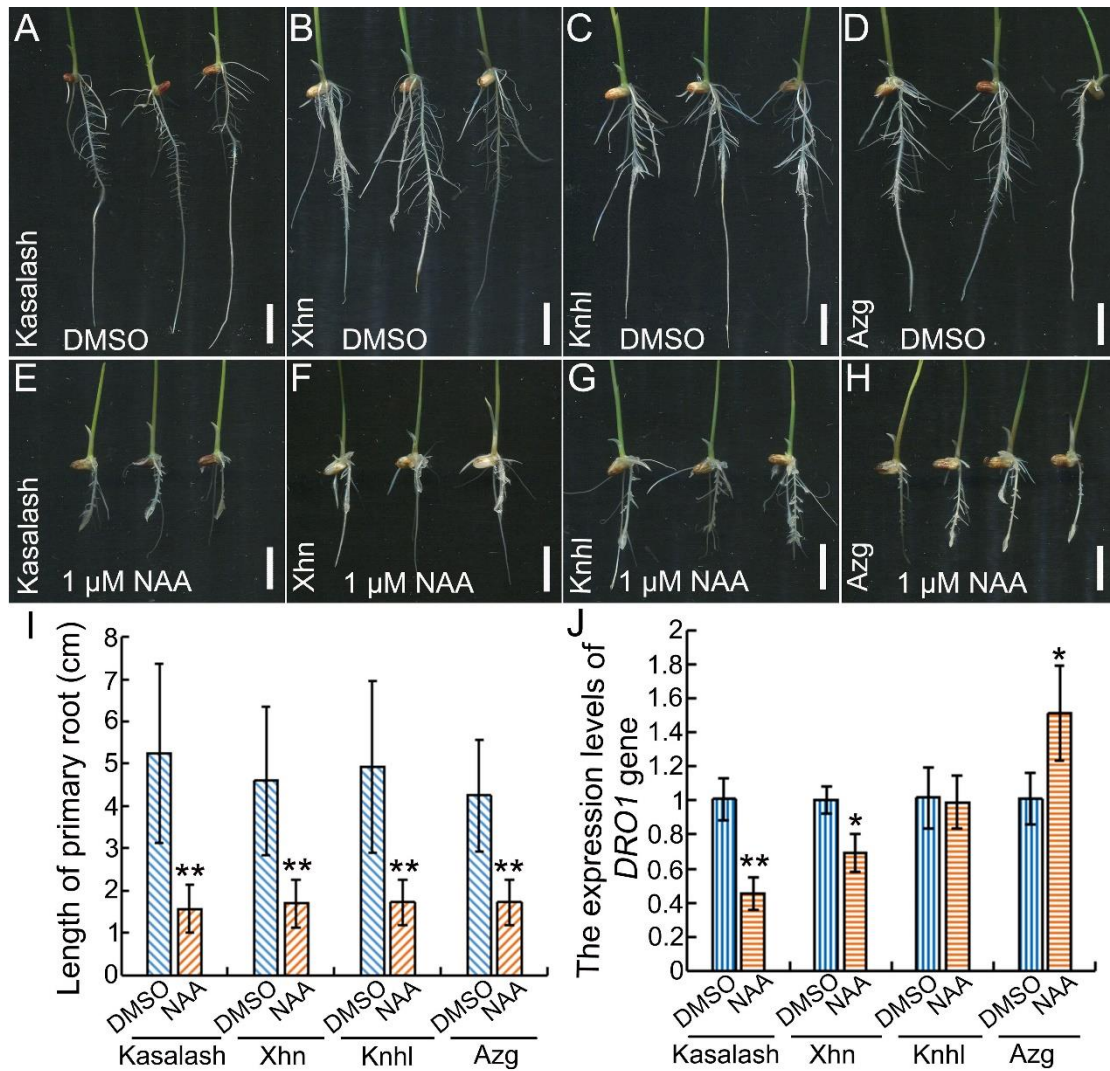


1402

1403 **Figure S23. Phenotypes of transgenic Nipponbare rice lines containing the**
 1404 ***INDITTO2* transposon in the *DRO1* promoter.**

1405 Schematic diagram of the expression construct containing an *INDITTO2* transposon
 1406 inserted into the Nipponbare *DRO1* promoter (A). Root phenotypes of wild-type
 1407 Nipponbare (B, F) and T1 transgenic rice lines expressing the *INDITTO2* transposon
 1408 (C-E, G-I) grown on MS medium with (F-I) or without (B-E) 15% PEG6000
 1409 supplementation. Quantification of the primary root lengths (J) (NPB: $n_{CK} = 20$, $n_{PEG} = 24$;
 1410 #8: $n_{CK} = 14$, $n_{PEG} = 9$; #11: $n_{CK} = 16$, $n_{PEG} = 12$; #14: $n_{CK} = 7$, $n_{PEG} = 10$). The
 1411 expression levels of *DRO1* (K) in the root meristem region of wild-type and
 1412 transgenic rice lines. The *OsActin* gene was used as an internal control. Data are
 1413 means \pm SD. * $P < 0.05$, ** $P < 0.01$ (Student's *t*-test for root length, SPSS analysis
 1414 for gene expression). *pDRO1N (+T)::DRO1N* = the Nipponbare *DRO1* promoter
 1415 containing the *INDITTO2* transposon and fused with Nipponbare genomic *DRO1*
 1416 gene. NPB = Nipponbare, CK = rice seedlings grown on MS medium, PEG = rice
 1417 seedlings grown on MS medium supplemented with 15% PEG6000. *gDRO1N* =
 1418 Nipponbare genomic *DRO1* gene. Bar = 1 cm.

1419

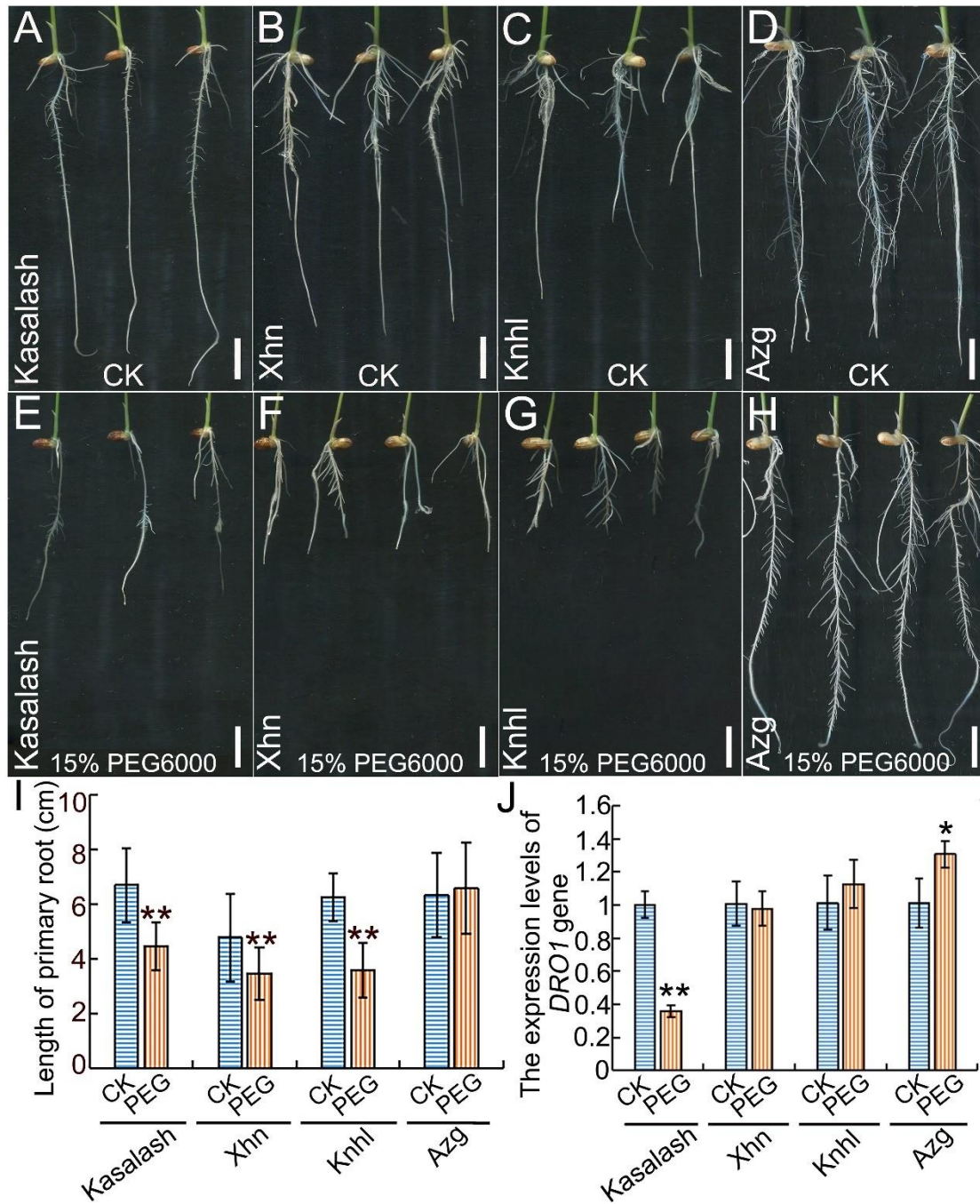


1420

1421 **Figure S24. The expression levels of *DRO1* in four rice varieties treated with**
 1422 **auxin.**

1423 Six-day-old seedlings of Kasalath (A, E), Xhn (B, F), Knhl (C, G) and Azg (D, H)
 1424 were grown on MS medium supplemented with DMSO (A-D) or with (E-H) 1 μM
 1425 NAA, and the expression levels of *DRO1* gene in root tip were checked by real-time
 1426 PCR (C). Seedlings grown on the MS medium containing DMSO was acted as a
 1427 control. The actin gene was used as an internal control. Data are the means ± SD. * P
 1428 < 0.05, ** $P < 0.01$ (SPSS analysis). Azg = Ai zhe gu, Knhl = Kou ni he lve, Xhn =
 1429 Xiao hua nuo.

1430

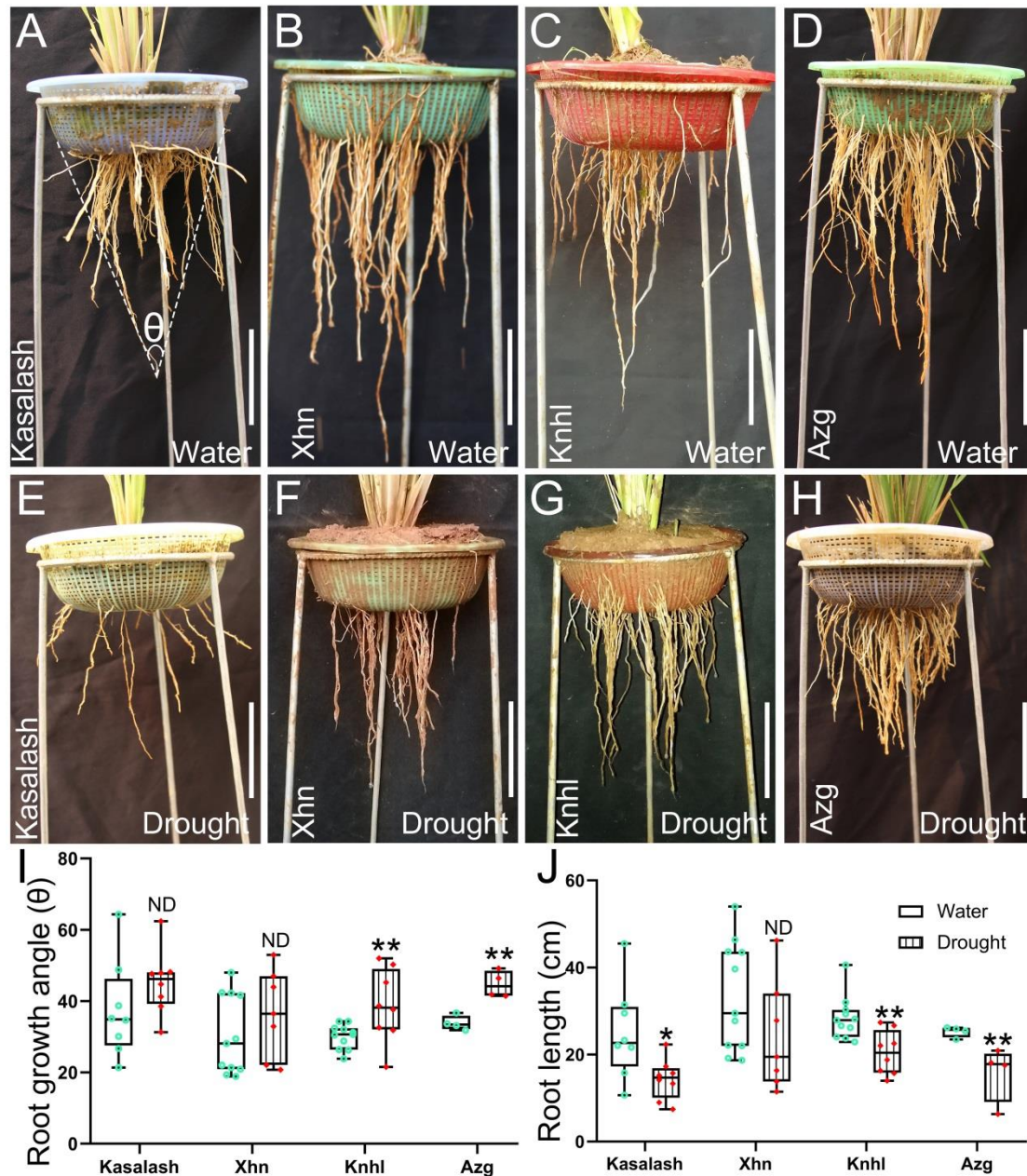


1431

1432 **Figure S25. Root lengths and the levels of *DRO1* in rice varieties grown under**
 1433 **drought stress.**

1434 Seedlings of Kasalath (A and E), Xhn (B and F), Knhl (C and G) and Azg (D and H)
 1435 grown on MS medium without (A-D) or with (E-H) 15% PEG6000 supplementation
 1436 for 6 days. The primary root lengths were measured and quantified (I) (Kasalath: n_{CK}
 1437 = 47, $n_{PEG6000}$ = 43, Xhn: n_{CK} = 42, $n_{PEG6000}$ = 42, Knhl: n_{CK} = 65, $n_{PEG6000}$ = 56, Azg:

1438 $n_{CK} = 12$, $n_{PEG6000} = 12$). The expression levels of *DRO1* (J) in the rice root meristem
1439 region were determined using real-time PCR. The *OsActin* gene was used as an
1440 internal control. Data are means \pm SD. * $P < 0.05$, ** $P < 0.01$ (Student's *t*-test for
1441 root length analysis, SPSS analysis for gene expression). CK = rice seedlings grown
1442 on MS medium, PEG = rice seedlings grown on MS medium supplemented with 15%
1443 PEG6000. Azg = Ai zhe gu, Knhl = Kou ni he lve, Xhn = Xiao hua nuo. Bar = 1 cm.
1444



1445

1446

Figure S26. Root architectures of rice varieties grown in the field.

1447

Kasalath (A, E), Xhn (B, F), Knhl (C, G) and Azg (D, H) were grown with irrigation

1448

conditions (A-D) or under drought stress (E-H) for 3 months. Quantification of the

1449

root growth angles (I) (Kasalath: $n_{\text{water}} = 8$, $n_{\text{drought}} = 8$, Xhn: $n_{\text{water}} = 11$, $n_{\text{drought}} = 7$,

1450

Knhl: $n_{\text{water}} = 11$, $n_{\text{drought}} = 8$, Azg: $n_{\text{water}} = 4$, $n_{\text{drought}} = 4$) and root length (J) (Kasalath:

1451

$n_{\text{water}} = 8$, $n_{\text{drought}} = 8$, Xhn: $n_{\text{water}} = 11$, $n_{\text{drought}} = 7$, Knhl: $n_{\text{water}} = 11$, $n_{\text{drought}} = 8$, Azg:

1452

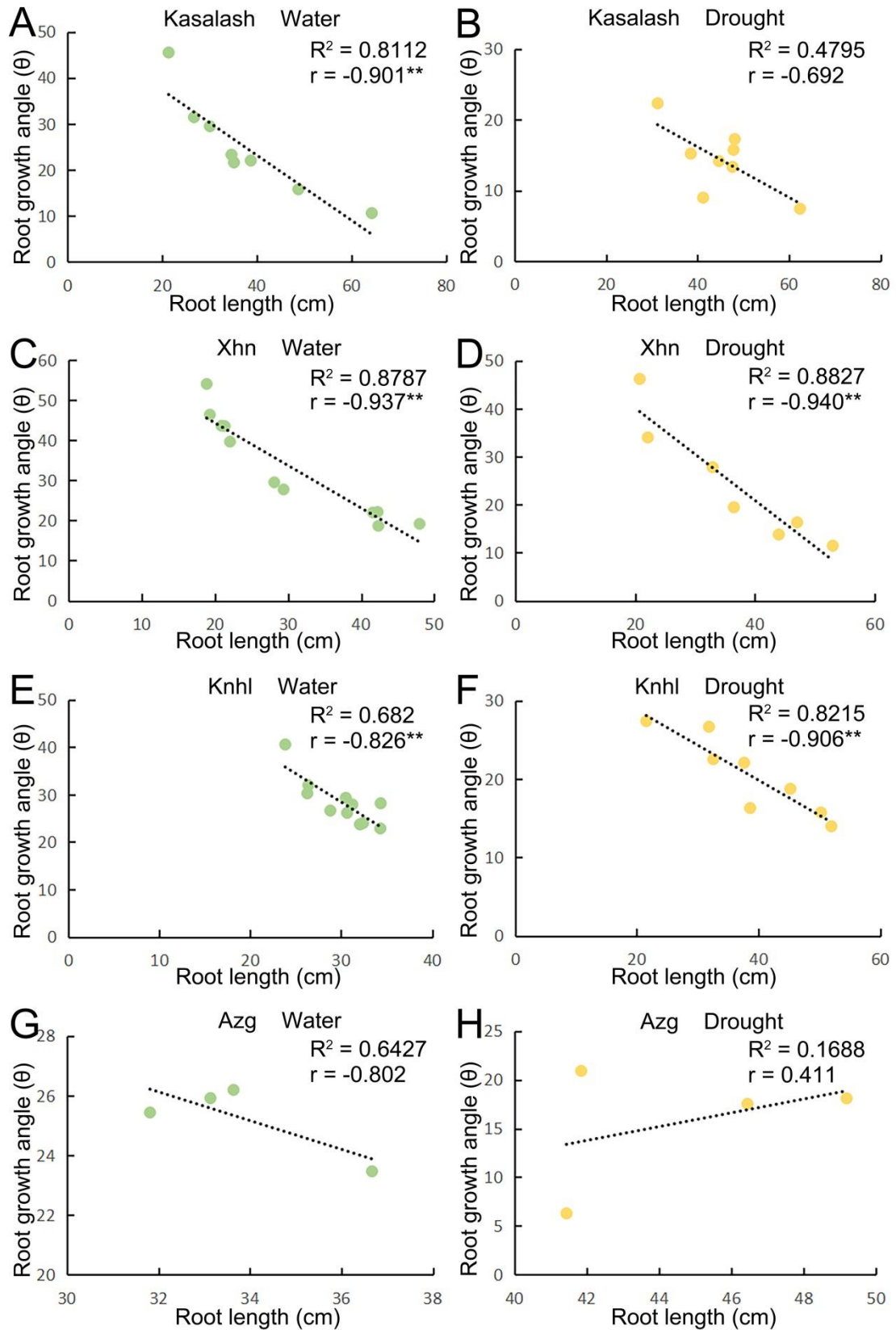
$n_{\text{water}} = 4$, $n_{\text{drought}} = 4$). Data are means \pm SD; * $P < 0.05$, ** $P < 0.01$ (Student's t -test).

1453

Azg = Ai zhe gu, Knhl = Kou ni he lve, Xhn = Xiao hua nuo, ND = no difference, $\theta =$

1454 root growth angle. Bar = 10 cm.

1455

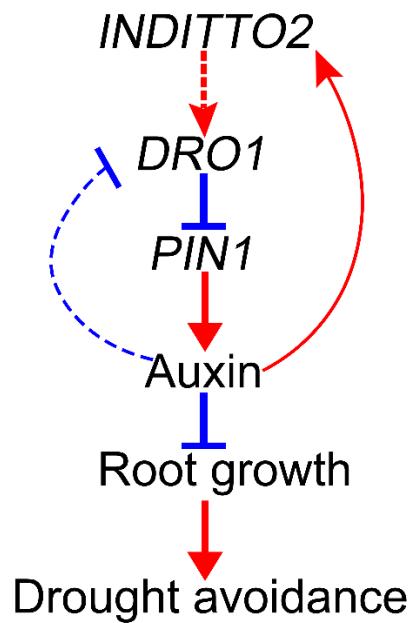


1456

1457 **Figure S27. Correlation analysis of root length and root growth angle in different**

1458 **rice varieties.**

1459 Kasalath (A, B), Xhn (C, D), Knhl (E, F) and Azg (G, H) were grown with irrigation
1460 conditions (A, C, E, G) or under drought stress (B, D, F, H) for 3 months. The
1461 correlation between root length and root angle was analyzed using SPSS software.
1462 Data are means \pm SD; ** $P < 0.01$ (double-tailed test) indicates a significant
1463 correlation. R^2 = Determination coefficient, r = Pearson's correlation coefficient; $r > 0$,
1464 positive correlation; $r < 0$, negative correlation. Azg = Ai zhe gu, Knhl = Kou ni he
1465 lve, Xhn = Xiao hua nuo.
1466



1467

1468 **Figure S28. A model of auxin-mediated *DRO1* transcription is conveyed by the**
 1469 ***INDITTO2* transposon to enhance rice drought avoidance.**

1470 *DRO1* is involved in negatively regulating the subcellular localization of the auxin
 1471 transporter *OsPIN1b* and controls auxin distribution; auxin negatively regulates the
 1472 expression level of the *DRO1* gene; *INDITTO2* transposon conveys the auxin signal to
 1473 mediate the *DRO1* transcription and regulate root growth and drought avoidance; thus,
 1474 providing a mechanism for rice to adapt to environmental drought stress. The dotted
 1475 line indicates that there may still be undiscovered factors in this pathway requiring
 1476 elucidation. → = promotion, ┘ = inhibition.

1477

Table S1. Rice landraces collected from the Yuanyang Hani's terraced fields

	Rice variety	Subspecies
1	Acuce	<i>indica</i> group
2	Ai jiao gu	<i>indica</i> group
3	Ai zhe gu	<i>indica</i> group
4	Bai gu	<i>indica</i> group
5	Ban jiu gu	<i>indica</i> group
6	Che bu	<i>indica</i> group
7	Che jia	<i>indica</i> group
8	Che zuo	<i>indica</i> group
9	Chuan bai gu	<i>indica</i> group
10	Da leng shui	<i>japonica</i> group
11	Da pi gu	<i>japonica</i> group
12	Duo dian	<i>indica</i> group
13	Ga niang hong gu	<i>indica</i> group
14	Gan di gu	<i>indica</i> group
15	Gan tian nuo	<i>indica</i> group
16	Hei gu	<i>japonica</i> group
17	Hong jiao lao geng	<i>indica</i> group
18	Hong yang 1	<i>indica</i> group
19	Hua ke nuo	<i>indica</i> group
20	Jian shui gu	<i>indica</i> group
21	Jiu yue nuo	<i>indica</i> group
22	Kou ni he lve	<i>indica</i> group
23	Le che che ma	<i>indica</i> group
24	Ma xian gu	<i>indica</i> group
25	Ma zha nuo	<i>indica</i> group
26	Man che hong nuo	<i>indica</i> group
27	Mao lai gu	unknown
28	Meng la gu	<i>indica</i> group
29	Meng la nuo	<i>indica</i> group
30	Qi xian gu	unknown
31	Shi yue bai gu	<i>indica</i> group
32	Si ma che	<i>indica</i> group
33	Xi bai gu	<i>indica</i> group
34	Xiao gu	<i>indica</i> group
35	Xiao hua gu	<i>indica</i> group
36	Xiao hua nuo	<i>indica</i> group
37	Xiao pi gu	<i>indica</i> group
38	Ye bai gu	<i>indica</i> group
39	Yun hui 290	<i>indica</i> group
40	Yun xiang	<i>japonica</i> group

1480 **Table S2.** Sequences of gene-specific primers

Target gene	Primer	Sequence of gene-specific primer	Locus
<i>OsDRO1</i>	DRO1-rFP	5'-AATGGAGAAGTTGCTCAAGGCA-3'	Os09g0439800
	DRO1-rRP	5'-TCATCGTCTAGATCACGCAGTG-3'	
<i>OsPIN1b</i>	OsPIN1b-rFP	5'-TCCTGCACGTCGCCATTGT-3'	Os02g0743400
	OsPIN1b-rRP	5'-GATGTAGTAGACGAGGGTGAT-3'	
<i>OsPIN2</i>	OsPIN2-5FP	5'-ACCAACGACCCCTACTCCATGAAC-3'	Os06g0660200
	OsPIN2-5RP	5'-AAGAGGGTGATGGTCCAGTCGAGC-3'	
<i>OsPIN3t</i>	OsPIN3t-FP	5'-TATGTATAGCCTGTTGTCGG-3'	Os01g45550
	OsPIN3t-RP	5'-TTGTACAAATGTCGCAGAGA-3'	
<i>Cas9</i>	Cas9-FP	5'-CACCATCTACCACCTGAGAA-3'	
	Cas9-RP	5'-CGAAGTTGCTCTTGAAGTTG-3'	
gRNA	PUV3-R	5'-CTGGCGAAAGGGGATGTGCTGCAA-3'	
	gRNA-R5	5'-ACGACCGGGTCACGCTGCACCT-3'	
<i>GUS</i>	GUS-rFP	5'-CGTGATGCGCGTCCAAGGA-3'	AF354045
	GUS-rRP	5'-TGATGGTGATGGTGATGGCTA-3'	
<i>NaActin</i>	NaActin-rFP	5'-GGTCGTACCACCGGTATTGTG-3'	JQ256516
	NaActin-rRP	5'-GTCAAGACGGAGAATGGCATG-3'	
<i>OsActin</i>	OsActin-FP	5'-GAGTATGATGAGTCGGGTCCAG-3'	Os11g0163100
	OsActin-RP	5'-ACACCAACAATCCCAAACAGAG-3'	
<i>ProDRO1A</i>	PrDRO1-FP	5'-CAGTGGTCTCATAGAGAGCTCATATATATTTTGAT-3'	Os09g0439800
	PrDRO1-RP	5'-CAGTGGTCTCAGTTGGGTACCGGCATGTCACTTCC-3'	
<i>ProDRO1N</i>	PrDRO1-FP	5'-CAGTGGTCTCATAGAGAGCTCATATATATTTTGAT-3'	Os09g0439800
	PrDRO1-RP	5'-CAGTGGTCTCAGTTGGGTACCGGCATGTCACTTCC-3'	
<i>INDITTO2</i>	PDI-FP	5'-GCCGCGCTGTACTTTATCTTA-3'	MN650123
	PDI-RP	5'-TTAGGACGAAGGTAGTATATCG-3'	
<i>INDITTO2</i>	Transposon-FP	5'-GAGCACCCGCAATGGTAAAGT-3'	MN650123
	Transposon-RP	5'-TTAGGGCACCCACAATGGTTAT-3'	
<i>INDITTO4</i>	Transposon-FP	5'-GAGCACCCGCAATGGTAAAGT-3'	MN650124
	Transposon-RP	5'-TTAGGGCACCCACAATGGTTAT-3'	

<i>OsDRO1</i>	OsDRO1-ccFP	5'-TCCCCTCAAGGAACAGGGAA-3'	Os09g0439800
	OsDRO1-ccRP	5'-TCGCCAATAGCAGCCACTAC-3'	
<i>OsYUCCA2a</i>	OsYUCCA2a-rFP	5'- TCAGAGAAAGATGGCTTCCCA -3'	Os01g0224700
	OsYUCCA2a-rRP	5'-CATATCGTGCAAACGCTGC-3'	
<i>OsYUCCA5b</i>	OsYUCCA5b-rFP	5'-AACGGATGGAAGGGTGAGT-3'	Os04g0128900
	OsYUCCA5b-rRP	5'-GCACGCCGTGCTCTTCTT-3'	

1481

1482 **Table S3.** Profiles of *INDITTO4* transposon homologues in the Nipponbare genome

Transposon	Chromosome	Start	End	E-value	Identity(%)	Remark	ARE
INDITT04	Chr1	1789089	1789352	3.44E-120	96.226	Os01g04110	-
INDITT04	Chr1	2546416	2546151	1.24E-119	95.88	not align to a gene	-
INDITT04	Chr1	4928955	4928690	2.66E-121	96.255	not align to a gene	-
INDITT04	Chr1	6014561	6014298	3.44E-120	96.226	not align to a gene	-
INDITT04	Chr1	6099685	6099945	7.40E-122	96.947	not align to a gene	-
INDITT04	Chr1	8712415	8712680	1.24E-119	95.88	not align to a gene	-
INDITT04	Chr1	9249970	9250232	1.24E-119	96.212	Os01g16310	-
INDITT04	Chr1	12319012	12318749	7.40E-122	96.604	not align to a gene	-
INDITT04	Chr1	24450817	24450552	1.23E-124	97.004	not align to a gene	-
INDITT04	Chr1	26507044	26506779	1.24E-119	95.88	not align to a gene	-
INDITT04	Chr1	27776411	27776676	2.64E-126	97.378	not align to a gene	-
INDITT04	Chr1	33086212	33086482	2.66E-121	95.956	not align to a gene	-
INDITT04	Chr1	34782540	34782277	7.40E-122	96.604	not align to a gene	-
INDITT04	Chr2	1049	784	2.55E-118	95.506	Os02g16940	-
INDITT04	Chr2	1085	1348	7.09E-119	95.849	Os02g45630	+
INDITT04	Chr2	4536323	4536588	2.66E-121	96.255	not align to a gene	+
INDITT04	Chr2	4589012	4588747	5.72E-123	96.629	not align to a gene	-
INDITT04	Chr2	8611637	8611900	3.44E-120	96.226	not align to a gene	-
INDITT04	Chr2	9454779	9454516	3.44E-120	96.226	not align to a gene	-
INDITT04	Chr2	23533755	23533492	3.44E-120	96.226	not align to a gene	-
INDITT04	Chr2	30575282	30575547	2.66E-121	96.255	Os02g50040	-
INDITT04	Chr2	32356824	32356559	2.66E-121	96.255	not align to a gene	-
INDITT04	Chr2	32636947	32637214	3.44E-120	95.911	not align to a gene	-
INDITT04	Chr2	32742755	32742490	1.24E-119	95.88	not align to a gene	-
INDITT04	Chr3	1927	1664	7.09E-119	95.849	Os03g22590	-
INDITT04	Chr3	8572827	8572608	2.13E-97	95.909	not align to a gene	-
INDITT04	Chr3	9787254	9787519	1.23E-124	97.004	Os03g17590	-
INDITT04	Chr3	11513912	11514175	7.40E-122	96.604	not align to a gene	-
INDITT04	Chr3	12673257	12673522	5.72E-123	96.629	not align to a gene	-
INDITT04	Chr3	12916441	12916706	5.72E-123	96.629	not align to a gene	-
INDITT04	Chr3	16060470	16060735	1.24E-119	95.88	not align to a gene	-
INDITT04	Chr3	21148823	21148558	5.72E-123	96.629	not align to a gene	-
INDITT04	Chr3	22604626	22604871	3.49E-110	95.951	not align to a gene	+
INDITT04	Chr3	27782605	27782342	1.59E-123	96.981	not align to a gene	-
INDITT04	Chr3	32622292	32622027	1.24E-119	95.88	not align to a gene	+
INDITT04	Chr3	34775226	34775491	1.23E-124	97.004	not align to a gene	-
INDITT04	Chr3	34931133	34930886	2.70E-111	95.984	not align to a gene	-
INDITT04	Chr3	35833625	35833890	5.72E-123	96.629	not align to a gene	-
INDITT04	Chr4	7704267	7704532	2.66E-121	96.255	Os04g13810	-
INDITT04	Chr4	28191069	28191334	1.24E-119	95.88	not align to a gene	-
INDITT04	Chr4	29486242	29486505	3.44E-120	96.226	Os04g49410	-
INDITT04	Chr4	30176489	30176752	7.40E-122	96.604	not align to a gene	-

INDITT04	Chr4	31782391	31782655	1.24E-119	95.88	not align to a gene	-
INDITT04	Chr5	334612	334347	1.23E-124	97.004	not align to a gene	-
INDITT04	Chr5	3496882	3497145	3.44E-120	96.226	not align to a gene	-
INDITT04	Chr5	5022414	5022149	5.72E-123	96.629	not align to a gene	-
INDITT04	Chr5	6941578	6941313	2.66E-121	96.255	not align to a gene	-
INDITT04	Chr5	13086371	13086634	3.44E-120	96.226	not align to a gene	-
INDITT04	Chr5	21060271	21060008	3.44E-120	96.226	not align to a gene	+
INDITT04	Chr5	27356360	27356623	3.44E-120	96.226	Os05g47750	-
INDITT04	Chr6	1831660	1831397	7.40E-122	96.604	Os06g04310	-
INDITT04	Chr6	8571622	8571887	1.24E-119	95.88	not align to a gene	-
INDITT04	Chr6	12848628	12848365	3.44E-120	96.226	not align to a gene	-
INDITT04	Chr6	17980600	17980861	4.45E-119	96.198	not align to a gene	-
INDITT04	Chr6	27708100	27708365	1.23E-124	97.004	not align to a gene	-
INDITT04	Chr6	29399341	29399604	1.59E-123	96.981	Os06g48590	-
INDITT04	Chr7	102786	103051	2.66E-121	96.255	not align to a gene	-
INDITT04	Chr7	5672370	5672633	3.44E-120	96.226	not align to a gene	-
INDITT04	Chr7	18837192	18837457	5.72E-123	96.629	not align to a gene	-
INDITT04	Chr7	19283173	19283438	5.72E-123	96.629	Os07g32420	-
INDITT04	Chr7	19447764	19447501	7.40E-122	96.604	not align to a gene	-
INDITT04	Chr7	21757809	21757546	3.44E-120	96.226	not align to a gene	-
INDITT04	Chr7	24097563	24097828	5.72E-123	96.629	not align to a gene	+
INDITT04	Chr8	600564	600299	1.24E-119	95.88	not align to a gene	+
INDITT04	Chr8	5237146	5237409	7.40E-122	96.604	not align to a gene	-
INDITT04	Chr8	5550744	5551007	1.59E-123	96.981	not align to a gene	-
INDITT04	Chr8	7583109	7582846	7.40E-122	96.604	not align to a gene	+
INDITT04	Chr8	21312747	21312482	1.24E-119	95.88	not align to a gene	-
INDITT04	Chr8	21940236	21939973	1.59E-123	96.981	not align to a gene	+
INDITT04	Chr8	23025352	23025087	1.24E-119	95.88	not align to a gene	+
INDITT04	Chr8	25611522	25611259	7.40E-122	96.604	Os08g40490	-
INDITT04	Chr8	27152477	27152214	7.40E-122	96.604	not align to a gene	-
INDITT04	Chr9	12105739	12105474	5.72E-123	96.629	not align to a gene	-
INDITT04	Chr9	13658520	13658783	7.40E-122	96.604	not align to a gene	-
INDITT04	Chr9	15196667	15196402	2.66E-121	96.255	not align to a gene	-
INDITT04	Chr9	18440510	18440245	2.66E-121	96.255	not align to a gene	+
INDITT04	Chr10	94153	93887	3.44E-120	95.896	not align to a gene	-
INDITT04	Chr10	2790768	2791031	3.44E-120	96.226	not align to a gene	-
INDITT04	Chr10	2799992	2800255	3.44E-120	96.226	not align to a gene	-
INDITT04	Chr10	11000532	11000797	2.66E-121	96.255	not align to a gene	-
INDITT04	Chr11	4470796	4470531	1.24E-119	95.88	not align to a gene	-
INDITT04	Chr11	6937844	6937581	7.40E-122	96.604	not align to a gene	-
INDITT04	Chr11	6938110	6937847	3.44E-120	96.226	not align to a gene	-
INDITT04	Chr11	16926034	16925771	7.40E-122	96.604	not align to a gene	-
INDITT04	Chr11	18570203	18570468	2.66E-121	96.255	not align to a gene	-
INDITT04	Chr11	22529778	22530043	1.23E-124	97.004	not align to a gene	-

INDITT04	Chr11	25170925	25171190	2.66E-121	96.255	not align to a gene	-
INDITT04	Chr11	27187297	27187032	1.24E-119	95.88	not align to a gene	-
INDITT04	Chr12	3987	3722	9.18E-118	95.506	Os12g41060	-
INDITT04	Chr12	2917445	2917710	1.23E-124	97.004	not align to a gene	-
INDITT04	Chr12	23973392	23973127	1.24E-119	95.88	not align to a gene	-
INDITT04	Chr12	23985997	23985732	1.23E-124	97.004	not align to a gene	-

1483 Note: Chr = chromosome, + and – means transposon containing with or without ARE,

1484 respectively. ARE = Auxin response element

1485

Table S4. Prediction of transcription factor binding sites in the *INDITTO2* transposon

Family	Start	Stop	Strand	p-value	q-value	Matched sequence
C2H2	17	34	-	2.34E-06	0.00106	TAGATAGCACCTTACTTT
BBR-BPC	169	189	+	6.21E-06	0.00188	TTTGCTCTCTCTTCATTTA
BBR-BPC	168	191	-	6.44E-06	0.00263	ATTAAATGAAGAGAGAGAGCAAAA
BBR-BPC	165	185	+	9.27E-06	0.00188	TAGTTTTGCTCTCTCTCTTCA
HD-ZIP	183	193	+	1.49E-05	0.00557	TCATTTAATAC
C2H2	198	209	-	1.51E-05	0.00762	TTTTCTTCTTG
HD-ZIP	183	193	+	2.09E-05	0.00777	TCATTTAATAC
BBR-BPC	167	187	+	3.10E-05	0.00419	GTTTTGCTCTCTCTTCATT
bZIP	210	224	-	3.16E-05	0.0159	ATCCATGTCAGCATA
bZIP	210	224	+	3.28E-05	0.0166	TATGCTGACATGGAT
bZIP	210	224	+	3.28E-05	0.0166	TATGCTGACATGGAT
HD-ZIP	183	193	-	6.53E-05	0.0121	GTATTAAATGA
MYB-related	160	173	-	9.70E-05	0.0352	GCAAAACTATCTAC